THE SMALL IRREGULAR ACTIVITY STATE IN THE RAT HIPPOCAMPUS

by

Beata Jarosiewicz

BS, University of Illinois, Champaign-Urbana, 1998

MS, University of Pittsburgh, 2001

Submitted to the Graduate Faculty of

Arts and Sciences in partial fulfillment

of the requirements for the degree of

Doctor of Philosophy

University of Pittsburgh

2003

UNIVERSITY OF PITTSBURGH

FACULTY OF ARTS AND SCIENCES

This dissertation was presented

by

Beata Jarosiewicz

It was defended on

25 November 2003

and approved by

Anthony Grace, Ph.D., Neuroscience

James McClelland, Ph.D., Neuroscience

Bruce McNaughton, Ph.D., Psychology and ARL, U. Arizona

David Touretzky, Ph.D., Computer Science, Carnegie Mellon University

External Examiner: James Ranck, Ph.D., Physiology, SUNY

Dissertation Chair: Carl Olson, Ph.D., Neuroscience

Dissertation Director: William Skaggs, Ph.D., Neuroscience

The Small Irregular Activity State in the Rat

Beata Jarosiewicz, PhD

University of Pittsburgh, 2003

The sleeping rat cycles between two well characterized physiological states, slow-wave sleep (SWS) and rapid eye-movement sleep (REM), often identified by the presence of large irregular activity (LIA) and theta activity, respectively, in the hippocampal EEG. Inspection of the activity of ensembles of hippocampal CA1 complex-spike cells along with the EEG reveals the presence of a third physiological state, distinctly different from both REM and SWS in both hippocampal EEG and population activity. The EEG during this state abruptly flattens for a few seconds, appearing very similar to the "small-amplitude irregular activity" (SIA) hippocampal EEG state reported in the literature to occur when rats are startled out of sleep. The flattening of the EEG is accompanied by a striking pattern of spike activity in the population of hippocampal pyramidal cells, wherein a small subset of cells becomes very active while the rest become quiet; the same subset of cells is usually active across long sequences of SIA. This dissertation shows (1) that these active cells are place cells whose place fields are in the location in which the rat is sleeping; (2) that the spontaneous SIA observed during sleep corresponds to the SIA state of increased alertness that has been reported in the literature to occur when rats are startled out of sleep; (3) that SIA is accompanied by a desynchronized neocortical EEG and low amplitude EMG; (4) that the cells active in SIA reflect a memory for the location in which the rat fell asleep, rather than an assessment of its location based on current sensory information; and (5) that the generation of SIA is likely to involve an increase of serotonin levels in the medial septal nucleus. It is proposed that SIA serves as a neural substrate for maintaining context memory during sleep, and that it reflects a partial arousal in response to internal or external stimuli that allows the animal to assess whether full awakening is warranted, without disrupting the sleep cycle.

ACKNOWLEDGEMENTS

This dissertation has been simultaneously the most challenging and the most rewarding enterprise I have ever undertaken. I am deeply grateful to everyone who helped me along the way. First and foremost, I'd like to thank my advisor, Bill Skaggs, who has never failed to astound me with his brilliant insight into matters scientific and his sagacious insight into matters meta-scientific. I've often found myself walking into his office confused and despondent, thinking that surely I must be the only scientist ever to have the pathetic problem I'm having, and walking out with not only a solution to my problem, but also with a profound sense of insight into the true nature of science and of how to "do it right." I am indebted to Bill for the whopping dose of skepticism I've acquired without squelching the whopping dose of optimism I brought with me to graduate school.

I would also like to thank the other members of my dissertation committee: Carl Olson, the chair of my committee, and one of the most sharply intelligent scientists I have ever met; Dave Touretzky, who generously supported the running of the laboratory after Bill's departure, and who has also been a great source of advice in my time here; Bruce McNaughton, my grand-advisor, so to speak, who has often taken time out from being one of the most influential scientists in the place cell literature to act as a second advisor to me; Jay McClelland, whose enthusiasm and insight into the "big picture" has always been an inspiration; Tony Grace, who wisely encouraged me to confront issues that have made my dissertation much more complete; and James Ranck, who has graciously agreed to serve as the external examiner on my committee.

I do not know what I would have done without my great friend and co-worker Nathaniel Daw, who has been incredibly helpful with all aspects of my graduate school career, most notably for managing the lab computers (along with Mark Fuhs), providing useful comments on drafts of manuscripts (including the Introduction and Chapter 5 of this thesis), and offering his keen insights on my work upon request; and Judith "Joy" Balcita, who greatly expedited my productivity in the last couple years by building drives, assisting with surgeries, managing the laboratory, and generally keeping me sane.

I would also like to thank György Buzsáki for providing helpful feedback on my first manuscript (Chapter 2 of this dissertation), Tony West for his advice on pharmacology, "Dr. Stan" Floresco for his advice on infusions, histology, and forehand swings in tennis, Kathy Kelly

for teaching me EMG, and Joel Brown for teaching me how to navigate about the lab and build drives when I first arrived. Thanks also to Andy Schwartz, my future postdoctoral advisor, for providing me with an office from which to finish writing my dissertation when the Skaggs lab space became unavailable.

I am also very grateful for the unbounded love and support from my wonderful friends and family.

Financial support for this work came from a National Science Foundation Graduate Fellowship, the Center for the Neural Basis of Cognition, and an Andrew Mellon Predoctoral Fellowship.

TABLE OF CONTENTS

LIST OF TABLES

LIST OF FIGURES

LIST OF ABBREVIATIONS

DG	dentate gyrus
EC	entorhinal cortex
EEG	electroencephalogram
EMG	electromyogram
LIA	large irregular activity
MnR	median raphe nucleus
MSDB	medial septum/vertical limb of the diagonal band of Broca
PH	posterior hypothalamus
PnO	nucleus pontis oralis
PPTg	pedunculopontine tegmental nucleus
REM	rapid eye-movement sleep
RF	reticular formation
SEM	standard error of the mean
SIA	small irregular activity
S-SIA	sleep-small irregular activity
SWS	slow-wave sleep

Chapter 1. INTRODUCTION

1.1. SLEEP

> Chuang Tzu once dreamed he was a butterfly. When he awoke, he no longer knew if he was a man who had dreamed he was a butterfly, or if he was a butterfly dreaming he was a man.
>
> *Chuang Tzu* (rough translation)

The duality of sentient existence, the waking life and the dream life, has fascinated philosophers throughout recorded history. Only in the last century, however, has it been possible to move beyond introspection and behavioral observation in the study of sleep and waking, with the advent of electrophysiological recording. Early sleep researchers were engrossed by the finding that the appearance of the electroencephalogram (EEG) recorded from scalps of human subjects changed systematically as they slept, and based on behavioral measures, subjective reports, and other variables, they found correlations between EEG patterns and levels of arousal and began delineating EEG patterns into defined sleep stages (Loomis et al., 1935a,b; Dement and Kleitman, 1957a,b). In 1968, Rechtschaffen and Kales, backed by a committee of prominent sleep researchers, revised and updated the sleep scoring systems developed by Loomis et al. and Dement and Kleitman, forming a standardized scoring system that is still widely used today. Based on EEG, electro-oculogram and electromyogram (EMG) characteristics, they divided sleep into non-REM stages 1-4, in sequential order of appearance and depth of sleep, and REM (rapid eye-movement sleep), so called because of the presence of rapid eye movements unique to this stage. REM has also been called “paradoxical sleep” because it is accompanied by nearly complete postural atonia, yet its EEG profile is more similar to waking than to the other sleep states. It is during REM that vivid, story-like dreams occur (Aserinsky and Kleitman, 1955; Dement and Kleitman, 1957b).

Because the limits imposed on human research are much more stringent than those imposed on animal research, and surface EEG recordings yield only limited, descriptive

information, it became desirable to study sleep states in animals as well, in whom local field potentials can be recorded from electrodes implanted inside the brain. In most mammals in which such recordings have been performed, non-REM (now commonly called "slow-wave sleep" [SWS] because of the presence of large slow waves in the neocortical EEG) and REM stages analogous to the human ones have also been found (for review, see Tobler, 1995). In animals lower than primates, it has been rare to subdivide these further.

Many animal sleep studies, including the ones in this dissertation, have used rats as subjects. In rats, REM and SWS are often distinguished by their hippocampal EEG. The hippocampal EEG state present during REM is theta activity, a strong ~7-8 Hz oscillation that is also present when rats are awake and actively exploring their environment. The hippocampal EEG state present during SWS is large irregular activity (LIA), an irregular activity of approximately the same amplitude as theta activity, but with no prominent rhythmicity; LIA is also present during quiet waking. The behavioral correlates of theta activity and LIA, their associated hippocampal cell activity, and mechanisms of generation, are discussed in detail in sections 1.4 and 1.5. Briefly, when the rat is actively exploring its environment, theta activity is present in the hippocampal EEG, accompanied by "desynchronized" (fast and small-amplitude) EEG in the neocortex (Green and Arduini, 1954; Gottesmann, 1964, 1992; Vanderwolf, 1969; Vanderwolf et al., 1975; O'Keefe and Nadel, 1978). During the awake theta state, many hippocampal CA1 pyramidal cells exhibit place specificity: these cells are only active when the rat enters a particular delimited portion of its environment (O'Keefe and Dostrovsky, 1971; O'Keefe, 1976; O'Keefe and Nadel, 1978; Best and Ranck, 1982). When the rat is awake but not actively exploring, LIA appears in the hippocampus while the neocortex remains desynchronized, and the activity of hippocampal CA1 pyramidal cells is diffuse, with large increases in spike activity across the population during occasional fluctuations called "sharp waves" (Buzsáki et al., 1992). When the rat falls asleep, it first enters SWS, during which LIA continues in the hippocampus, and the neocortex exhibits large-amplitude slow waves with occasional oscillations called "spindles" (Gottesmann, 1964, 1992; Steriade et al., 1993; McCormick and Bal, 1997; Siapas and Wilson, 1998). After a few minutes of SWS, the rat may enter a period of REM. The hippocampal and neocortical physiology of REM appears remarkably similar to that of the awake theta state: hippocampal theta activity and neocortical desynchronization are present (Swisher, 1962; Gottesmann, 1964, 1992; Vanderwolf, 1969), and

individual pyramidal cells show occasional brief periods of activity surrounded by virtual silence (Skaggs and McNaughton, 1998; Louie and Wilson, 2001), as though the rat is dreaming of running through their place fields.

This dissertation arises from observations that a third physiological state, differing from both theta activity and LIA, is revealed when hippocampal population activity patterns are inspected along with hippocampal EEG of the sleeping rat (Skaggs, 1995). During this state, the hippocampal EEG becomes very low in amplitude, and a small subset of cells becomes active while the rest of the cells remain nearly silent; the same cells are usually active across long sequences of such episodes. This state, lasting on the order of a few seconds, occurs repeatedly within periods of SWS and immediately follows nearly every REM episode. Chapter 3 provides evidence that this state corresponds to the "small irregular activity" (SIA) state that Vanderwolf (1971) observed when an animal was startled out of sleep without moving, and during active waking states when it abruptly stopped its motion but remained alert. The focus of this dissertation is to more fully characterize the SIA state that occurs spontaneously during sleep; to investigate the level of arousal during SIA relative to the other well-characterized states, testing its correspondence to the SIA reported in the literature; to investigate the correlates of its associated hippocampal cell ensemble activity; and to explore possible mechanisms by which SIA is generated.

It might at first seem trivial to assess the level of an animal's arousal; it seems that checking to see if it is moving should suffice. However, when the animal is not moving, it is surprisingly difficult to find a definition that is scientifically rigorous. Two commonly used measures are EMG amplitude and the presence or absence of desynchronization in the neocortical EEG. EMG amplitude is a measure of muscle tone, and is thus closely associated with the "obvious" assessment of whether or not an animal is moving around. EMG amplitude is highest in active waking (during theta activity), decreases in quiet waking (during LIA), and decreases further during SWS, reaching a minimum during REM (Timo-Iaria et al., 1970; Kohn et al., 1974; Johns et al., 1977). Neocortical EEG is also commonly used to assess arousal level; desynchronization is taken as a sign of cortical arousal because it is present during active waking (Pravdich-Neminsky 1913; Berger 1929; Moruzzi and Magoun 1949; Green and Arduini, 1954; Pickenhain and Klingberg, 1967; O'Keefe and Nadel, 1978; Vanderwolf, 1969; Whishaw, 1972; Gottesmann, 1992). However, this assessment fails to align with EMG in the case of REM, in

which desynchronization is also present but whose EMG level is the lowest of all the physiological states. This misalignment is often evaded by postulating that the cortex is also very active during REM, and that vivid dreams are the product of this cortical activity.

A third common approach to assessing level of arousal is by testing the animal's responsiveness to sensory stimuli. One difficulty with this strategy is in finding a satisfactory definition of an "arousal response," because this ultimately requires an assumption that some behavioral or electrophysiological measure axiomatically defines arousal, thus begging the question. For example, in some studies, neocortical desynchronization is considered a sufficient arousal response (Neckelmann and Ursin, 1993); the problem arises when one desires to test the level of arousal of a state that is already accompanied by neocortical desynchronization, such as REM or SIA (as will be shown in Chapter 3), by checking the latency to neocortical desynchronization. The other difficulty with this approach is in choosing an appropriate stimulus to which to test the animal's responsiveness. If the stimulus is meaningless, the animal rapidly habituates to it with repeated exposure and ceases to respond in any physiological state. For example, Dillon and Webb (1965) reported that "on some occasions the animal would awaken from either type of sleep as a chair creaked or a pencil fell, and on other occasions they would sleep through our maximum stimulus (approximately 100 db)" (p. 447).

Habituation can be avoided by making a stimulus meaningful, for example by training the animal to respond to the stimulus in a certain way to obtain a reward or to avoid a punishment. Using this strategy in rats, the latency to a trained behavioral response was found to be fastest during awake states, slower during SWS and slowest during REM (Van Twyver and Garrett, 1972), consistent with the EMG data suggesting that REM is a "deeper" sleep state than SWS. This is also consistent with results of studies using meaningful stimuli to which there was no trained response, e.g. when the stimulus was a ramping shock to the neck musculature (Dillon and Webb, 1965) or vibration of the floor, to which animals do not habituate as readily as to auditory stimuli (Davis et al., 1972), and the measured response was movement. However, results can vary depending on the nature of the stimuli used. In one study (Neckelmann and Ursin, 1993), the stimulus was a tone of gradually increasing intensity to which the animal had been repeatedly exposed prior to the sleep experiments, and the measured arousal response was latency to neocortical EEG desynchronization and EMG amplitude increase. In this study, REM

actually had a lower response threshold than SWS (Neckelmann and Ursin, 1993), suggesting that SWS is a deeper sleep state than REM.

In humans, in whom SWS is divided into 4 stages of increasing depth (Rechtschaffen and Kales, 1968), the level of arousal of REM appears to fall somewhere between the lighter 2 stages and the deeper 2 stages of SWS, and the results can be extremely variable even within a single experiment. For example, Rechtschaffen et al. (1966) found that, when an auditory stimulus of ramping intensity was used as the stimulus, the threshold to awakening during REM appeared to depend on the extent to which the stimulus was incorporated into the subject's dream! When subjects were awakened by tones that become extremely loud during REM, they reported dreams such as the following:

> "I was in my room with a friend. We were arguing over the pronunciation of a German word. Suddenly my friend said that he had hidden a voltmeter in the closet which was going all the time. I said I had one too, and we both compared voltmeters. My friend's was unusual in that it lit up and made a noise every time he plugged it into a higher voltage. As he plugged it into higher and higher voltages, the sound got louder and louder."
>
> "I was at a lecture or something or other. Then I found myself in a laboratory giving sound tests to mice in a cage. I don't know what the mice were supposed to do or how they would react. As I gave louder sounds, they just seemed to ignore it." (Rechtschaffen et al., 1966, p. 928)

When a non-ramping, meaningful stimulus was used, the responsiveness during REM was found to be less variable, significantly lower than in SWS stages 3-4, and comparable to that of SWS stage 2 (Rechtschaffen et al., 1966).

Thus, the assessment of the level of arousal of a particular physiological state can vary greatly depending on the precise methods by which it is measured. No single measure of arousal level is universally accepted as being the ultimate measure, and indeed, there is no reason to believe that arousal level has any true ultimate measure. Simultaneous consideration of multiple commonly used measures can provide a general idea of the relationship between different physiological states.

1.2. HIPPOCAMPAL ANATOMY

Before discussing the physiological states of the hippocampus in detail, it is useful to review the relevant hippocampal anatomy. It is summarized here only briefly, emphasizing the characteristics that are thought to be important for the hippocampus's unique physiological properties. Except where noted, the following description is based on Amaral and Witter (1995).

In the rat, the hippocampal formation is a relatively large structure, its surface area rivaling that of the neocortex. The bilateral hippocampal formation appears similar to the curved horns of a ram, hence its early name "*Cornu Ammonis*" (Ammon's horn), after which its CA1-3 fields are named. Each roughly C-shaped side extends from the septal nuclei dorsally and caudally over the diencephalon, and then ventrally and rostrally tucks under the temporal lobe (Fig. 1.1).

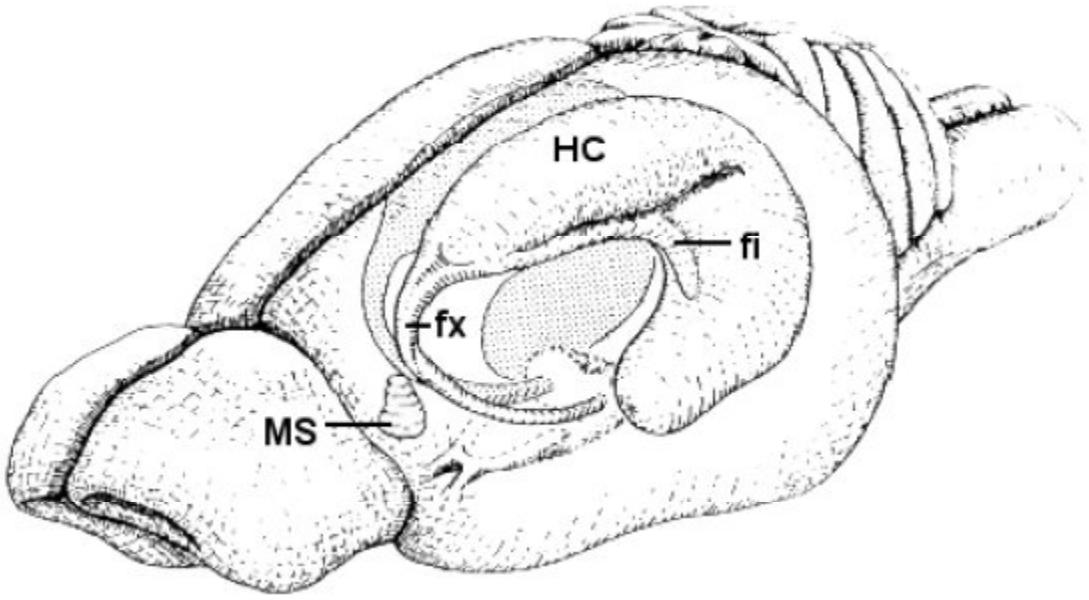

Figure 1.1. Layout of hippocampus in rat brain.

Left is anterior, right is posterior. Abbreviations: HC = hippocampus; fx = fornix; MS = medial septum; fi = fimbria. Modified from Amaral and Witter (1995) by Ikonen (2002). Reproduced with permission.

The hippocampal formation includes the entorhinal cortex (EC); dentate gyrus (DG); hippocampus proper, which is subdivided into fields CA1, CA2, and CA3 (although the existence of CA2 in the rat is controversial and rarely mentioned in the physiology literature); and the subicular complex, consisting of the subiculum, presubiculum, and parasubiculum. The major intrinsic hippocampal connections are summarized schematically in Figure 1.2. The EC,

which has strong projections to and from most areas of neocortex except primary sensory areas, provides the sole cortical input and major cortical output of the hippocampal formation (CA1 and subiculum also project directly to some cortical areas, bypassing the EC). The superficial layers of the EC project to all the other fields of the hippocampal formation via the "perforant path": EC layer 2 projects primarily to the dentate gyrus and CA3, and EC layer 3 projects primarily to CA1 and the subiculum. In addition, the granule cells of the DG project to CA3 as the "mossy fibers"; CA3 contains extensive recurrent collaterals, such that the primary input of its projection cells (pyramidal cells) are other CA3 pyramidal cells; CA3 pyramidal cells project to CA1 as the "Schaffer collaterals"; and CA1 pyramidal cells project to the subiculum. The deep layers (4-6) of the EC receive hippocampal output via the subiculum and CA1. Also, DG granule cells project to the contralateral DG, and CA3 and perhaps some CA1 pyramidal cells project to the contralateral CA3, CA2, and CA1, as the associational/commissural fibers. All of the aforementioned projections are glutamatergic.

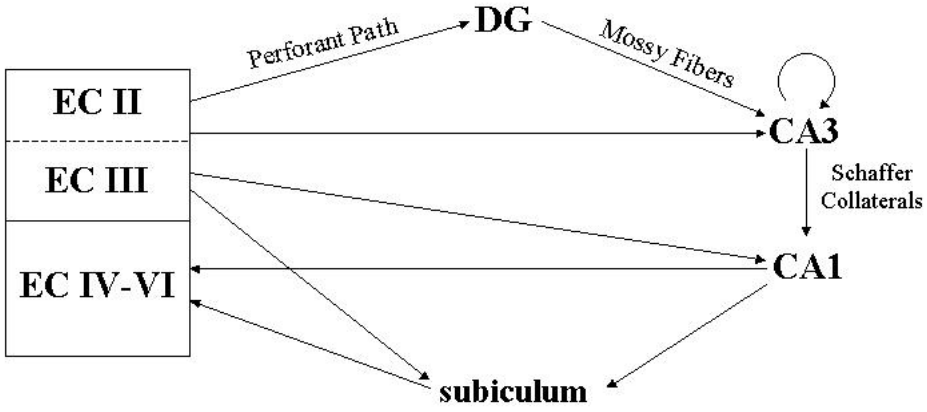

Figure 1.2. Major intrinsic connections of the hippocampal formation.
Abbreviations: EC = entorhinal cortex; DG = dentate gyrus; INs = interneurons.

The hippocampal formation also has interconnections with subcortical structures, primarily coursing through the fimbria/fornix. The medial septum/vertical limb of the diagonal band of Broca (MSDB) projects to all fields of the hippocampal formation, providing both GABAergic and cholinergic input. These projections are critical for the generation of theta activity (see Section 1.3.3). MSDB input into the hippocampus is topographically organized:

more medial regions of the MSDB project primarily to the septal pole of the hippocampus, and more lateral regions of the MSDB project primarily to the temporal pole of the hippocampus. Additionally, Amaral and Kurz (1985) have shown that septal levels of the hippocampus obtain most of their cholinergic input from the nucleus of the diagonal band, which is more ventral, whereas temporal levels obtain most of their cholinergic input from the medial septal nucleus, which is more dorsal. Also, the supramammillary nucleus (SuM) projects to the DG, the subicular complex, and EC; the locus coeruleus provides noradrenergic input to the DG, CA3, CA1, presubiculum, parasubiculum, and EC; and the raphe nuclei provide serotonergic input to DG, CA3, CA1, and EC. CA1 also receives input from the basolateral amygdala and nucleus reuniens of the midline thalamus, and the anterior thalamus is interconnected with the subiculum and parasubiculum. The major targets of subcortical output from the hippocampus include the lateral septum, which receives input from CA3, CA1, and subiculum; the diagonal band of Broca, which receives input from CA1; the mammillary nuclei and nucleus accumbens, which receive input from the subiculum; and the anterior thalamus and medial and lateral nuclei of the mammillary complex, which receive input from the presubiculum and parasubiculum.

The cross-section of the hippocampal formation has a striking laminar profile. Each field (DG, CA1, and CA3) contains a thin plane of projection cell bodies, called granule cells in the DG and pyramidal cells in fields CA1-3. These principal cells are the ones that show spatial firing correlates (see Section 1.3.2). The anatomical layout of these principal cell layers and a subset of their intrahippocampal projections, the classical "trisynaptic circuit" (Andersen et al., 1971), are shown schematically in Figure 1.3. All of the projection cells are neatly aligned with their apical dendrites extending toward the hippocampal fissure (the division between the dentate gyrus and CA1) and the basal dendrites and axons extending toward the outer surface of the hippocampus. This polarized arrangement of the principal cell bodies and their dendrites is responsible for the dipole that determines the laminar profile of theta activity (see Section 1.3.3).

In the DG, there are 2 other layers, the *molecular layer*, which is closest to the hippocampal fissure, and the *polymorphic layer*, more often called the *hilus*, on the other side of the granule cell layer, closest to CA3. In the CA fields, the narrow, cell-free layer just deep to the pyramidal cell layer is called *stratum oriens*, in which most of the basal dendritic tree is located, and deep to this is the fiber-containing *alveus*. In the CA3 field, but not in CA2 or CA1, there is a narrow layer called the *stratum lucidum*, containing the mossy fiber projections from the

dentate gyrus. Just above the pyramidal cell layer in CA2 and CA1, and just above the stratum lucidum in CA3, is the *stratum radiatum*, in which the CA3 recurrent collaterals and CA3-CA1 Schaffer collaterals are located. The most superficial (i.e. closest to the hippocampal fissure) layer is the stratum *lacunosum-moleculare*, in which perforant pathway fibers from the EC travel and terminate. In addition to the projection cells, each layer of each field also contains a heterogeneous mix of interneurons, the vast majority of which are GABAergic. The interneurons receive inputs from the same regions as the principal cells in that field, and they also project to and receive inputs from the local principal cells. They are predominantly local circuit neurons, but some are also known to project outside their subfields.

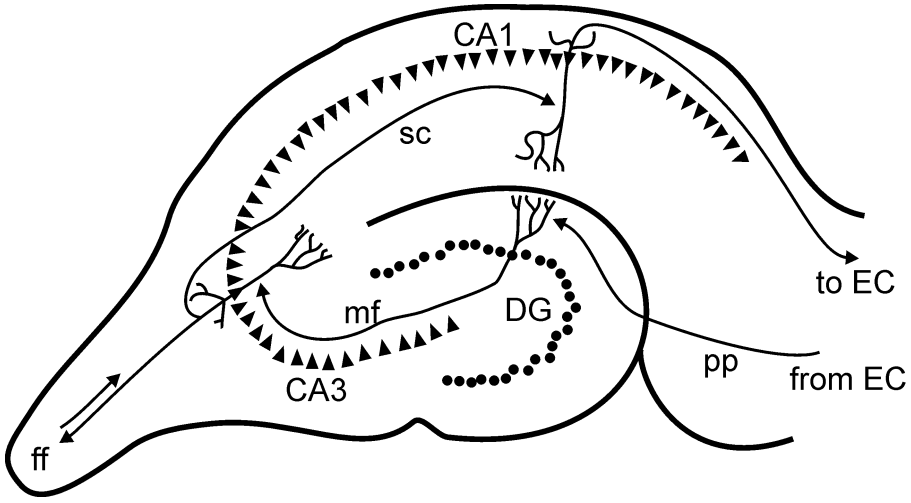

Figure 1.3. Cross-section of hippocampus.

This schematic of the coronal cross-section of dorsal hippocampus illustrates the layout of the principal cell layers of DG, CA3, and CA1. It also illustrates the layout of a subset of the intrinsic outputs of these principal cells, known classically as the "trisynaptic circuit" (Andersen et al., 1971): EC to DG (synapse 1), DG to CA3 (synapse 2), and CA3 to CA1 (synapse 3). The projections from CA1 back to EC are also shown. It is now known that the projections through the hippocampus, although still primarily feed-forward, are more elaborate than this (see text). Abbreviations: EC = entorhinal cortex; DG = dentate gyrus; pp = perforant pathway; mf = mossy fibers; sc = Schaffer collaterals; ff = fimbria/fornix. Reproduced with permission from Ikonen (2001).

1.3. THETA ACTIVITY

1.3.1. Behavioral Correlates

In 1954, Green and Arduini published the first large-scale study of spontaneous hippocampal electrical activity. They observed an intermittent, strikingly regular oscillation around 5-7 Hz in the hippocampus of the cat and rabbit, and more rarely in the monkey. This "rhythmic slow activity," now usually called "theta activity," often (but not always) coincided with periods of neocortical desynchronization, from which they conjectured that theta activity might reflect hippocampal arousal. An explosion of research on the behavioral correlates of the hippocampal theta rhythm in different species using different behavioral paradigms produced a confused mass of data relating theta activity to phenomena such as inhibiting the orienting reflex (Grastyán et al., 1959), approach behavior (Grastyán et al., 1966), and learning and attention (Adey 1966, 1977; Elazar and Adey 1967a,b).

C. H. Vanderwolf, an influential hippocampal physiologist and an adamant behaviorist, opposed the trend to link brain signals to poorly defined "inferred processes" like arousal and attention; he favored searching for correlates with objectively observable behaviors (Vanderwolf 1967, 1969, 1971; Vanderwolf et al., 1975). He found that, in the rat, theta activity was nearly always present during what he called "type 1" or "voluntary" behaviors, defined as those "that can be brought under the control of many different drive states and can be performed in a variety of combinations and sequences…. Thus, running may be controlled by hunger, thirst, fear, sexual or material drive, etc., on different occasions" (p. 84, Vanderwolf, 1971). Thus, behaviors such as walking, running, swimming, and manipulating objects were associated with theta activity. On the other hand, theta activity was nearly always absent during "type 2" or "involuntary" behaviors, defined as "reflexes as well as a number of activities which… occur only in association with particular drive states… Thus, 'feeling cold' is associated with cutaneous vasoconstriction, shivering, a crouched posture, etc." (p. 84, Vanderwolf, 1971). A more irregular but still large-amplitude EEG pattern was observed instead, which Vanderwolf called "large irregular activity" (LIA). Thus, LIA was present during automatic behaviors such as eating, grooming, and sitting still. Vanderwolf was careful to point out that his terms "voluntary" and "involuntary" were not intended to describe any inferred mental processes subserving these

classes of movements, but were rather meant as mnemonic tags for classes of behaviors that would otherwise take more words to describe.

Vanderwolf's behaviorist description of the correlates of theta activity, although appealingly elegant, does not generalize to species other than rodents: in rabbits and cats, theta activity occurs in response to sensory stimuli even while the animal is motionless (Green and Arduini, 1954; Brown, 1968; Bennett, 1969; Harper, 1971; Klemm, 1971; Sakai et al., 1973; Whishaw and Vanderwolf, 1973; Kramis et al., 1975; Sainsbury and Montoya, 1984). The frequency of this immobility-related theta is lower than the "type 1 theta" spontaneously present during type 1 behaviors in these animals, and is thought to correspond to the "type 2 theta" present under urethane anesthesia (Kramis et al., 1975; Bland, 1986) because of its similar frequency and sensitivity to muscarinic blockers such as atropine (Kramis et al., 1975; Vanderwolf, 1988). In humans, the correlates of theta activity seem even more complicated: theta activity has been observed during the performance of various cognitive tasks, such as virtual navigation (Kahana et al., 1999; Caplan et al., 2003), digit working memory (Jensen and Tesche, 2003), and word-list learning (Fell et al., 2003). It is difficult to interpret these human studies because different groups have different definitions of the frequency of human theta activity, and most human EEG studies are performed either on epileptic patients, whose results may or may not generalize to the normal population, or using surface electrodes, which are unlikely to reflect hippocampal activity. Much work is still needed to sort out the correlates of hippocampal theta activity in humans, if it actually exists; it seems unlikely from the evidence thus far that it will be possible to define them in purely behavioristic terms.

Even in rats, the association between theta activity and type 1 behaviors is not absolute: theta activity is present during REM (Swisher, 1962; Vanderwolf, 1969; Gottesmann, 1964, 1992), and theta activity can be abolished by lesions or pharmacological manipulations while sparing type 1 behaviors (Green and Arduini, 1954; Winson, 1978; Givens and Olton, 1990; Mizumori et al., 1989; Lawson and Bland, 1993). Nevertheless, when considering only the awake, intact, undrugged rat, theta activity does appear to have strong behavioral correlates, and Vanderwolf's description of those behavioral correlates is still considered quite accurate. In general, it is now widely accepted that theta activity in rats predominantly occurs when and only when the rat is actively moving through or manipulating objects in its environment, and also

during REM sleep, when (one might speculate) the rat might be dreaming of performing such activities.

1.3.2. Associated Cell Activity: Place Cells

Perhaps not surprisingly, research on the correlates of hippocampal cell activity had a similar history to research on the correlates of theta activity. Many of the early studies were done in restrained animals exposed to arrays of various stimuli (e.g. Vinogradova, 1970; Vinogradova et al., 1970) or in classical conditioning paradigms (e.g. Olds, 1967; Olds and Hirano, 1969), and the correlates of the recorded cells were determined by comparing their firing rates during presentations of stimuli or during different phases of the experiment (for review, see O'Keefe and Nadel, 1978). Based on average increases or decreases in firing rate under different conditions or phases of the task, researchers hypothesized that hippocampal cells represented phenomena like the animal's arousal level, phases of learning, etc.

O'Keefe and Nadel (1978) argued that, in the initial stages of attempting to characterize the correlates of any brain activity, it is important to place the animal in as naturalistic a setting as possible, and to permit the widest possible range of natural behaviors, in order to maximize the possibility of finding behaviors or stimuli that best drive the cell: "When we first venture into the unknown, we need not the incisive beam of the proud penetrating laser, but the gentle diffuse illumination of the humble torch. There will be plenty of time later for detailed investigation of the nooks and crannies; first we must find the mountains" (O'Keefe and Nadel, 1978, p. 194). To point out the shortcomings of using the rigidly structured "neuropsychological" approach commonly used at that time (as opposed to the unstructured "neuroethological" approach they advocated) in early phases of determining the neural correlates of a particular brain area, O'Keefe and Nadel (1978) quoted the following clever passage written by Vanderwolf, who expressed a similar sentiment about the importance of considering the animal's behavior when looking for correlates of brain activity:

> Consider the case of Professor Omega, an imaginary researcher who suspected that the somatic muscles had a direct role in mental processes. Omega began his research by recording electromyographic activity (EMG) from m. pectoralis major during behaviour in animals. His first finding was that on exposure of an animal to an unfamiliar Skinner box, EMG activity was high initially but declined progressively during continued exposure. Presentations of

> tones and flashing lights led to temporary increases in EMG activity. These findings suggested a role of the muscle in habituation and attention. When the animal was trained to press a lever in the box, EMG activity rose to a high level. Extinction procedures resulted in a decline to pretraining levels. These facts suggested a role for the muscle in conditioning and learning. Further research showed that EMG activity rose during food deprivation and fell after feeding, suggesting a role in motivational phenomena. Amphetamine increased EMG activity sharply, but anaesthetics abolished it. Tranquillizers had an intermediate effect. Omega concluded that the pectoralis muscle was probably the site of action of many drugs.
>
> To his surprise, Omega had great difficulty in publishing his results in scientific journals. In response to criticisms of his work, he pointed out that the methods and experimental design he had used were identical to those adopted by many researchers who had published papers purporting to show that the slow wave or unit activity of the neocortex, the hippocampus, and many other parts of the brain is related to attention, learning, motivation, etc. (Vanderwolf, 1983, p. 92[*]).

Presumably led by this neuroethological sentiment, O'Keefe and Dostrovsky (1971) recorded from single hippocampal units while carefully observing the animal's behavior. They placed rats on a small arena on which they were allowed to eat, drink, groom, walk around, and sleep as they pleased. Out of 76 total recorded hippocampal units, 8 had firing correlates different from any previously reported: these cells appeared to be maximally driven when the rat entered particular places on the arena. Numerous other ("movement") cells appeared to be related to the rat's ongoing behavior, firing most during behaviors that Vanderwolf had associated with theta activity. Along with a couple of studies indicating that rats with hippocampal lesions had difficulty with, among other things, spatial tasks (Douglas, 1967; Kimble, 1968), these 8 place-related cells led O'Keefe and Dostrovsky (1971) to put forth the hypothesis that the hippocampus serves as a spatial, or cognitive, map. O'Keefe and collaborators subsequently extended and confirmed these studies, naming these cells "place cells" and their preferred firing fields "place fields" (O'Keefe, 1976; O'Keefe and Nadel, 1978).

[*] Vanderwolf had written the chapter containing this passage in 1976, but the book containing this chapter was not published until 1983.

Ranck (1973), also led by a neuroethological philosophy, enumerated various behavioral correlates of hippocampal cells in freely moving rats. Importantly, he found that two distinct classes of hippocampal cells could be identified based on their electrophysiological characteristics: "complex spike cells" and "theta cells." By definition, complex spike cells at least on occasion show complex spikes (a burst of several spikes within a few milliseconds of each other, each successive spike usually decreasing in amplitude), whereas theta cells never do. In addition, these physiological cell types differ in their waveform and firing rate characteristics (Ranck, 1973; Fox and Ranck, 1975, 1981; Barnes et al., 1990): theta cells have narrower waveforms and much higher mean firing rates than complex spike cells. Theta cells were so named because most of them increase their firing rate during theta activity, both in waking and in REM. Complex spike cells appeared to have much more complicated behavioral correlates; Ranck (1973) noticed but did not emphasize their spatial aspects. Fox and Ranck (1975, 1981) later found that complex spike cells correspond anatomically to projection cells, and that theta cells correspond anatomically to interneurons, a correspondence that is now widely accepted. O'Keefe (1976) observed that all of the place cells he recorded had the properties of Ranck's complex spike cells (and were thus probably projection cells), and all of his movement-related cells had the properties of theta cells (and were thus probably interneurons). Best and Ranck (1982) verified this correspondence in an interesting experiment designed to test the behavioral correlates of hippocampal cells as described by Ranck (1973) versus those described by O'Keefe and Dostrovsky (1971) and O'Keefe (1976): they asked naïve observers to watch videotapes of a behaving rat while listening to the spike train of a hippocampal cell to see if they can determine the cell's behavioral correlates. This experiment confirmed O'Keefe and Dostrovsky's (1971) and O'Keefe's (1976) findings that theta cells are related to movement, and that most complex spike cells are related to the animal's spatial location. Best and Ranck (1982) also observed that many place-related cells only had spatial correlates when the rat was *moving* through their place fields, not when sitting still inside them. In agreement with this finding, O'Keefe and Nadel (1978) reported that firing rates of complex spike cells were strongly modulated by place only in the presence of theta activity; on the other hand, during LIA, most place cells fired at about 1 Hz, irrespective of the animal's location.

As mentioned previously, during REM, the temporal structure of hippocampal ensemble activity, like the hippocampal EEG, appears strikingly similar to the awake theta state (Skaggs

and McNaughton, 1998; Louie and Wilson, 2001): individual complex spike cells are silent most of the time, but occasionally fire in bursts a few seconds long, as though the rat is dreaming of running through their place fields. The temporal patterns of activity that occur during REM statistically resemble the patterns of activity in the preceding waking pattern more than expected by chance, as though the hippocampus is replaying memories of the rat's trajectories in the preceding waking period (Louie and Wilson, 2001).

The spatial correlates of hippocampal complex spike cells have been verified in hundreds of subsequent studies. It has since been shown that in dorsal CA1, in which most place cell studies are done because of its easy accessibility, only about 10-25% of place cells have place fields in a given environment, and that the particular subset of cells that have place fields is random and independent across environments (Thompson and Best, 1989). When cells have place fields in multiple environments, their topological relationship to one another is unrelated across environments (Kubie and Ranck, 1983; Thompson and Best, 1989). A single place cell can have multiple place fields in a single environment, although multiple fields are observed less commonly with better cell isolation (O'Keefe and Conway, 1978; Wilson and McNaughton, 1993).

Place fields are controlled by an interaction of visual and self-motion cues. If the visual cues in an environment are rotated, place fields rotate by an equal amount (O'Keefe and Conway, 1978; Muller and Kubie, 1987; Bostock et al., 1991), but only if the rat has previously learned that the cues are stable (Knierim et al., 1995; Jeffery and O'Keefe, 1999). Also, if the rat is first exposed to an environment in the light, and then the lights are turned off, place fields persist in the dark, although they can drift over time (Quirk et al., 1990; Markus et al., 1994). When landmark cues are dissociated from one another (O'Keefe and Nadel, 1978; Shapiro et al., 1997; Tanila et al., 1997; Brown and Skaggs, 2002; Knierim, 2002) or from idiothetic (self-motion) cues (Knierim et al., 1998; Sharp et al., 1995), ensembles of simultaneously recorded place fields select one source of spatial information or the other (probably depending on which the rat believes to be more reliable, as evidenced above), or they entirely remap, as though the rat has encountered a novel environment. In these situations, there is some evidence that place fields rotate together, all following one set of cues (Quirk et al., 1990; Markus et al., 1994; Brown and Skaggs, 2002), but there is also evidence that they can split into groups, some fields rotating with one set of cues and some rotating with the other (Shapiro et al., 1997; Tanila et al., 1997;

Knierim, 2002). Consistent with the hypothesis that the hippocampal cell population activity reflects the rat's internal spatial map, in tasks in which spatial location is relevant to the rat's behavior (e.g. in which the rat obtains a reward only if it goes to the correct arm of a maze), mistakes in the rat's behavior correspond to misalignments in place cell firing (O'Keefe and Speakman, 1987; Lenck-Santini et al., 2002; Rosenweig et al., 2003).

Despite the prominence of the place cell phenomenon, it is clear that place is not the only correlate of hippocampal complex spike cells. Many cases of complex spike cells with non-spatial correlates were reported in early studies; for example, one of Best and Ranck's (1982) complex spike cells only fired when the rat was drinking, irrespective of whether the rat was drinking from a water tube, dish, or dropper, and no matter where the drinking was taking place, even if the rat was following a dish or dropper that the experimenter was moving around. Two other cells fired only during particular body movements, irrespective of where those movements took place (Best and Ranck, 1982). More recently, Markus et al. (1995) found that a large subset of simultaneously recorded place cells changed the location of their place fields when the rat switched from a random foraging task to shuttling between specific points within the same arena. Similarly, Wood et al. (2000) found that most complex spike cells fired differentially on the central stem of a T-maze depending on whether the rat was eventually going to make a left or right turn on that trial, even though the rat's behavior and location at that point in the maze did not differ between trial type. It has been suggested that the hippocampus does not encode solely space, but more generally *context*, of which space is just one component (Eichenbaum et al., 1999; Redish, 1999). This view is meant to help bridge the place cell literature with the equally expansive literature supporting a role for the hippocampus in learning and memory (e.g. see Scoville and Milner, 1957; Squire, 1992; McClelland et al., 1995).

1.3.3. Generation Mechanisms

Over the last 50 years, evidence has accumulated in support of the existence of an "ascending brainstem synchronizing system" that induces theta activity in all parts of the hippocampal formation (for reviews, see Vertes, 1982; Bland and Colom, 1993). The brainstem reticular formation (RF) and the MSDB were implicated in theta generation from the start: Green and Arduini (1954) showed that hippocampal theta activity could be elicited by stimulation of the RF, and that theta activity could be abolished by lesions to the MSDB. It was soon found that

cells of the MSDB fire rhythmically with the theta rhythm, and that this rhythmic firing can be driven by tonic stimulation of the brainstem RF (Petsche et al., 1962, 1965; Stumpf et al., 1962), leading Petsche, Stumpf and colleagues to postulate that the MSDB is the "pacemaker" of the theta rhythm, because it appears to transform tonic input from the reticular formation into rhythmic firing that induces rhythmic field oscillations in downstream limbic structures. The pacemaker hypothesis gained support from numerous replications of the findings that lesioning or inactivating the MSDB abolishes theta activity (Winson, 1978; Givens and Olton, 1990; Mizumori et al., 1989; Kirk and McNaughton, 1993; Lawson and Bland, 1993; Oddie et al., 1996), and that stimulating the RF induces theta activity in the hippocampus (Macadar et al., 1974; Vertes et al., 1993). It gained further support from subsequent findings that brainstem RF stimulation also drives rhythmic firing in MSDB neurons (Brazhnik et al., 1985; Bland et al., 1994; Oddie et al., 1994) and that increasing the intensity of tonic stimulation of the RF increases the initial frequency of the elicited hippocampal theta activity (Klemm, 1972; Macadar et al., 1974; Brazhnik et al., 1985; Vertes, 1980, 1981; Oddie et al., 1994) and a corresponding increase in the discharge rate of MSDB neurons (Bland et al., 1994). The most effective RF stimulation site for theta generation was pinned down to the nucleus pontis oralis (PnO) (Macadar et al., 1974; Vertes, 1981), which most of the RF stimulation experiments above targeted, although the pedunculopontine tegmental nucleus (PPTg) has also been implicated in theta generation (Macadar et al., 1974; Vertes et al., 1993).

The PnO-MSDB ascending brainstem synchronizing system model was complicated by anatomical findings that the PnO has only very sparse projections to the MSDB (Vertes, 1984, 1988; Vertes and Martin, 1988). Vertes postulated that the supramammillary nucleus of the hypothalamus (SuM), a structure he found to have strong projections to the MSDB (Vertes, 1988, 1992) and to receive strong projections from the PnO (Vertes and Martin, 1988), relayed the actions of the PnO to the MSDB. Evidence for this came from findings that electrical stimulation in the vicinity of the SuM or the neighboring posterior hypothalamus (PH) generates hippocampal theta activity (Torii, 1961; Yokota and Fujimori, 1964; Anchel and Lindsley, 1972; Bland and Vanderwolf, 1972; Whishaw et al., 1972; Wilson et al., 1976; Vertes, 1981; Oddie et al., 1994) and produces rhythmic firing of MSDB cells (Wilson et al., 1976; Bland et al., 1990, 1994), and that inactivation of the PH prevents PnO stimulation from inducing theta activity

(Oddie et al., 1994; Bland et al., 1994) and rhythmic discharges in the MSDB (Bland et al., 1994).

In fact, there is evidence that theta rhythmicity is already present before reaching the MSDB, at the level of the SuM: when the PnO is stimulated, cells in the SuM fire rhythmically in phase with the hippocampal theta rhythm (Kirk and McNaughton, 1991; Kocsis and Vertes, 1994; Bland et al., 1995), and they maintain their rhythmic firing even when the MSDB has been inactivated with procaine, abolishing hippocampal theta (Kirk and McNaughton, 1991). Furthermore, Kirk and McNaughton (1993) showed that inactivation of either the MSDB or the SuM suppressed the *amplitude* of hippocampal theta activity resulting from PnO stimulation; however, the *frequency* of theta activity was reduced when the SuM was inactivated, but not when the MSDB was inactivated. They interpreted this to mean that the MSDB must already be receiving frequency-coded information, and that the SuM, not the MSDB, might actually set the pace of the hippocampal theta rhythm. This interpretation is consistent with the finding that stimulation of the MSDB at frequencies near normal theta range, between ~ 5 and 35 Hz, produces hippocampal theta activity at the same frequency as the MSDB stimulation, but stimulation of the MSDB at high frequencies (greater than ~100 Hz) does not (Brücke et al., 1959; Ball and Gray, 1971; Klemm and Dreyfus, 1975; Stumpf, 1965; James et al., 1977; Brazhnik et al., 1985), providing evidence that the MSDB actually requires theta-like input to produce theta-like output.

To complicate matters further, it was recently found that in awake, behaving rats, lesion or inactivation of the SuM does not suppress either the amplitude or the frequency of theta activity nearly as much as it does in urethane-anesthetized rats (McNaughton et al., 1995; Thinschmidt et al., 1995). One possible explanation for this finding is that, in the awake behaving rat, a network of brainstem and hypothalamic nuclei are involved in theta production; the PH and the SuM are likely to have parallel functions so that one can compensate at least partially in the absence of the other (Woodnorth et al., 2003). Support for a parallel role of the PH comes from the stimulation and inactivation studies described above, and from the findings that the PH has significant projections to the SuM and MSDB and receives projections from the PnO and PPTg (Vertes et al., 1995; Bland and Oddie, 1998); that PH cells increase their discharge rate during spontaneous theta activity in the awake behaving rat (Bland et al., 1995; Kirk et al., 1996) and during hippocampal theta elicited by PnO stimulation in the urethane-

anesthetized rat (Kirk et al., 1996), and they maintain this increased discharge rate even when the MSDB is inactivated by procaine injection (Kirk et al., 1996). In summary, then, the ascending brainstem synchronizing system is thought to begin in the PnO and the PPTg, which project to the SuM and PH, which in turn project to the MSDB. The frequency appears to be established at the level of the SuM, and the MSDB appears to provide the direct theta drive to each field of the hippocampus. The details of the precise role of each structure and their interactions have yet to be worked out.

The cellular mechanisms by which the MSDB drives hippocampal theta activity are another topic of intense research. The classical model assumes that theta activity reflects the summed postsynaptic potentials of the neatly aligned hippocampal principal cells that receive coherent inhibitory input directly and indirectly (via feed-forward inhibitory neurons) onto their cell bodies from the rhythmically bursting MSDB cholinergic and GABAergic neurons and coherent excitatory input directly onto their distal dendrites from the perforant path (for reviews, see Stewart and Fox, 1990; Smythe et al., 1992; Vertes and Kocsis, 1997). This scheme is supported by current-source density analysis (Mitzdorf, 1985) showing a sink in the CA1 stratum lacunosum-moleculare and a source in the pyramidal cell layer (Buzsáki et al., 1986; Brankack et al., 1993). It is also supported by the finding that the theta activity remaining after EC lesion or deafferentation is missing the dipole at the distal dendrites near the hippocampal fissure (Ylinen at al, 1995b; Kamondi et al., 1998). Interestingly, the theta activity remaining after EC lesion can be abolished by atropine (Buzsáki et al., 1983; Vanderwolf and Leung, 1983). This pharmacological and laminar profile is very similar to that of type 2 theta (Ylinen at al, 1995b; Kamondi et al., 1998; Kramis et al., 1975; Vanderwolf, 1988), suggesting that the mechanistic differences between type 1 and type 2 theta are in the presence versus absence, respectively, of the entorhinal cortical contribution. Buzsáki (2002) provides evidence that NMDA receptors, recurrent connections in the dentate gyrus and CA3, and intrinsic resonant properties of various hippocampal neurons may also play a role in theta generation, but the precise mechanisms are still far from being worked out.

1.4. LARGE IRREGULAR ACTIVITY (LIA)

1.4.1. Behavioral Correlates

LIA is defined as the absence of a regular oscillation in the hippocampal EEG, with amplitude similar to that of theta activity. A prominent feature of LIA is the occasional large 30-120 ms spike called a sharp wave. Sharp waves are largest in amplitude near the stratum radiatum, and are usually accompanied by a fast sinusoidal "ripple" (~4-10 waves with periods of ~4-8 ms) in the pyramidal cell layer, where the sharp wave abruptly reverses polarity (O'Keefe and Nadel, 1978; Buzsáki, 1986).

As discussed in Section 1.3.1, Vanderwolf (1971) found that, in the rat, theta activity is present during "type 1" or "voluntary" behaviors such as walking, running, swimming, and manipulating objects, whereas LIA is present during "type 2" or "involuntary" behaviors, such as eating, grooming, and sitting still. LIA is also present during SWS, although the neocortical EEG pattern is different between SWS and quiet waking: during waking, the neocortex remains desynchronized, but during SWS, the neocortex exhibits large-amplitude slow waves and spindles (Gottesmann, 1964, 1992; Steriade et al., 1993; McCormick and Bal, 1997; Siapas and Wilson, 1998).

1.4.2. Associated Cell Activity

As mentioned in section 1.3.2, the firing of hippocampal pyramidal cells is most strongly place-modulated during theta activity. In LIA, place selectivity is highly degraded (Foster et al., 1989; Kubie et al., 1985) or absent (O'Keefe and Nadel, 1978; Best and Ranck, 1982). Instead, the population of hippocampal CA1 cells has a diffuse pattern of activity, with transient increases during sharp waves (Buzsáki et al., 1992). The patterns of activity during LIA, particularly during sharp waves, statistically resemble the patterns of activity during the preceding waking period more than expected by chance, but unlike the reactivation during REM, the reactivation during LIA is highly compressed in time (Pavlides and Winson, 1989; Wilson and McNaughton, 1994; Skaggs and McNaughton, 1996; Nádasdy et al., 1999).

1.4.3. Generation Mechanisms

Many studies of hippocampal physiology treat LIA as the default hippocampal EEG state in the absence of theta activity, and relatively little research has been devoted to LIA's mechanisms of generation. The bulk of studies on LIA generation, coming largely from Buzsáki's laboratory, have focused on the mechanisms of its more prominent subcomponents: sharp waves, ripples, and the fast (~100-140 Hz) oscillations that occur between sharp waves (O'Keefe and Nadel, 1978; Buzsáki et al., 1983, 1992; Buzsáki, 1986; Ylinen et al., 1995a; Csicsvari et al., 1999a,b).

Buzsáki and collaborators (Buzsáki et al., 1983, 1992; Buzsáki, 1986) have shown that all of the subcomponents of LIA probably arise within the hippocampus. Evidence for this comes from their observations that sharp waves are not abolished by MSDB lesions, fornix transection, or EC lesions or isolation. Based on their findings that sharp waves are accompanied by increased firing rate in both hippocampal pyramidal cells and interneurons, which are generally quiet between sharp waves; that the histogram of pyramidal cell spike activity has peaks coinciding with the negative peaks of the associated ripple oscillations; that peaks of interneuron cross-correlograms are time-shifted by about ½ a cycle from pyramidal cells; and that CA1, but not CA3, shows a high spatiotemporal coherence of ripples over large regions of hippocampus, Buzsáki and collaborators concluded that sharp waves are probably initiated within CA3 as a result of temporary disinhibition from afferent control, that the sharp waves recorded from the stratum radiatum of CA1 represent summed post-synaptic potentials of CA1 pyramidal cells and interneurons by the Schaffer collaterals, and that the interneurons probably do not contribute to the oscillations but help to determine the precise timing of pyramidal cell spikes in the background of excitatory CA3 barrage. A faster (~180 Hz) oscillation in the pyramidal cell layer of CA1 that occurs between large-amplitude ripples (~110 Hz) is thought to be initiated by strong input from CA3 pyramidal cells but its frequency determined by the characteristics of the CA1 field (Chrobak and Buzsáki, 1996; Csicsvari et al., 1999b).

1.5. SMALL IRREGULAR ACTIVITY (SIA)

1.5.1. Behavioral Correlates

As mentioned above, a third physiological state, differing from both theta and LIA, is revealed when hippocampal population activity patterns are inspected along with hippocampal EEG of the sleeping rat (Skaggs, 1995). The EEG of this state appears similar to a pattern that has been called "low-amplitude irregular activity" (Pickenhain and Klingberg, 1967), also called "small-amplitude irregular activity" or SIA (Vanderwolf, 1971; Whishaw, 1972; see O'Keefe and Nadel, 1978, for a review). In a study designed to test the behavioral correlates of theta activity, Pickenhain and Klingberg (1967) found an unexpected "low-amplitude irregular activity" in rats in response to novel or unfamiliar stimuli when no orienting movements were made; e.g., when a click awakened them from sleep. When orienting movements were made, theta activity occurred instead. Vanderwolf (1971) applied the nomenclature "small-amplitude irregular activity" to this sudden suppression of hippocampal activity, under the assumption that it corresponds to the EEG pattern named by Stumpf (1965), who described SIA in the rabbit as a "fast activity" sometimes superimposed upon theta (probably corresponding to what is now called "gamma activity") and sometimes occurring in isolation under experimental conditions like septal lesions or reticular stimulation (Stumpf, 1965). Vanderwolf (1971) observed SIA, usually lasting about 1-2 sec, in rats that abruptly stop an ongoing movement: e.g. when they are startled onto their feet, without running; when they jump to the edge of a box and almost go over the edge (requiring a sudden halt); and when they cling to a motor-driven wheel, riding back on it instead of moving forward. Whishaw (1972), Vanderwolf's PhD student at the time, defined SIA as hippocampal electrical activity with smaller amplitude than the smallest theta observed in that animal (LIA had approximately the same amplitude as theta, but was irregular in frequency and amplitude). He also observed SIA when rats suddenly arrest voluntary movement or change from a resting or sleeping state to an alert state, as indicated by neocortical desynchronization, without moving. Neither Pickenhain and Klingberg (1967) nor Vanderwolf (1971) recorded during sleep; they only described SIA as a waking state. Whishaw (1972) reported only continuous LIA during sleep.

Similar EEG states have also been reported in the sleeping rat by other groups of researchers: Roldán et al. (1963) observe "arousal-like periods" of EEG desynchronization in both neocortex and hippocampus at the end of REM and sometimes during SWS; this state is similar to the state they report to occur when the rat is startled out of sleep. Bergmann et al. (1987) report the existence of "low-amplitude sleep," characterized by low hippocampal and cortical EEG amplitude and low EMG amplitude; this is similar to the state they observe when the rat is startled during waking states. It is likely that "arousal-like periods," and "low-amplitude sleep" correspond to the SIA-like state that we observe during sleep, and Chapter 3 provides evidence that this in turn corresponds to Vanderwolf's SIA. Thus, we have adopted Vanderwolf's terminology and refer to this sleep state as SIA.

1.5.2. Associated Cell Activity

The hippocampal cell activity during SIA was first described by Skaggs (1995): most pyramidal cells fall silent, except for a small proportion of them, which become very active at SIA onset and remain active throughout the episode. The same subset of cells is active across many SIA episodes. Chapter 2 of the current dissertation shows that these "SIA-active" cells are place cells whose place fields are in the location in which the rat is sleeping (Jarosiewicz et al., 2002), and Chapter 4 shows that this population activity reflects a memory for the location in which the rat fell asleep, rather than an on-line assessment based on current sensory input.

1.5.3. Possible Generation Mechanisms

The mechanisms by which SIA is generated are not addressed in the few studies characterizing its behavioral correlates. However, a hippocampal "desynchronization" resembling SIA has been reported under three sets of experimental conditions. (1) It occurs when the MSDB has been lesioned or temporarily inactivated, and theta activity would otherwise normally be expected, e.g. during running or REM sleep (Green and Arduini, 1954; Winson, 1978; Givens and Olton, 1990; Mizumori et al., 1989; Lawson and Bland, 1993) or during stimulation of the reticular formation (Kirk and McNaughton, 1993; Oddie et al., 1996). (2) Stimulation of the MSDB at frequencies near normal theta range, between ~ 5 and 35 Hz, produces hippocampal theta rhythm of the same frequency as the stimulation, but when the MSDB is stimulated at frequencies

beyond physiological theta range (greater than ~100 Hz), hippocampal desynchronization occurs instead (Brücke et al., 1959; Stumpf, 1965; Ball and Gray, 1971; Klemm and Dreyfus, 1975; James et al., 1977; Brazhnik et al., 1985). Together, these two sets of results suggest that SIA might occur when LIA is precluded (either behaviorally or by electrical stimulation) but external theta drive is somehow disrupted.

A third set of results sheds some light on a possible neural trigger of SIA: (3) Stimulation of the median raphe nucleus ("MnR") produces hippocampal desynchronization (Macadar et al., 1974; Assaf and Miller, 1978; Vertes, 1981). This effect appears to be mediated by serotonergic projections to the MSDB, as continuous theta activity results under manipulations that suppress the activity of MnR serotonergic neurons (for review, see Vertes and Kocsis, 1997); MnR serotonergic fibers directly inhibit a subset of septohippocampal cholinergic projection cells via 5HT-1A receptors (Milner and Veznedaroglu, 1993; Kia et al., 1996) and directly excite septohippocampal GABAergic projection cells via 5-HT-2A and possibly other receptor subtypes (Alreja, 1996; Leranth and Vertes, 1999); and MnR stimulation inhibits irregularly firing septal neurons and disrupts the rhythmicity of regularly bursting septal neurons (Assaf and Miller, 1978). Furthermore, serotonergic MnR cells have been shown to increase their firing at the offset of REM episodes and in response to phasic visual or auditory stimuli during waking and sleep (Rasmussen et al., 1984), when naturally occurring SIA would be expected. These results suggest a possible mechanism of naturally occurring SIA: when the animal is suddenly aroused, the MnR suddenly increases its activity. The increase of serotonin in the MSDB causes it to send a sudden stream of non-rhythmic input into the hippocampus, shutting down the intrinsic mechanisms producing LIA without driving theta activity, resulting in SIA. Some predictions of these hypotheses are tested in this dissertation; the results are reported in Chapter 5.

1.6. SUMMARY AND AIMS

In summary, during SWS and drowsy waking states, the EEG at the level of the hippocampal fissure exhibits predominantly LIA, and the hippocampal population activity is generally diffuse, with increases of activity during sharp waves. In REM, as well as in active waking states, the rat hippocampal EEG exhibits theta activity, and hippocampal population activity resembles awake

exploration, in that individual pyramidal cells show occasional brief periods of activity surrounded by virtual silence. When hippocampal population activity patterns are inspected along with hippocampal EEG of the sleeping rat, a third physiological state is revealed, probably corresponding to the waking SIA state described by Vanderwolf (1971) (see Chapter 3). During SIA, the EEG becomes very low in amplitude, and a small subset of cells becomes active while the rest of the cells remain nearly silent; the same cells are usually active across long sequences of such episodes. The goal of this dissertation is to characterize SIA in order to better understand its relationship to the other, well-characterized physiological states. Chapters 2 and 3 characterize the hippocampal and neocortical EEG, EMG, hippocampal population activity, and incidence of SIA relative to REM and LIA; Chapters 2 and 4 determine the significance of the hippocampal population activity during SIA; Chapters 3 and 4 assess by various measures the level of arousal of SIA; Chapter 3 provides evidence that the spontaneous SIA that occurs during sleep corresponds to the waking SIA state elicited by auditory stimuli; and finally, Chapter 5 explores possible mechanisms by which SIA is generated.

Chapter 2. HIPPOCAMPAL POPULATION ACTIVITY DURING THE SMALL-AMPLITUDE IRREGULAR ACTIVITY STATE IN THE RAT

2.1. PREFACE

This Chapter is based on Jarosiewicz B, McNaughton BL, Skaggs WE (2002), Hippocampal population activity during the small-amplitude irregular activity state in the rat, J Neurosci 22:1373-1384. It comprises a preliminary characterization of the hippocampal population activity and EEG of SIA. In this paper, we called the state "sleep-SIA," abbreviated "S-SIA" to specify that the SIA we are characterizing is the one we observe to occur spontaneously during sleep, which may or may not correspond to the SIA previously reported as a waking state. In Chapter 3, we provide evidence that these really are the same state, and thenceforth collapse the terminology and call it "SIA."

2.2. INTRODUCTION

The sleeping rat cycles between two well characterized physiological states, slow-wave sleep (SWS) and rapid eye-movement sleep (REM), often defined by their cortical and hippocampal EEG (for review, see O'Keefe and Nadel, 1978; Gottesmann, 1992; and Skaggs and McNaughton, 1998). During SWS and drowsy waking states, the EEG at the level of the hippocampal fissure exhibits predominantly large-amplitude waves with power distributed across a broad range of frequencies, often called "large-amplitude irregular activity" (LIA), punctuated by fluctuations called "sharp waves" (Buzsáki, 1986). The population activity of CA1 pyramidal cells in LIA is generally diffuse, with large increases of activity during sharp waves (Buzsáki et al., 1992). The neocortex exhibits large-amplitude, slow waves with occasional brief 7-14 Hz oscillations called "spindles" (Gottesmann, 1964, 1992; Steriade et al., 1993; McCormick and Bal, 1997; Siapas and Wilson, 1998). In REM, corresponding in humans to dream sleep (Dement and Kleitman, 1957a,b), as well as in active waking states, the rat hippocampal EEG exhibits

strong 7-8 Hz rhythmicity, called "theta activity," and the neocortical EEG exhibits small-amplitude, fast ("desynchronized") activity (Green and Arduini, 1954; Gottesmann, 1964, 1992; Vanderwolf, 1969; Vanderwolf et al., 1975; O'Keefe and Nadel, 1978). CA1 population activity during REM also resembles that during awake exploration (Skaggs and McNaughton, 1998; Louie and Wilson, 2001), in that individual pyramidal cells show occasional brief periods of activity surrounded by virtual silence.

The present study arises from observations that a third physiological state, differing from both theta and LIA, is revealed when hippocampal population activity patterns are inspected along with hippocampal EEG of the sleeping rat. During this state, the EEG becomes very low in amplitude, and a small subset of cells becomes active while the rest of the cells remain nearly silent; the same cells are usually active across long sequences of such episodes. This state occurs repeatedly within periods of SWS and immediately after every REM episode, but never just before REM. The EEG appears similar to a pattern that has been called "low-amplitude irregular activity" (Pickenhain and Klingberg, 1967), also called "small-amplitude irregular activity" or SIA (Vanderwolf, 1971; Whishaw, 1972; for review, see O'Keefe and Nadel, 1978). These early studies reported the presence of SIA in rats on occasions when an ongoing movement was abruptly stopped, or when they suddenly changed from a resting or sleeping state to an alert state (as indicated by neocortical desynchronization) without moving. Similar EEG states have also been reported in the sleeping rat, called "arousal-like periods" (Roldán et al., 1963) or "low-amplitude sleep" (Bergmann et al., 1987). Because the hippocampal physiology of the sleep state we observe is similar to that of SIA, but to distinguish the general physiological state from its more specific manifestation during sleep, we will refer to the episodes that occur during sleep as "Sleep-SIA" (S-SIA).

Our aim is to characterize the EEG, hippocampal population activity, and incidence of S-SIA relative to REM and LIA and to explore the possible functional significance of the cells active in S-SIA. Many hippocampal pyramidal cells have strong spatial correlates; each hippocampal "place cell" fires rapidly only when the rat is in a particular delimited portion of its environment, called its "place field" (O'Keefe and Dostrovsky, 1971; O'Keefe, 1976; for review, see O'Keefe and Nadel, 1978). The possibility that S-SIA is a state of heightened arousal suggests a possible functional correlate of the cells active during S-SIA: they might be cells with place fields in the current location of the rat. The correspondence between the cells active during

S-SIA and the cells with place fields in the "nest" (where the rat sleeps) is therefore assessed. Preliminary observations were reported by Skaggs (1995) and Jarosiewicz and Skaggs (1999).

2.3. MATERIALS AND METHODS

2.3.1. Subjects

Data were collected from six male Sprague-Dawley rats, weighing between 350 and 500 gm at the time of surgery. Each rat was housed individually in a 12-hour light/dark cycle in a temperature-controlled room with food and water available *ad libitum*. For approximately 1 week before surgery, each rat was handled and gradually accustomed to the recording room environment for several hours a day and was food-deprived to 80–95% of its *ad libitum* weight to motivate it to run for randomly-scattered food pellets so that recordings could be tracked between sleep and waking behavior. Recordings were made during the light phase of the cycle.

2.3.2. Surgery

All surgery was performed under sterile conditions. The rat was anesthetized with Equithesin (3 ml/kg, i.p.), and boosts of Metofane (inhalant) or additional Equithesin were given during surgery as necessary. Once deeply anesthetized, the rat was secured in earbars in a Kopf stereotaxic frame (David Kopf Instruments, Tujunga, CA). A small (~1 cm) incision was made along the midline of the scalp to expose the cranium. Skin and connective tissue were retracted, and five to six small holes were drilled into the cranium to accommodate jeweler's screws, one of which was later connected to a ground channel. Another larger hole was drilled over the right hippocampus (~2 mm diameter, centered on 3.5 mm posterior and 2-3 mm lateral from Bregma). The dura was retracted, and the exposed cortex was covered with sterilized petroleum jelly. The base of a "hyperdrive," which contained 12 individually drivable tetrodes and 2 single-channel reference/EEG electrodes all bundled to ~1.5 mm diameter at the base, was lowered toward the exposed cortex. The hyperdrive was cemented in place with dental acrylic, which was anchored to the cranium by the jeweler's screws. Just after surgery the tetrodes and reference electrodes were lowered ~680 μm toward the hippocampus and the wound was covered with antibiotic

ointment and a mild local anesthetic ointment. Over the next few days, the wound was cleaned and ointment was reapplied daily until the animal recovered. Tetrodes were gradually lowered over a few hours each day until they arrived at the hippocampal CA1 pyramidal cell layer (about 2 mm deep), which was identified by its well-characterized EEG and spike waveform characteristics (Ranck, 1973; Fox and Ranck, 1975, 1981; O'Keefe, 1976; O'Keefe and Nadel, 1978; McNaughton et al., 1983a; Buzsáki et al., 1992; Skaggs et al., 1996).

2.3.3. Electrophysiology and Recording

For data acquisition, the top of the hyperdrive was connected to a headstage containing pre-amplifiers and a ring of light-emitting diodes used for position tracking by a camera mounted on the ceiling over the recording chamber. The headstage was attached to a pair of soft, flexible cables, partially suspended by a counterweight system to help ease the load on the rat's head. The cables ascended through the ceiling of the recording chamber into the adjoining room, where they connected to the Cheetah recording system (Neuralynx, Tucson, AZ) consisting of eight 8-channel amplifiers with software-configurable high- and low-pass filters, feeding their output to a custom-made controller and analog-to-digital processor. During recording, signals from each channel of each tetrode were filtered to 600–6000 Hz, sampled at 32 KHz per channel, formatted, and fed to a Sun Ultrasparc 2 workstation (Sun Microsystems, Palo Alto, CA), running custom-written acquisition and control software. Each time the signal on any one of the tetrode channels crossed a specified threshold, a 1 ms sample of data from all four channels of that tetrode was written to disk, beginning 0.25 ms before the threshold was crossed, capturing the spike waveform on each channel along with its timestamp. An EEG was also recorded from one specified channel on each tetrode and from an EEG electrode near the hippocampal fissure, at a bandwidth of 1-100 or 1-500 Hz and a sampling rate of 2461 Hz. At the same time, position records containing information about the distribution of light across the video image were acquired at 60 Hz and written to disk. The rat's velocity was calculated off-line as the change in position two timestamps before and two timestamps after the current timestamp, divided by the elapsed time. The error of the tracker is approximately one-half the width of the ring of light-emitting diodes on the headstage, or 2.5 cm.

Cheetah recording software on a Sun workstation was used to monitor spike waveforms on each of the four channels of each of the twelve tetrodes and one EEG trace from each tetrode

and the EEG electrode, and an audio monitor could be used to listen to signals from any single channel. Once an adequate number of stable CA1 complex-spike cells were obtained and robust theta activity was visible on one of the EEG channels during locomotion, a recording session was performed. EEG signals, spike waveforms, and the position of the rat were recorded simultaneously while the rat either slept, ran for randomly scattered food pellets, or some sequential combination of the two. Approximately ten to thirty recording sessions ("data sets"), each on separate days, were performed for each animal, until damage from the tetrodes made cells difficult to find or until the animal otherwise became unusable, at which point the animal was humanely killed and its hyperdrive was removed for reuse.

2.3.4. Cell Isolation

Spike waveforms, EEG signals, and the rat's position data, along with their respective timestamps, were recorded onto disk during the recording session for off-line analysis. Spikes were assigned to individual cells by cluster-cutting in Xclust (written by M. Wilson, Massachusetts Institute of Technology, Cambridge, MA), which plots any two selected parameters (e.g. spike height, spike width, spike root-mean-square area, spike time, rat position, etc.) of all spikes recorded from that tetrode against one another as a scatterplot. For each tetrode in each data set, the experimenter drew polygons around clusters of spike parameter values in these various two-dimensional projections; ideally, each cluster in the multidimensional parameter space contained spikes from a single potential unit. Units were then judged to be complex-spike cells, theta cells (corresponding to pyramidal cells and interneurons, respectively) (Fox and Ranck, 1981), noise or chewing artifact, according to their waveforms, inter-spike interval histograms, spatial selectivity, etc.; only those units judged to be relatively clean, well-isolated complex-spike cells were included in further analysis.

2.3.5. Behavioral Task

In some data sets, recordings were performed only while the rats were asleep in a round bowl or small (25 x 20 cm) cardboard box lined with a towel (i.e. the nest). In others, the sleep session was preceded and/or followed by a run session, in which the rat ran around eating randomly scattered food pellets; the run sessions allowed cell activity to be compared across sleep and

waking states. The recording environment was either a square blue plastic table top (70 cm^2) surrounded by distant blue curtains containing four cues, or a round paper-covered plywood floor bounded by a large gray cylindrical wall (76 cm diameter, 50.8 cm tall) with a white card covering 90^o of arc on one side. The nest in these data sets was placed on the floor of the recording environment such that the rat could freely enter and exit the nest during the run session, allowing the possibility to be tested that the cells active in S-SIA had place fields in the nest.

2.3.6. Data Analysis

Delineation of sleep states. Sleep states were delineated into categories using two methods. The first method was entirely manual: plots containing rasters of all the simultaneously recorded spikes, at least one good EEG signal, and the rat's velocity were examined by the experimenter. LIA, REM, and S-SIA onsets and offsets were delineated by hand to the nearest 100 msec according to the following criteria: periods during which LIA was present in the EEG were classified as LIA; periods in which theta activity was present in the EEG and the rat was not moving were classified as REM; and periods in which SIA was present in the EEG and the population activity was sparse and fairly constant were classified as S-SIA. Periods in which theta was present in the EEG and the rat was moving were classified as waking.

To reduce the level of subjectivity in the delineation of sleep states, a more objective method was developed for some analyses that relied on the consistent structure of population activity across S-SIA episodes. The "mean S-SIA population activity vector" was constructed for each data set by calculating the mean firing rate for each cell during all of the hand-delineated S-SIA episodes in that data set. This vector was then compared with the population activity vector in each 500 msec time bin throughout the sleep period. Those time bins with a population activity vector that was highly correlated with the mean S-SIA population activity vector (with threshold $r = 0.6$ or 0.8, depending on the correlation histogram for that particular data set) were grouped into S-SIA and the rest were grouped into non-S-SIA. This method of sleep state delineation has coarser temporal resolution, but it has the advantage of being more objective. The correlation between the categorization of each 100 msec epoch of sleep in hand-delineated sleep states versus population activity correlation-delineated sleep states was on average 0.45 ± 0.064,

with the correlation-based delineation generally being more conservative than hand delineation in labeling a time period as S-SIA.

Sparseness. The population activity differences between S-SIA and the other hand-delineated sleep states were also quantified in terms of "sparseness" of population activity (Treves and Rolls, 1991), defined as the ratio $\langle \mathbf{r} \rangle^2 / \langle \mathbf{r}^2 \rangle$, where **r** is the vector of mean firing rates of the cells in a short interval of time. This ratio can also be written as $(1/N \times \Sigma r_i)^2 / (1/N \times \Sigma r_i^2)$, where r_i is the mean firing rate of the i^{th} cell over a given interval of time and N is the total number of cells. Thus, sparseness is 1 when all cells are active at the same firing rate, and approaches 0 when a very small fraction of cells are active and the rest are silent. When no cells are active, the sparseness is undefined. The mean sparseness was calculated for each of the hand-delineated sleep states (LIA, REM, and S-SIA) for each data set, using 500 ms time bins. Because S-SIA has a characteristic population activity profile in which a small percentage of cells are active, S-SIA was expected to have the lowest mean sparseness.

EEG total power. The difference in EEG between S-SIA and the other sleep states was quantified in terms of mean total power in the EEG signal for that state. Total power is the root-mean-square area under the curve; thus, the higher the amplitude of the EEG in a given time interval, the higher its total power. The mean total power was calculated for each hand-delineated sleep state (LIA, REM, and S-SIA) in each of the above data sets, and to verify that the differences in EEG power were not attributable to subjectivity in the delineation of sleep states, the total power in the EEG was also calculated for sleep states delineated solely by population activity correlations (non-S-SIA versus S-SIA). Because EEG amplitude varies with electrode depth, the power in hand-delineated S-SIA and REM was normalized by the mean power in LIA in its data set, and the power in correlation-delineated S-SIA was normalized by the mean power in non-S-SIA in its data set. Thus, powers were expressed as a proportion of the mean power during LIA or non-S-SIA. Because S-SIA has a flattened EEG relative to LIA and REM, it was expected to have the lowest mean power.

Incidence of S-SIA relative to REM. The incidence of S-SIA episodes relative to REM episodes was also examined to quantify the observations that S-SIA never immediately precedes a REM

episode (i.e. there is always some LIA before every REM episode), and that almost every REM episode is immediately followed by S-SIA. The first observation was quantified by cross-correlating the offsets of S-SIA episodes with the onsets of REM episodes in each data set, using 5 sec bins. Because S-SIA never occurs just before REM, S-SIA offsets were expected to never coincide with REM onsets, producing a *dip* in the cross-correlation just before and at 0. The second observation was quantified by cross-correlating the offset of REM with the onset of S-SIA over all the episodes in all the data sets. Because nearly all REM episodes were immediately followed by an S-SIA episode, REM offsets were expected to coincide with S-SIA onsets, producing a *peak* at 0 in the cross-correlation.

To reduce the level of subjectivity in the delineation of onsets and offsets of REM and S-SIA, these observations were also quantified by comparing the population activity before and after REM episodes with the mean S-SIA population activity vector. To quantify the incidence of S-SIA episodes over time before REM, the population activity for one min preceding each REM episode was divided into 5 sec bins, and the correlation between the population activity vector of each bin and the mean S-SIA population activity vector was calculated. (Because REM often evolves out of LIA gradually, the hand-delineated REM onset times were somewhat arbitrary; thus, there is still some subjectivity to this analysis.) To quantify the occurrence of S-SIA episodes immediately after REM episodes, the population activity for 30 sec after each REM episode was divided into 2 sec bins, and the correlation between the population activity vector of each bin and the mean S-SIA population activity vector was calculated. (The transition out of REM was always quite abrupt, so the REM offset times were more accurate.)

Population activity in S-SIA compared to awake behavior. To test whether the cells active during S-SIA were cells with place fields in the location in which the rat was sleeping, "correlation maps" were made using data sets in which a fairly long sleep session was recorded in the same data set as a run session, the rat entered the nest repeatedly during the run session, and abundant cells were tracked between the sleep and run sessions. A vector of the mean firing rate of each cell was constructed for each pixel in the environment (the "mean run population activity vector"). The "S-SIA population activity vector" was constructed in one of two ways: if the sleep states had been delineated previously by hand, then the mean of the population activity across all the episodes of S-SIA was used, as above. For the rest of the data sets, an idealized S-SIA

population activity vector was constructed: the raster of population activity was examined to determine which cells were S-SIA-active and which were not (these groups were fairly consistent across S-SIA episodes) and the population activity vector consisted simply of 1's for S-SIA-active cells and 0's for the rest of the cells (because the firing rates of the S-SIA-active cells in these data sets were fairly similar to one another, this approximation did not severely impair subsequent analysis because correlation coefficients are insensitive to scale). Then, for each pixel in the environment, the correlation coefficient between the S-SIA population activity vector and the mean run population activity vector was determined and the result was a "correlation map" of the population activities during the run session and S-SIA. Peaks in the correlation map correspond to locations in the environment in which the population activity during the run session most resembles the population activity during S-SIA. For instance, if the S-SIA-active cells are place cells with fields spanning the location in which the rat is sleeping, the peak of the correlation map should occur in the location of the rat's nest.

2.4. RESULTS

2.4.1. Structure of Population Activity and EEG in LIA, REM, and S-SIA

Consistent with the results of many previous studies (for review, see O'Keefe and Nadel, 1978), we find that, during SWS and drowsy waking states, the EEG at the level of the hippocampal fissure exhibits predominantly LIA with occasional sharp waves, often accompanied at the pyramidal cell layer by ripples. The population activity during LIA (Fig. 2.1*C*) is generally diffuse, with large increases of activity across the whole population during sharp waves. REM (Fig. 2.1*B*) resembles awake exploration (Fig. 2.1*A*) in both EEG and CA1 population activity: theta activity is present in the EEG, and individual cells occasionally show bursts of activity surrounded by silence, as when the rat is running through the place fields of recorded cells. However, we also observed in all animals the existence of a third physiological state, intermixed with LIA during all periods of SWS and following nearly every REM episode, in which the EEG abruptly becomes very low in amplitude for a few seconds and a small subset of cells (~3-5%) becomes very active while the rest of the cells remain nearly silent (Fig. 2.1*D*, 2.6*A,C,E,F*); the same subset of cells is usually active across many consecutive episodes (Fig. 2.1*D*,*E*, 2.6*A,E,F*).

Toward the end of these episodes, the active cells gradually decrease their activity and the EEG amplitude gradually increases, sometimes exhibiting some low-amplitude, low-frequency (type 2) theta, and often terminating abruptly with a sharp wave before returning to LIA (see Figs. 2.1*E*, 2.6*A,C,E*). The duration of episodes ranges from ~200 msec to many seconds. The EEG during this state most likely corresponds to the previously described "low-amplitude irregular activity" (Pickenhain and Klingberg, 1967), also called "small-amplitude irregular activity" or SIA (Vanderwolf, 1971; Whishaw, 1972). To distinguish the general physiological state of SIA from its more specific manifestation during sleep, we refer to the SIA that we observe during sleep as "Sleep-SIA" (S-SIA).

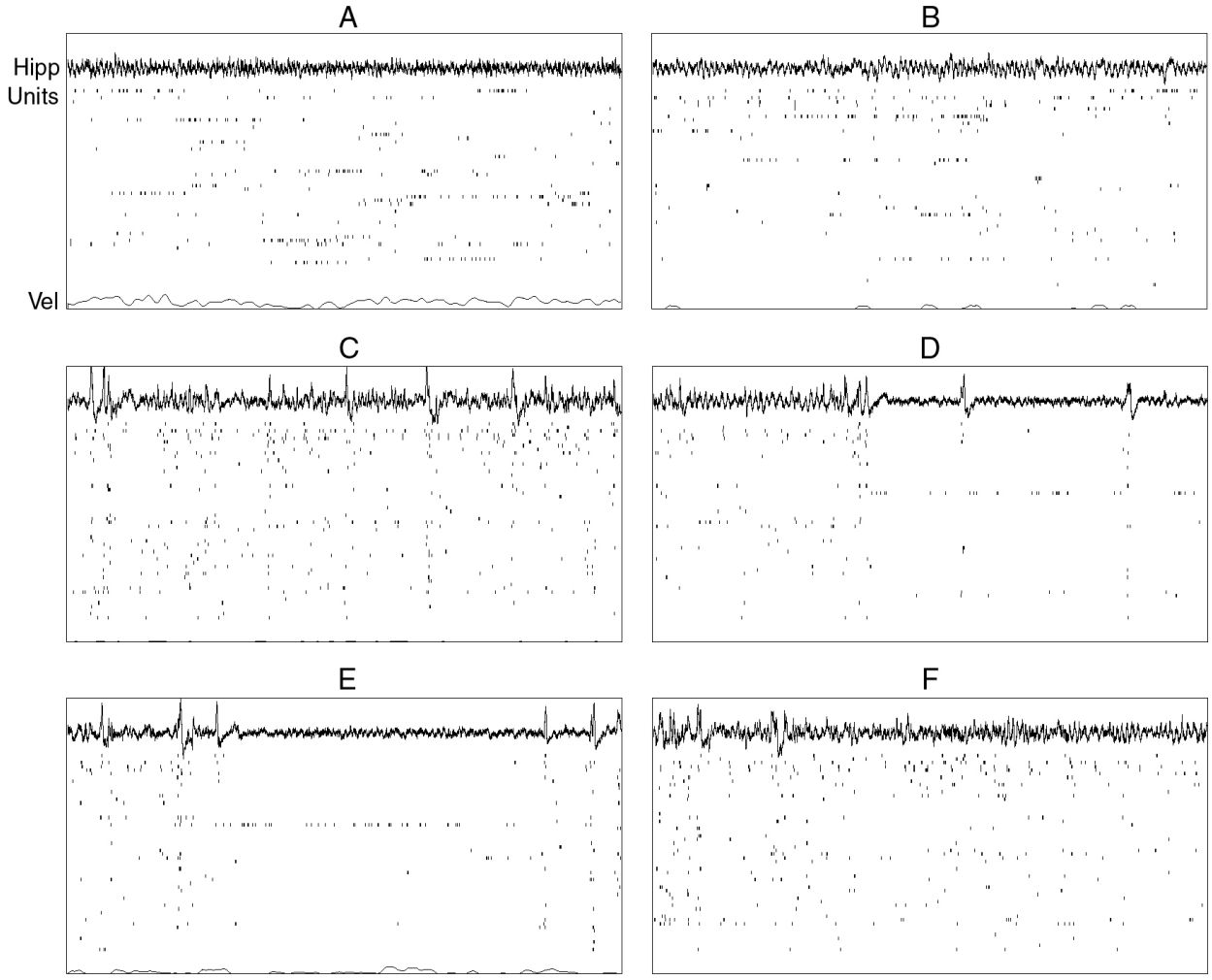

Figure 2.1. Hippocampal physiological states.

Fifteen second sample epochs from a single recording session (p119-03) showing EEG recorded near the hippocampal fissure (*Hipp*); a raster of spikes from the ensemble of 54 simultaneously recorded CA1 pyramidal

cells (*Units*); and the animal's velocity, with zero aligned at the bottom of the plot (*Vel*). *A*, Awake exploration of recording environment. Note the theta activity in the EEG trace, the population activity reflecting the place selectivity of the recorded cells, and the nonzero velocity, indicating movement. *B*, REM. Note the regular theta oscillation in the EEG and the characteristic population activity, both similar to run. The velocity trace is mostly 0, indicating lack of gross movement. (The occasional transients in the velocity traces are attributable to noise in the position data.) *C*, SWS. Note the large-amplitude irregular activity and occasional sharp waves in the EEG, corresponding, respectively, to periods of diffuse population activity and sudden increases in activity across the CA1 population. *D*, S-SIA emerging from a REM episode. Note the reduced-amplitude EEG and the unusual population activity profile, with a small percentage of cells continuously active and the rest nearly silent. During the two sharp waves, the population activity transiently increases. The transition into S-SIA is always quite abrupt, and often follows one or two sharp waves. *E*, A later episode of S-SIA, this time occurring within LIA during SWS. Note that the same subset of cells is active as in *D*. *F*, An example of the transition into REM, which always evolves gradually out of LIA.

2.4.2. Quantification of Population Activity and EEG Characteristics

The existence of repeating patterns of activity can be seen in population autocorrelation plots, in which each pixel shows the correlation of the population activity vectors at two points in time. Figure 2.2*A* shows such a plot, constructed from data recorded during 12 min of SWS; the red blocks are areas of high correlation, corresponding to S-SIA episodes. The fact that the level of red does not decrease outward from the diagonal indicates that S-SIA population activity patterns are strongly correlated across the entire 12 min. Indeed, similar plots made from much longer SWS periods often show the same level of correlation across time. Three data sets (p081-16, p121-01, and p121-04) contained S-SIA-active cells that could be followed between pre-run sleep and post-run sleep; out of the 13 such cells, 6 were active in both pre-run S-SIA and post-run S-SIA, and each of these data sets contained at least one cell that was active in both and one cell that was not.

For an initial examination of the relationship between population activity and EEG throughout sleep, episodes of LIA, REM, and S-SIA were delineated by visual inspection of EEG and CA1 population activity. In S-SIA, a small subset of cells is very active while the rest are nearly silent; this effect was quantified using sparseness of population activity. As described in Materials and Methods, sparseness is 1 when all cells are active at the same firing rate and approaches 0 when only a small fraction of cells are active; thus, S-SIA was expected to have a low average sparseness. The finding that the EEG flattens during S-SIA relative to LIA and REM was quantified using "total power" in the EEG, which is the root-mean-square amplitude; thus, S-SIA was expected to have a low total power. As an example, the sparseness of population activity and total power in the EEG were calculated for a single data set and a scatterplot was

constructed of sparseness versus EEG power for each 2 sec bin (Fig. 2.2*B*). Each point in the scatterplot was color-coded according to the hand-delineated sleep state that occupies at least one-half of the 2 sec period that the point represents. This data set exhibits a robust clustering corresponding to periods of LIA, REM, and S-SIA: LIA has high EEG power and high sparseness, REM has high EEG power and low sparseness, and S-SIA has low EEG power and low sparseness.

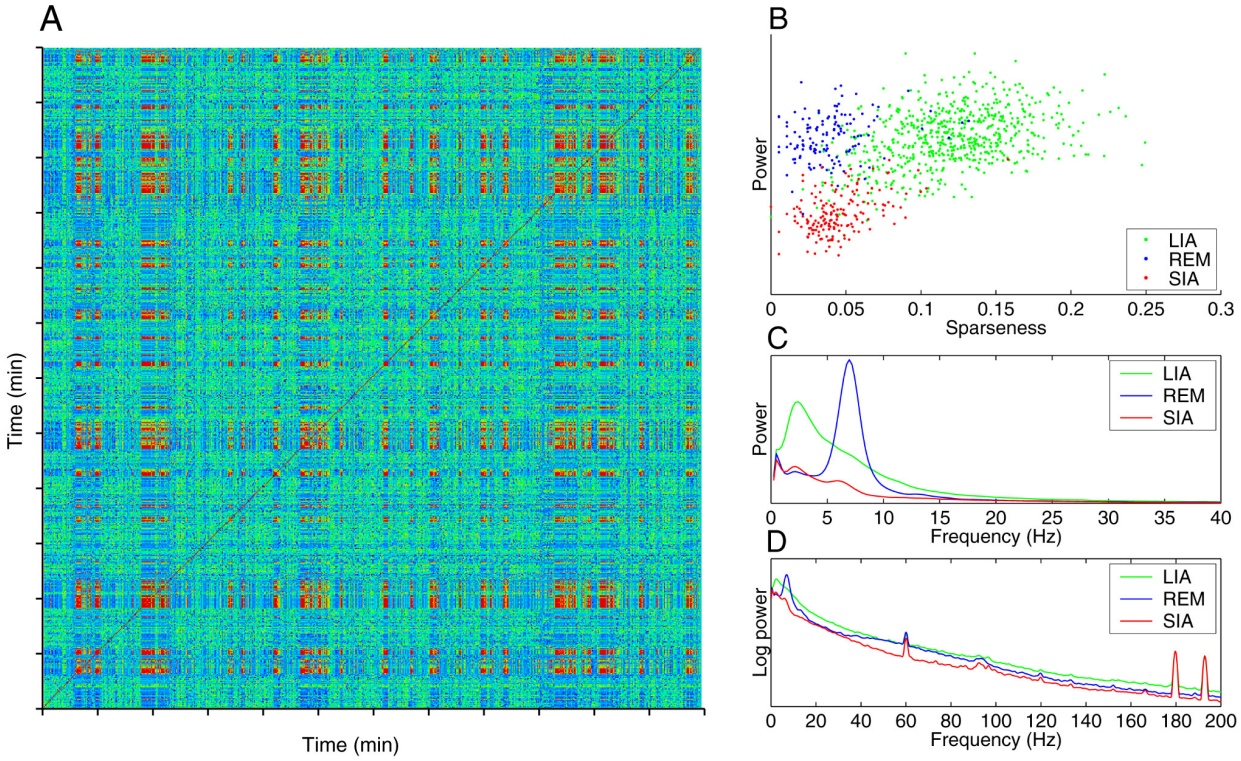

Figure 2.2. EEG and population activity structure of S-SIA.

A, Population activity vector autocorrelation matrix from a 12 min sample of SWS, using 500 msec bins (from data set p108-03). *Blue areas* correspond to low correlation values and *red areas* to high correlation values. The red blocks off the diagonal reveal highly consistent patterns of population activity occurring repeatedly throughout the 12 min time interval; these correspond to episodes of S-SIA. *B*, Scatterplot of sparseness versus EEG total power for each 2 sec epoch from the entire sleep period in data set p108-03. This data set exhibits a robust clustering corresponding to periods of LIA, REM, and S-SIA: LIA has high EEG power and high sparseness, REM has high EEG power and low sparseness, and S-SIA has low EEG power and low sparseness. Each point is color-coded according to the hand-delineated sleep state that occupies at least one-half of the 2 sec period that the point represents. *C*, *D*, Power spectra of hand-delineated sleep states. Power spectra were constructed using Welch's averaged, modified periodogram method, with a window size of 1 sec and sampling frequency of 492.2 Hz. Only episodes at least 2 second long were included in this analysis, totaling 1615.3 seconds of S-SIA, 1293.9 sec of REM, and 5749.9 sec of LIA. *C*, S-SIA has a lower power across the frequency spectrum than either LIA or REM. It has a small peak in the low-frequency (type 2) theta range (~ 6 Hz). REM shows a peak at type 1 theta frequency (~7 Hz), and LIA has a wide peak around 2-4 Hz and remains higher than REM and S-SIA across the spectrum. *D*, The same data are plotted against log power to reveal the power differences in the high frequencies. Again, S-SIA has a lower

power than LIA throughout the spectrum. REM has another peak around gamma frequency (35-90 Hz), which does not occur in LIA or S-SIA. The source of the peak near 90-95 Hz in all spectra is unknown. The sharp peaks at 60, 180, and 195 Hz are attributable to artifact.

EEG power spectra. To check for differences in the frequency content of the EEG in the different sleep states, power spectra were constructed for manually delineated LIA, REM, and S-SIA episodes (Fig. 2.2*C*,*D*) using five data sets from four different animals with good EEG signals, abundant cells including at least one S-SIA-active cell, and fairly long bouts of continuous sleep including at least one REM episode (data sets p094-04, p108-03, p119-03, p119-07, and p121-04). S-SIA had a lower power across the frequency spectrum than either LIA or REM, corresponding to its low amplitude, and had a small peak in the low-frequency theta range (~6 Hz), possibly corresponding to low-amplitude type 2 theta frequency, which was sometimes visible in the raw EEG toward the end of longer episodes (see Figs. 2.1*E*, 2.6*C,F*). REM showed a peak at type 1 theta frequency (~7 Hz), and LIA had a wide peak around 2-4 Hz and remained higher than REM and S-SIA across the spectrum.

Changes in mean population activity associated with S-SIA. In six data sets from five different animals (p094-04, p098-01, p108-03, p119-03, p119-07, and p121-04), contributing 157 hand-delineated S-SIA episodes of at least 3 sec duration, changes in population activity associated with S-SIA episodes were investigated by constructing perievent time histograms of the mean population activity surrounding the onset (Fig. 2.3*A*) and offset (Fig. 2.3*B*) of S-SIA episodes. The mean population activity transiently increased slightly at the onset of S-SIA episodes (Fig. 2.3*A*), which is probably the combined effect of the increase in activity across the entire population associated with the one or more sharp waves that often precede S-SIA episodes and the sudden burst of activity from the few S-SIA-active cells. The mean population activity then decreased into the episode as the S-SIA-inactive cells remained nearly silent and the S-SIA-active cells decreased their activity. These changes in mean population activity over time around S-SIA onset were highly significant (two-way ANOVA with 20 and 156 df; $F = 9.512$; $p<10^{-15}$). The mean population activity decreased in the last few seconds of S-SIA, reflecting a gradual decline of activity of the S-SIA-active cells near the end of the episode (Fig. 2.3*B*); the decline in the last 3 sec of S-SIA is not an artifact of averaging across long and short episodes, because only S-SIA episodes lasting ≥3 sec were used in this analysis. The population activity abruptly

increased again just after S-SIA offset, almost always being terminated by a sharp wave, and returned to baseline levels associated with LIA. These changes in population activity over time around S-SIA offset were highly significant (two-way ANOVA with 20 and 156 df; $F = 11.2$, $p < 10^{-15}$).

Sparseness. In five data sets from four different animals with good EEG signals, abundant cells including at least one S-SIA-active cell, and fairly long bouts of continuous sleep including at least one REM episode (data sets p094-04, p108-03, p119-03, p119-07, and p121-04), the sparseness of population activity of both hand-delineated sleep states and correlation-delineated sleep states was calculated across animals (Fig. 2.3*C,D*). These data sets contributed 1/33, 2/47, 2/57, 1/60, and 5/46 S-SIA-active/total recorded cells, respectively, for a total of 11/243 cells. Note that this ratio slightly overestimates the mean percentage of S-SIA-active cells because only data sets containing at least one S-SIA-active cell were used in this analysis; when those data sets with no S-SIA-active cells are taken into account, the average percentage of cells active in S-SIA was ~3%.

Because S-SIA has a characteristic population activity profile in which a small percentage of cells are continuously active and the rest are nearly silent, S-SIA was expected to have a low average sparseness. Using 500 msec time bins, the mean and SEM of the sparseness were calculated for hand-delineated LIA, REM, and S-SIA; these were 0.11 ± 0.01, 0.070 ± 0.010, and 0.053 ± 0.006, respectively (Fig. 2.3*C*). These means were significantly different (two-way ANOVA with 2 and 8 df; $F = 11.17$; $p = 0.0048$). *Post-hoc* paired *t* tests verified that the sparseness during S-SIA was significantly smaller than during LIA ($p = 0.016$), but it was not significantly different from REM. The difference between the sparseness in S-SIA and REM was not expected to be large because the cell activity during REM resembles that of awake exploration, during which cells are fairly silent most of the time but become active at fairly high rates when the rat enters their place fields. The mean and SEM of sparseness were also calculated for correlation-delineated non-S-SIA and S-SIA; these were 0.098 ± 0.008 and 0.054 ± 0.011, respectively (Fig. 2.3*D*). The sparseness during S-SIA was significantly smaller than during non-S-SIA (one-tailed *t* test, $p = 0.0059$). Note once again that the sparseness during S-SIA is probably slightly overestimated because only those data sets containing at least one S-SIA-active cell were used in these analyses.

EEG total power. The finding that the EEG flattens during S-SIA relative to LIA and REM was quantified using total power in the EEG, which is the root-mean-square of the EEG amplitude. The average total power was calculated for hand-delineated and population activity-delineated sleep states from the same data sets as those used in the sparseness analysis above. Because EEG amplitude varies with electrode depth, the total power was normalized by the mean total power during LIA in each data set. With the power during LIA set to 1, the mean relative power was 0.95 ± 0.08 during REM and 0.59 ± 0.04 during S-SIA (Fig. 2.3*E*). The LIA, REM, and S-SIA means were significantly different (two-way ANOVA with 2 and 8 df; $F = 19.63$; $p = 0.0008$). *Post-hoc t* tests verified that the total power in the EEG during S-SIA was significantly smaller than both LIA ($p = 0.00001$) and REM ($p = 0.0063$).

To verify that these differences in EEG power across sleep states were not attributable to experimenter bias during manual sleep-state delineation, the total power in the EEG was also calculated for sleep states delineated solely by population activity correlations. In each data set, the total power was normalized by the mean total power during non-S-SIA; thus, the power in the EEG during S-SIA was expressed as a proportion of the mean power of non-S-SIA in that data set. Indeed, the mean relative power during S-SIA was 0.83 ± 0.04 (Fig. 2.3*F*), which was significantly smaller than non-S-SIA (*t* test; $p = 0.0049$). Thus, the power in the EEG is significantly lower during S-SIA than during non-S-SIA, even when S-SIA episodes are defined by population activity patterns alone; this finding confirms that the differences in EEG power across sleep states are not attributable to experimenter bias during manual delineation of sleep states, and fortifies the claim that population activity patterns are consistent across long sequences of S-SIA episodes. In summary, LIA, REM, and S-SIA differ from one another in EEG power and sparseness of population activity in the following way: LIA has high EEG power and high sparseness, REM has high EEG power and low sparseness, and S-SIA has low EEG power and low sparseness.

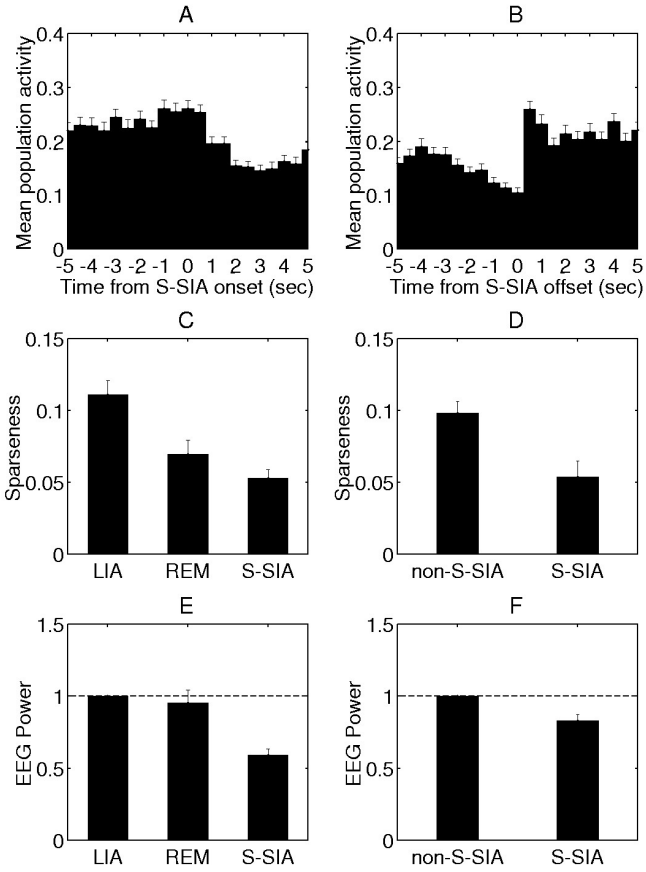

Figure 2.3. EEG and population activity structure of S-SIA, cont.

A, *B*, Changes in mean population activity associated with S-SIA. Peri-event time histograms were constructed for 5 sec windows around S-SIA onsets and offsets. The average firing rate of the population of recorded cells was calculated by dividing the total number of spikes across the population in each 500msec bin by the total number of cells in the population. Only episodes lasting >3 second were used in this analysis to ensure that any structure emerging in the 3 sec after S-SIA onset and before S-SIA offset reflected actual population activity changes within episodes rather than an artifact of averaging episodes of varying lengths. *A*, Peri-event time histogram of population activity aligned at S-SIA onset. The mean population activity slightly increases at the onset of S-SIA episodes, a combined effect of the increase in activity across the entire population associated with the one or more sharp waves that often precede S-SIA episodes and the sudden burst of activity from the few S-SIA-active cells. The mean population activity then decreases into the S-SIA episode as the S-SIA-inactive cells remain nearly silent and the S-SIA-active cells gradually decrease their activity ($F = 9.512$; $p<10^{-15}$). *B*, Peri-event time histogram of population activity aligned at S-SIA offset. The total population activity decreases as the activity of the S-SIA-active cells declines in the last few seconds of S-SIA and increases transiently just after S-SIA offset because sharp waves often terminate S-SIA episodes ($F = 11.2$, $p < 10^{-15}$). *C, D*, Sparseness = $\langle \mathbf{r} \rangle^2 / \langle \mathbf{r}^2 \rangle$, where **r** is the vector of mean firing rates of the cells, using 500 ms time bins. *C*, Sparseness in hand-delineated LIA, REM, and S-SIA episodes. The mean sparseness during S-SIA is significantly smaller than during LIA but is not significantly different from REM ($F = 11.17$; $p = .0048$). *D*, Sparseness in correlation-delineated sleep states (S-SIA and non-S-SIA). The mean sparseness during S-SIA is significantly smaller than during non-S-SIA ($p = 0.0059$). *E*, *F*, EEG total power, the root-mean-square area under the curve of the EEG, using 492.2 samples/sec. The *horizontal dashed lines* at EEG power = 1 represent the normalized power during LIA (*E*) and non-S-SIA (*F*). E, EEG total power in hand-delineated LIA, REM and S-SIA episodes, normalized by the total power in LIA in each data set. The mean total power in the EEG is significantly smaller in S-SIA than both REM and LIA ($F = 19.63$; $p = 0.0008$). *F*, EEG total power in correlation-delineated sleep states (non-S-SIA and S-SIA), normalized by the total power in non-S-SIA. The mean total power in the EEG is significantly smaller in S-SIA than in non-S-SIA ($p = 0.0049$).

2.4.3. Temporal Structure of S-SIA.

Duration and interepisode interval. In six data sets from five different animals with good EEG signals, abundant cells, and fairly long bouts of continuous sleep (p094-04, p098-01, p108-03, p119-03, p119-07, and p121-04), contributing 262 total hand-delineated S-SIA episodes, the temporal structure of hand-delineated S-SIA states was quantified in terms of duration of episodes and time interval between consecutive episodes. S-SIA is irregularly intermixed with LIA during periods of SWS (Fig. 2.4*A*), occupying 33.4 ± 6.6% of SWS and 20.6 ± 3.8% of total sleep. A typical S-SIA episode lasts ~2 sec, but the mean duration is higher (7.9 ± 0.6 sec) because of the positive skew of the duration histogram (Fig. 2.4*B*). Longer S-SIA episodes are interrupted every few seconds by sharp waves and an associated firing rate increase across the entire pyramidal cell population; thus, longer S-SIA episodes could also have been counted as a sequence of shorter S-SIA episodes. The mean interepisode interval is 36.9 ± 3.4 seconds, and its distribution is also positively skewed (Fig. 2.4*C*).

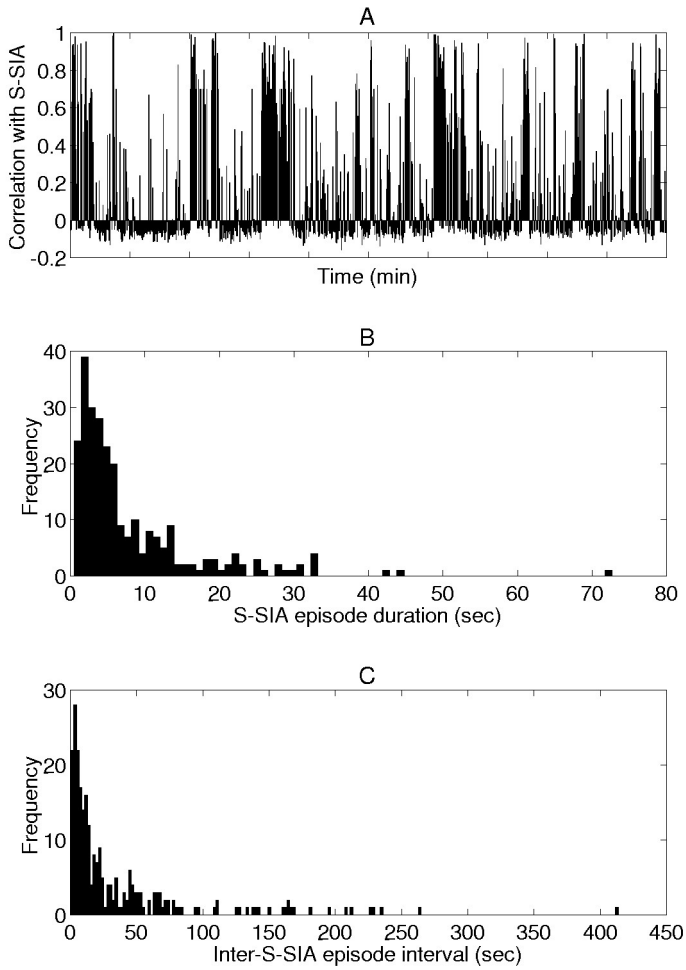

Figure 2.4. Temporal structure of S-SIA episodes.

A, Correlation of population activity with the mean S-SIA population activity vector in 500 msec bins during a 10 min interval of LIA from data set p108-03, showing the detailed structure of S-SIA episode occurrence. Periods of high correlation generally correspond to S-SIA episodes. Note that S-SIA is irregularly intermixed with LIA during periods of SWS. *B*, Histogram of S-SIA episode durations. The mean duration is 7.9 ± 0.55 sec, but shorter episodes are more frequent than long ones. Longer S-SIA episodes are interrupted every few seconds by sharp waves and could also have been counted as a sequence of short episodes. *C*, Histogram of inter-S-SIA episode intervals. The mean is 36.9 ± 3.42 sec, and its distribution is also positively skewed.

Relation to REM episodes. In five data sets from four different animals with good EEG signals, abundant cells including at least one S-SIA-active cell, and fairly long bouts of continuous sleep including at least one REM episode (data sets p094-04, p108-03, p119-03, p119-07, and p121-04), the incidence of S-SIA with respect to REM was analyzed. These data sets contributed 3, 5, 7, 7, and 2, REM episodes and 45, 33, 39, 41, and 36 S-SIA episodes, respectively, for a total of 24 REM episodes and 194 S-SIA episodes. S-SIA was never observed to immediately precede

REM, but it immediately followed nearly every REM episode. The first observation was quantified by cross-correlating the offsets of S-SIA episodes with the onsets of REM episodes in each data set (Fig. 2.5*A*); the dip in the mean cross-correlation histogram just before and at 0 illustrates that no S-SIA episodes immediately preceded any REM episodes in these data sets. The sec observation was quantified by cross-correlating the offset of REM with the onset of S-SIA over all the episodes in all the data sets (Fig. 2.5*B*); the peak at 0 illustrates that REM episodes were often immediately followed by S-SIA episodes.

To verify that these results were not purely due to the subjective delineation of onsets and offsets of both REM and S-SIA, these observations were also quantified by plotting the population activity correlations with the mean S-SIA population activity vector, a robust indicator of the presence of S-SIA, in the time periods before and after hand-delineated REM episodes. To quantify the decrease in S-SIA episodes over time before REM episodes, the population activity for 1 min preceding each REM episode was divided into 5 sec bins, and the correlation between each bin and the mean S-SIA population activity vector was plotted to verify that, on average, the correlation decreases over time (Fig. 2.5*C*). Because the number of REM episodes varied across data sets, correlation plots for all 24 REM episodes were used as independent observations in a two-way ANOVA rather than using the means for each data set. The decrease in the mean correlations across time bins was significant (two-way ANOVA with 12 and 276 df, $F = 2.509$, $p = 0.0038$), supporting the observation that S-SIA episodes become less and less frequent over the minute before a REM episode and rarely occur within seconds of REM. To quantify the observation that S-SIA episodes immediately follow most REM episodes, the population activity for 30 sec after each REM episode was divided into 2 sec bins, and the correlation between each bin and the mean S-SIA population activity vector was plotted (Fig. 2.5*D*). On average, the correlation with S-SIA just after REM is very high, indicating the robust presence of S-SIA episodes, and it decreases to baseline levels over the next few seconds, corresponding to the termination of the S-SIA episodes of various lengths. Again, the decrease in the correlation across time bins was significant (two-way ANOVA with 15 and 345 df, $F = 14.3$, $p < 10^{-15}$), supporting the observation that most REM episodes are immediately followed by S-SIA episodes.

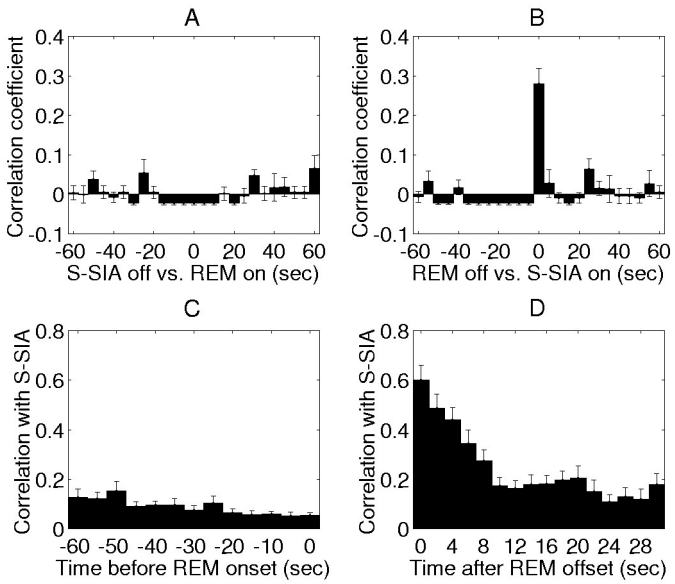

Figure 2.5. Incidence of S-SIA relative to REM.

Based on 24 REM episodes and 194 S-SIA episodes from 4 animals. *A*, Cross-correlation of hand-delineated S-SIA offsets versus REM onsets. The dip before and at 0 represents the observation that S-SIA episodes never occur just before REM episodes. *B*, Cross-correlation of hand-delineated REM offsets versus S-SIA onsets. The peak at 0 represents the observation that REM offsets frequently correspond to S-SIA onsets (i.e., that most REM episodes are immediately followed by an S-SIA episode). *C*, Mean correlation of population activity with S-SIA in 5 sec bins for one min preceding each REM episode. On average, the correlation decreases significantly over time ($F = 2.509$, $p = 0.0038$), demonstrating that the incidence of S-SIA, as determined by population activity correlations, decreases over time before REM episodes. *D*, Mean correlation of population activity with S-SIA in 2 sec bins for 30 sec after each REM episode. The peak just at REM offset and rapid decline in correlation with S-SIA ($F = 14.3$, $p < 10^{-15}$) demonstrate that REM episodes are often immediately followed by S-SIA episodes.

2.4.4. Functional Correlates of Population Activity in S-SIA

The cells active during S-SIA are otherwise physiologically indistinguishable from those not active during S-SIA (at least in terms of extracellularly observable properties); thus, the question arises as to whether S-SIA-active cells have any special functional correlates. Indeed, the population activity patterns during S-SIA appear similar to the population activity patterns that occur while the rat is awake and moving around inside the nest (Fig. 2.6*A,B*). Furthermore, when the rat changes its location within the nest and falls back asleep, the cells active while it moves sometimes change from one subset to another (i.e. the rat moves between place fields within the nest), and the cells active in subsequent S-SIA episodes change accordingly (e.g., Fig. 2.6*C-F*). Thus, the possibility is raised that S-SIA-active cells are cells with place fields encompassing the

location where the rat is sleeping; i.e. that S-SIA is a state of increased alertness in which the animal's location in the environment is represented in the brain.

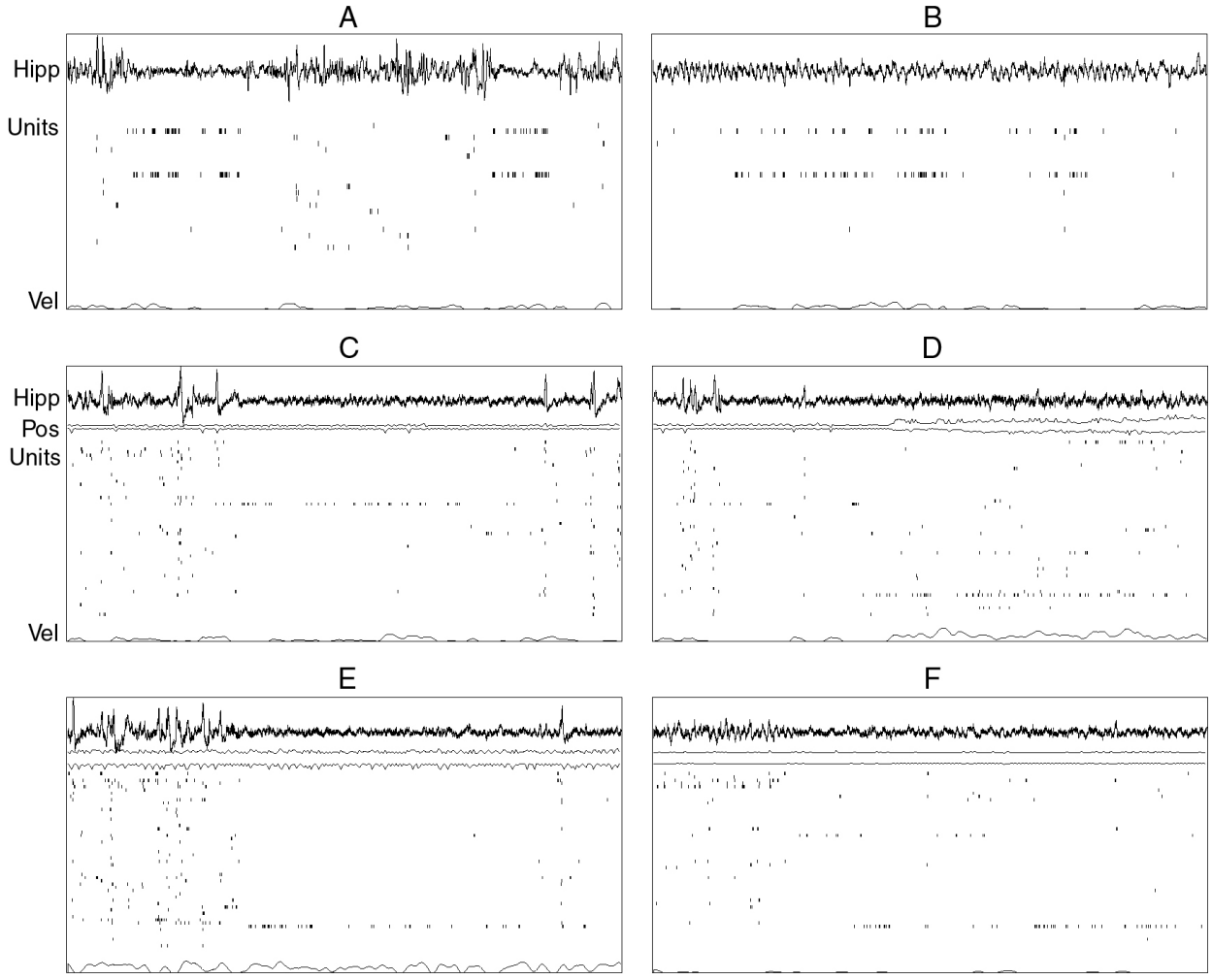

Figure 2.6. The population activity in S-SIA may reflect the rat's current location: raw data.

Time base = 15 sec. *A*, Two short S-SIA episodes within LIA. Note the flattening of the EEG and the characteristically sparse population activity. *B*, Later in the recording, the rat is awake and moving around inside the nest. Note that the same subset of cells that was active in S-SIA is active here. *C*-*F*, SIA-active cells change as the rat changes position in the nest (from p119-03). Same format as before, except now with two additional traces: the rat's *x* and *y* coordinates (*Pos*) are plotted as a function of time so that changes in the rat's location within the nest can be seen along with the raster. *C*, S-SIA while rat is in first location. Note the S-SIA-active cell. (This is the same period of time as Fig. 2.1*E*; another example of S-SIA from this recording can be seen in Fig. 2.1*D*.) *D*, The rat enters S-SIA and then wakes up and changes its location inside the nest; note that a different cell becomes active in this new location. *E*, An S-SIA episode shortly after the change in location. Note that the same cell that was active while the rat was awake in the new location is active in S-SIA. *F*, A later S-SIA episode. While the rat is sleeping in this new location, this new cell continues to be S-SIA-active.

To quantify the observation that S-SIA-active cells appear to have place fields in the location of the nest, correlation maps were made using six data sets from four different animals in which a good sleep session was recorded in the same data set as a run session, the rat entered the nest repeatedly during the run session, and at least one S-SIA-active cell was tracked between the sleep and run sessions (data sets p094-14, p116-05, p116-06, p119-03, p121-02, and p121-04). These data sets contributed 2/20, 3/45, 2/40, 2/44, 3/21, and 5/39 S-SIA-active/total recorded cells, respectively, that were tracked between run and sleep sessions (total: 17/209). For each pixel in the environment, the correlation coefficient between the S-SIA population activity vector and the mean population activity vector during run was determined, and the result was a correlation map (Fig. 2.7*A*). Peaks in the correlation map correspond to locations in the environment where the population activity during run most resembles the population activity during S-SIA. If the S-SIA-active cells are place cells with fields in the location in which the rat is sleeping, the peak of the correlation map should occur in the location of the rat's nest.

In the data set with the square environment (p094-14), the nest was a circular bowl in the center of the environment, and there was a clear peak in the correlation map in the nest (Fig. 2.7*A*, top left). In the round environments, the nest was a box in the lower right-hand corner of the environment. The mean of the correlation values in all of the pixels inside the nest versus in the environment outside of the nest was 0.44 versus –0.12, 0.17 versus 0.077, 0.46 versus 0.17, 0.17 versus 0.097, 0.26 versus 0.036, and 0.34 versus 0.028 for each data set, respectively, with a mean value across data sets of 0.31 ± 0.05 inside the nest versus 0.047 ± 0.040 outside the nest. To test the hypothesis that the mean correlation in the nest was greater than chance (0), the inside-nest means for each data set were compared to 0 using a one-tailed *t* test. The results were significant ($p < 0.001$), supporting the hypothesis that the activity during S-SIA resembles the place field activity inside the nest during run more than would be expected by chance. To rule out the possibility that the S-SIA-active cells were simply more active than other cells everywhere in the environment, which would increase the correlation values everywhere, the mean inside-nest correlation values were compared with the mean outside-nest correlation values. Indeed, the mean inside-nest correlation values were significantly greater than the mean outside-nest correlation values (two-way ANOVA with 1 and 5 df; $F = 12.54$; $p = 0.016$), supporting the hypothesis that S-SIA-active cells are more likely to have place fields inside the nest than outside the nest.

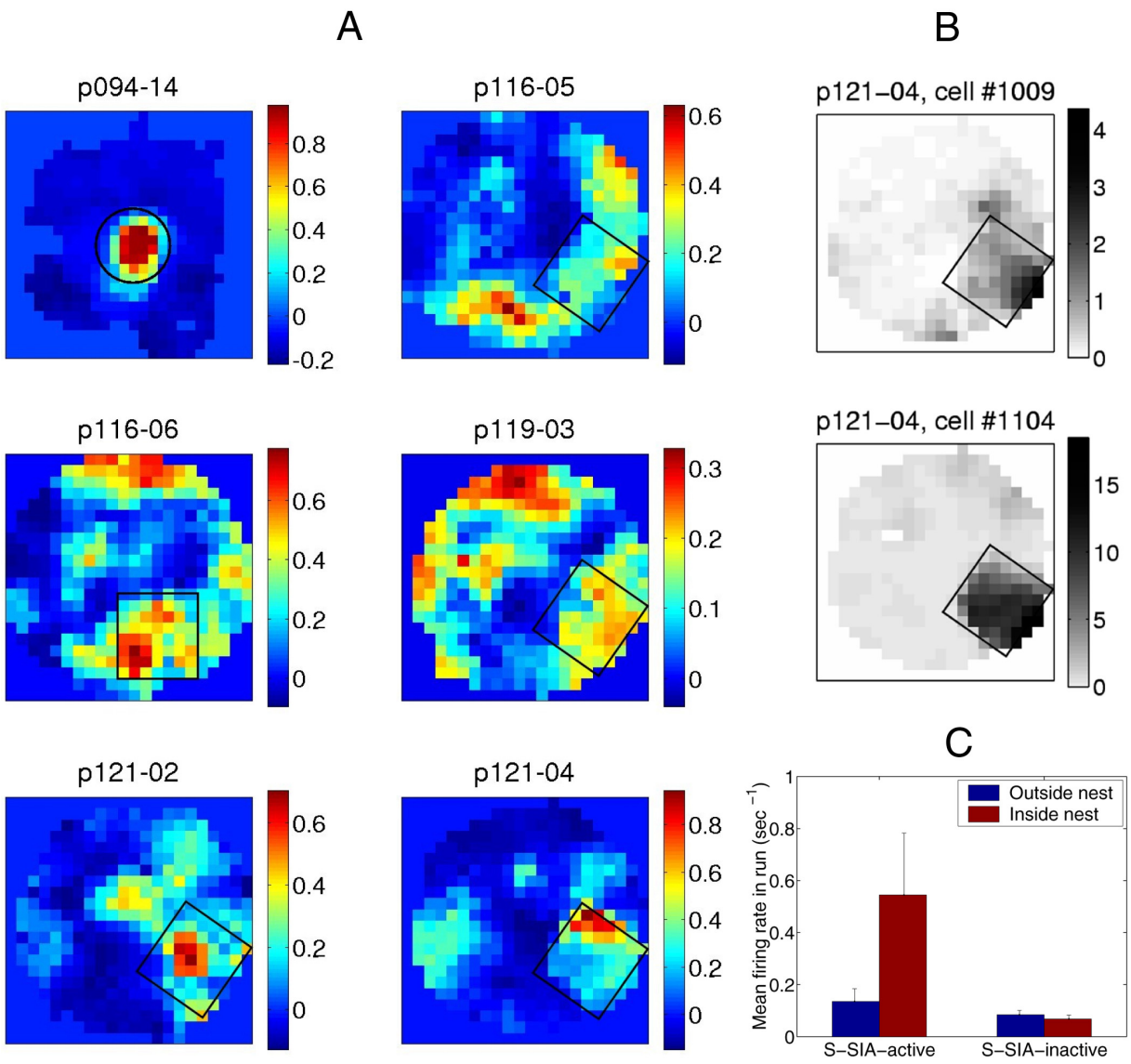

Figure 2.7. The population activity in S-SIA reflects the rat's current location: quantification across data sets.

A, S-SIA population activity correlation maps. For each data set, the correlation between the S-SIA population activity vector and the mean population activity vector during run was plotted for each pixel of the environment. *Blue areas* correspond to low correlation values and *red areas* correspond to high correlation values (as shown by the scales to the *right* of each map). The peaks correspond to places in the environment where the population activity during run most closely resembles the population activity during S-SIA. The location of the sleeping nest within the environment is shown in *black outline* for each data set. The nest in p116-06 is rotated and shifted toward the left with respect to the nest in the other round environments, because the rat pushed it there early in the run session. The mean correlation in the nest was greater than expected by chance ($p < 0.001$), supporting the hypothesis that S-SIA-active cells tend to have place fields extending into the location in which the rat is sleeping. The mean inside-nest correlation values were also significantly higher than the mean outside-nest correlation values ($F = 12.54$; $p = .016$), demonstrating that the place fields of S-SIA-active cells are significantly more likely to be inside the nest than outside the nest. *B*, Two examples of cells which were not active during S-SIA but whose place fields in the run session extended into the nest. *Black* corresponds to areas in the environment where that cell had a high firing rate, and *white* corresponds to areas where that cell had a low firing rate (as shown by the scales to the *right* of each map); the *black outline* again corresponds to the location of the nest. The mean firing rate during S-SIA of cell 1009 (*top*) is 0.16 sec^{-1} and that of cell 1104 (*bottom*) is 0.36 sec^{-1}; although these rates are toward the high end of S-

SIA-inactive cells in this data set, they are significantly lower than those of the 5 cells that were clearly active during S-SIA in this data set (mean = 1.83 ± 0.63 sec^{-1}; p = 0.002 and 0.0032, respectively). *C*, Mean firing rate of S-SIA-active and S-SIA-inactive cells outside and inside the nest during the run session. On average, cells that were S-SIA-active were more active inside the nest than outside the nest during run, and cells that were S-SIA-inactive were more active outside the nest than inside the nest during run. Paired 1-tailed *t* tests confirmed that both of these differences were significant (p = 0.03 and 0.02, respectively), supporting the hypothesis that the hippocampal population activity during S-SIA reflects the rat's awareness of its current location in space.

Although most of the correlation maps clearly had at least one peak inside the nest, sometimes the peaks extended outside the nest, and sometimes peaks occurred entirely outside the nest. The peaks outside the nest are attributable to S-SIA-active cells with multiple place fields, or, less frequently, S-SIA-active cells with place fields located entirely outside of the nest. The converse, cells with place fields extending into the nest that were not clearly S-SIA-active, were also observed occasionally (Fig. 2.7*B*). The factors that determine whether particular S-SIA-active cells will have place fields in the nest and whether particular cells with place fields in the nest will be S-SIA-active are as yet unclear. On average, however, cells that were S-SIA-active were more active inside the nest (mean firing rate = 0.54 ± 0.24 sec^{-1}) than outside the nest (mean = 0.13 ± 0.05 sec^{-1}) during run, and cells that were S-SIA-inactive were more active outside the nest (mean = 0.085 ± 0.017 sec^{-1}) than inside the nest (mean = 0.068 ± 0.014 sec^{-1}) during run (Fig. 2.7C). These means were significantly different (paired one-tailed *t* test, p = 0.03 and 0.02, respectively), supporting the hypothesis that the hippocampal population activity during S-SIA reflects the rat's current location in space.

2.4.5. Comparison of Population Activity in the S-SIA vs. Theta State

The following analyses were added to this Chapter after the publication of the article upon which it is based, using data sets from Chapters 3 and 4. The previous sections provided evidence that the hippocampal CA1 pyramidal cells show place-related activity during S-SIA, resulting in a population activity pattern resembling a pattern that might be expected if the theta state were frozen in time. The question thus arises whether the population activity in S-SIA is also similar to that of the awake theta state in features beyond those captured by the correlation coefficient of their population activity vectors. For example, correlation coefficients are scale-invariant, so a high correlation between the population activity vector from S-SIA and the population activity vector from that location in run does not imply that the level of activity is comparable between these states. To test whether the population activity vectors in S-SIA and

active waking were comparable in magnitude, the Euclidian lengths were calculated of the mean S-SIA population activity vector and the mean run population activity vector from the pixel of the environment in which the rat slept. The Euclidean length of a vector **x** is defined as $(x_1^2 + x_2^2 + \ldots + x_n^2)^{1/2}$, where x_i is the firing rate of cell *i*; thus, the higher the firing rates in the population, the larger the magnitude of the population activity vector. The run population activity vectors were found to have a significantly higher magnitude than the population activity vectors from S-SIA (2-tailed t-test; $p < 0.005$, based on 9 pairs of mean population activity vectors, one mean vector from baseline S-SIA and one from the pre-rotation run session from each of the 9 data sets used in Chapter 4). This difference may be partially accounted for by the fact that the run session contained periods of LIA, during which the population activity level is known to increase during sharp waves. But in any case, the firing rates of place cells during active waking are modulated by the rat's running speed (McNaughton et al., 1983a; Rivas et al., 1996; Czurkó et al., 1999; Hirase et al., 1999), so it is unclear how the level of activity during S-SIA, during which the rat is motionless, would be predicted to compare to the level of activity during active waking.

Another property of place-related activity during the theta state is that the spiking probability of CA1 pyramidal cells is modulated by the hippocampal theta rhythm (Buzsáki et al., 1983; Fox et al., 1986), a finding that has influenced the conception that place-related activity and the theta rhythm are functionally intertwined. Although there is little or no theta activity visible in the EEG during S-SIA, it is possible that there are subthreshold theta oscillations that modulate the probability of spiking. To test whether there is any residual theta modulation in S-SIA, despite the absence of overt theta activity, autocorrelograms were constructed of the spike trains from S-SIA-active cells and averaged across S-SIA episodes, and autocorrelograms of these cells' spike trains from the entire run session were constructed for comparison (Fig. 2.8). S-SIA-active cells were found to show normal theta modulation during active waking, but little or no theta modulation during S-SIA, demonstrating that place-related cell activity can occur in the absence of theta activity. Thus, although the hippocampal population activity during S-SIA shows place-related activity, it differs from the place-related activity present during the awake theta state in its total population activity level and in its lack of strong theta modulation.

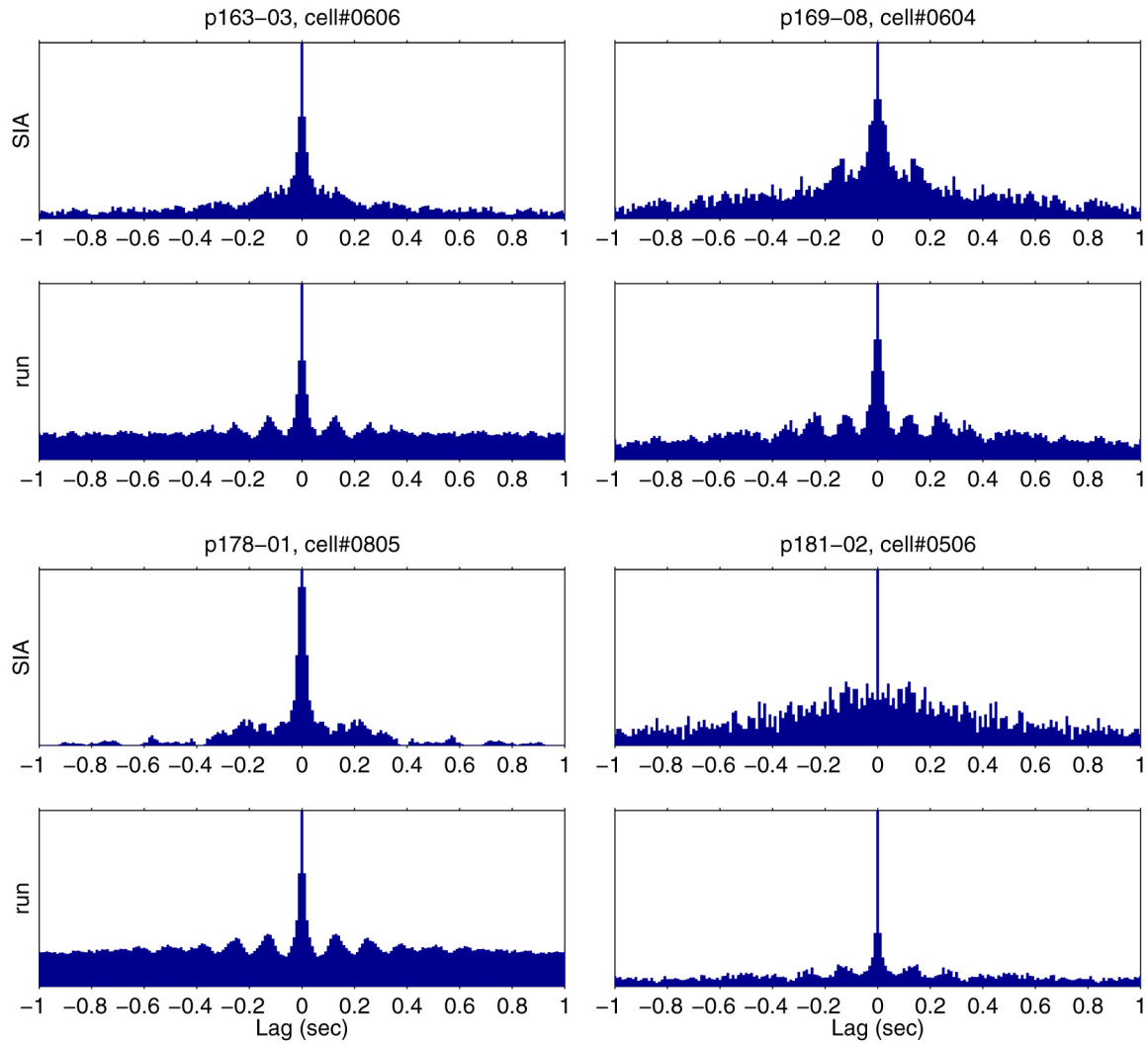

Figure 2.8. Autocorrelograms of S-SIA-active cells during S-SIA and run.

Cells that were active during S-SIA showed normal theta modulation during active foraging (*run*), as demonstrated by the periodic peaks at theta frequency in their autocorrelograms. During S-SIA (*SIA*), these cells did not exhibit the strong rhythmicity normally present during the theta state, although some slight low-frequency theta modulation may have been present. The left 2 S-SIA-active cells are taken from Chapter 3 data sets, and the right 2 from Chapter 4. The mean firing rates of these cells during S-SIA were 4.2, 4.0, 3.3, and 5.0 Hz, respectively for cells 0606, 0805, 0604, and 0506.

2.5. DISCUSSION

This study shows that SIA occurs frequently during sleep (S-SIA) in the rat and that hippocampal CA1 pyramidal cell activity during S-SIA is sparse, with the same subset of cells (3-5% of the total recorded population) active across long sequences of episodes. S-SIA episodes

are irregularly intermixed with LIA during periods of SWS, occupying ~33% of SWS and 20% of total sleep, usually lasting ~2 seconds but occasionally much longer, and occurring on average 30-44 seconds apart. Although the possibility has not been ruled out that S-SIA-active cells are a different morphological class of cells, this seems unlikely, because S-SIA-active cells are otherwise similar to ordinary complex-spike (pyramidal) cells: they are recorded in the same layer of the hippocampus as other complex-spike cells, they fire complex spikes, they often have place fields, and the subset of cells active during S-SIA can change over time. The population activity during S-SIA statistically resembles the population activity during waking states while the rat is in the location of the nest, and S-SIA-active cells sometimes change when the rat changes its position in the nest, suggesting that S-SIA is a state of heightened arousal during which the rat's current location in space is represented in the brain. Although the correspondence between cells that are active during S-SIA and cells with place fields in the nest is not perfect, it is significantly higher than expected by chance, supporting the hypothesis that the hippocampal population activity during S-SIA reflects the rat's awareness of its current location in space.

The findings that hippocampal CA1 pyramidal cells show place-related activity during S-SIA, and that S-SIA-active cells show little or no theta modulation during S-SIA, are novel and important in light of the growing confidence among hippocampal physiologists that place-related activity and the theta rhythm are functionally intertwined. For example, the findings that pyramidal cell spike times are modulated by the theta rhythm (Buzsáki et al., 1983; Fox et al., 1986), and that spikes advance to earlier phases of the theta cycle as the rat passes through a place field, a phenomenon termed "phase precession" (O'Keefe and Recce, 1993; Skaggs et al., 1996), have inspired numerous computational models of how the phase relationship of place cell spike timing might influence the properties of place-related activity and underlie the various forms of learning and memory that have been attributed to the hippocampus (e.g. Skaggs, 1995; Skaggs et al., 1996; Tsodyks et al., 1996; Wallenstein and Hasselmo, 1997; Sohal and Hasselmo, 1998; Jensen and Lisman, 2000; Huxter et al., 2003; Sato and Yamaguchi, 2003). Our finding that place-related CA1 cell activity also occurs during S-SIA with little or no theta modulation demonstrates a dissociation between place selectivity and theta activity, which will need to be considered in future models of hippocampal function.

In this study, S-SIA states were identified in two ways: by visual inspection and by correlation with the mean of the population activity vectors from the visually identified periods.

Neither of these methods is completely objective, although the latter is more so. There are several possible approaches toward a completely objective way of identifying SIA epochs, using for example the clustering observable in Figure 2.2*B* or the high interevent correlations observable in Figure 2.2*A*. In the present article, it was considered desirable to aim for the most precise possible separation of S-SIA from non-S-SIA states, but other approaches are certainly possible and may be more useful in future studies.

Despite the similar appearance of the EEG during S-SIA to the waking SIA state described in the literature (Pickenhain and Klingberg, 1967; Vanderwolf, 1971; Whishaw, 1972), there is as yet no definitive evidence that they are actually the same physiological state. A more direct test would be to purposely wake a sleeping rat with a controlled stimulus, in the spirit of Pickenhain and Klingberg (1967), and to test whether the elicited EEG and population activity profile coincides with that of spontaneous S-SIA episodes in that data set. Furthermore, one could startle the rat during a run session while it is outside of the nest to test whether SIA appears in the EEG and S-SIA-like population activity occurs, with the active cells now representing the rat's current location rather than the location of the nest. If so, these findings would provide evidence that S-SIA actually corresponds physiologically to the SIA state reported in the literature, and furthermore, that the population activity in both forms of SIA represents the rat's current location.

A related question is whether S-SIA is actually the same behavioral state as waking SIA. Is S-SIA a sleep state whose physiology resembles that of waking SIA, in the same way that REM is a sleep state whose physiology resembles waking theta, or is it actually a waking state that repeatedly interrupts sleep? There is no consensus in the literature on an absolute definition of sleep and waking, but several characteristics are used heuristically to distinguish whether an animal is asleep or awake: motion, EEG, EMG, etc. During LIA and theta activity, whether a rat is awake or asleep can be determined by whether or not it is moving. In the case of S-SIA, such an assessment is inconclusive, because rats are reported to be motionless during waking SIA as well. Our observations that S-SIA occurs so frequently within LIA during SWS (often within minutes of REM onset), that it consistently occurs just after REM, and that its occurrence during sleep is consistent across animals support the idea that S-SIA is a sleep state. Conversely, our findings that the hippocampal population activity during S-SIA reflects an awareness of self-

location and that S-SIA rarely occurs immediately before or during REM support the idea that S-SIA is a waking state.

Neocortical EEG might help shed some light on this issue, because it is often used along with hippocampal EEG to delineate physiological states (Green and Arduini, 1954; Pickenhain and Klingberg, 1967; O'Keefe and Nadel, 1978; Vanderwolf, 1969; Whishaw, 1972; Gottesmann, 1992). For example, Gottesmann (1992) divides the sleep-waking cycle of the rat into seven states; in both of the waking states, the neocortical EEG is desynchronized, and in all the sleep states, it is not, with the exception of REM, during which neocortical desynchronization is present despite behavioral evidence of sleep (he does not characterize SIA at all). According to Roldán et al. (1963) and Bergmann et al. (1987), neocortical desynchronization does occur during S-SIA. Although their finding supports the idea that S-SIA is a state of heightened neocortical arousal, it should not be treated as definitive evidence that S-SIA is a waking state, because neocortical desynchronization also occurs during REM, a sleep state. Thus, the desynchronization of neocortical EEG during S-SIA does not distinguish whether S-SIA is a waking state or simply another "paradoxical" sleep state of heightened neocortical arousal.

EEG-based criteria were developed as a secondary, post hoc measure of behavioral state transitions; perhaps EMG, a measure of muscle tone, would be more useful in distinguishing sleep and waking states, because it directly measures behavioral phenomena that originally motivated the conception of this dichotomy. In Gottesmann's (1992) characterization, all of the waking states exhibit higher-amplitude EMG signals, evidencing more muscle tone, than any of the sleep states; again, Gottesmann did not characterize SIA. Bergmann et al. (1987) did record EMG during S-SIA, finding it to be very low; they called this state "low-amplitude sleep," basing the "sleep" part of their terminology on its low EMG amplitude. However, they also report observing low EMG amplitude in a waking state that fulfills their EEG criteria for SIA; thus, their data also fail to resolve whether S-SIA is a waking or a sleep state. The literature on neocortical EEG, then, suggests that S-SIA should be thought of as a waking state, and the literature on EMG suggests that S-SIA should be thought of as a sleep state; neither result provides a conclusive answer. It would be useful to compare the neocortical EEG and EMG profiles more systematically between waking SIA, elicited S-SIA, spontaneous S-SIA, and the other behavioral states; perhaps a systematic study could shed more light on this issue.

A third possibility to consider is that S-SIA (indeed, possibly all manifestations of SIA) is neither distinctly a sleep or waking state; instead, it might fall somewhere toward the middle of a continuum of levels of arousal. Such a continuum appears to exist, for instance, in humans, in whom the transition from waking to sleep is more accurately depicted as an interval of time rather than an instant, when both EEG and behavioral responsiveness are taken into account (Ogilvie and Wilkinson, 1988). Furthermore, during normal sleep in humans, transitory states of heightened arousal exist, lasting on the order of seconds to tens of seconds and occurring every 4-5 minutes, called "phases d'activation transitoire" (Schieber et al., 1968, 1971; Ehrhart and Muzet, 1974) or "micro-arousals" (Halász et al., 1979; for review, see Terzano et al., 1991). These resemble arousal in EEG, EMG, and heart rate; they are often accompanied by shifts in posture or other movements; they occur more frequently during "lighter" stages of sleep than "deeper" stages; and they can be elicited by auditory stimuli, supporting the idea that they are states of increased arousal. Conversely, eliciting a large number of them seems to reduce the number of spontaneously occurring ones, so that their total incidence throughout the night is preserved (Ehrhart and Muzet, 1974); they do not reset the sleep cycle; and they are rarely recalled by the sleeper upon awakening, supporting the idea that they are nevertheless a natural part of sleep. These micro-arousals are likely to be the human analogue of S-SIA; like micro-arousals, perhaps S-SIA episodes are simply transient states of relatively heightened arousal that occur during normal sleep.

What, then, is the functional significance of SIA? Perhaps the most reasonable suggestion, based on the available evidence, is that SIA is a state in which the animal takes in and processes information from the sensorium without immediately acting on it. In contrast, the theta state occurs when information is actively used to guide ongoing locomotor behavior, and the LIA state occurs when information from the sensorium is either ignored or at least less deeply processed than in the other states. This study shows that SIA is not, as might have been thought, a rarely occurring curiosity but rather is comparable in prevalence to the LIA and theta states, and it provides a compelling functional correlate of its neural activity.

Chapter 3. LEVEL OF AROUSAL DURING THE SMALL IRREGULAR ACTIVITY STATE IN THE RAT

3.1. PREFACE

This chapter is based on a manuscript recently submitted to Journal of Neurophysiology. Various different methods of assessing an animal's arousal level were discussed in Section 1.1. In this Chapter, two of those measures are employed to assess the level of arousal during SIA. The first is EMG amplitude, which has the most direct association with the "obvious" behavioral assessment of an animal's arousal level. The second is neocortical EEG, in which desynchronization is commonly taken to be a sign of cognitive arousal. Neocortical EEG is not a perfect measure of arousal level, because it is present in both classically defined wakefulness and in REM sleep; nevertheless, it is a very common measure that has been characterized for the other physiological states, and characterizing it for SIA would be useful to at least complete our understanding of the similarities and differences across physiological states. Additionally, two other factors speak to the issue of arousal level in SIA. One relates to the finding that a visually similar hippocampal EEG state can be elicited by playing auditory stimuli during REM or SWS (Pickenhain and Klingberg, 1967; Vanderwolf, 1971; Whishaw, 1972). This Chapter shows that SIA elicited by an auditory stimulus during sleep has the same EEG, EMG, and cell activity profile as spontaneously occurring SIA, suggesting that spontaneous SIA is also a state of heightened arousal relative to REM and SWS. The other factor is the finding that the population activity during SIA reflects the rat's awareness of its current sleeping location. Chapter 5 shows that this population activity does not reflect the processing of incoming sensory information, but rather a memory for the location in which the rat fell asleep. This finding suggests that SIA is not as high a state of arousal as the active theta state, during which current sensory information does affect the rat's assessment of its current location in space. We conclude that the level of arousal during SIA lies somewhere between classically defined sleep and waking, sharing characteristics with both.

3.2. INTRODUCTION

Three physiological states have been recognized in the rat hippocampus, generally known as the *theta*, *large irregular activity* (LIA), and *small irregular activity* (SIA) states, after the type of EEG associated with each. The properties of these hippocampal states and their relationship to global physiological states are summarized in Table 3.1. The literature on theta and LIA in the rat is quite extensive; in contrast, the literature on SIA is relatively scarce. Perhaps the main reason for this is that when EEG alone is examined, SIA appears, mainly during sleep, in frequent but brief (~2 sec) flattenings of the voltage trace. Given the overall complexity of the EEG, the importance of these events is not obvious. However, when rasters of substantial numbers of simultaneously recorded CA1 pyramidal cells are added to the picture, the distinctiveness of the SIA state becomes very clear (Skaggs, 1995; Jarosiewicz and Skaggs, 1999, 2001; Jarosiewicz et al., 2002; see also Fig. 3.1). SIA is characterized by a sparse pattern of population activity, in which a small subset (~3-5%) of pyramidal cells shows continuous activity while the rest are nearly silent. Moreover, the same group of cells is usually active across long sequences of SIA episodes. Jarosiewicz et al. (2002) showed that the SIA-active cells largely correspond to place cells whose place fields encompass the location where the rat sleeps, suggesting that SIA might be a state of increased arousal.

The literature provides some additional support for such a suggestion. Pickenhain and Klingberg (1967) reported a "low-amplitude irregular activity" in the hippocampus of rats in response to novel or unfamiliar stimuli when no orienting movements are made; e.g., when a click awakens them from sleep. Vanderwolf (1971) and Whishaw (1972) reported a similar suppression of hippocampal activity, which they called SIA, when rats suddenly arrest voluntary movement or change from a resting or sleeping state to an alert state, as indicated by neocortical desynchronization, without moving. Other groups of researchers have reported similar EEG states during sleep: Roldán et al. (1963) observed "arousal-like periods" of EEG desynchronization in both neocortex and hippocampus at the end of REM and sometimes during SWS, similar to the state they observed when the rat is startled out of sleep. Bergmann et al. (1987) reported the existence of "low-amplitude sleep," characterized by low hippocampal and cortical EEG amplitude and low EMG amplitude, similar to a state they observed when the rat is startled while awake. Both "arousal-like periods" and "low-amplitude sleep" probably correspond to Vanderwolf's SIA; we have chosen to adopt Vanderwolf's terminology.

The aim of the current study was to determine whether spontaneous and arousal-elicited SIA correspond to a single physiological state, and to characterize the level of arousal during SIA. There is no consensus in the literature on an absolute definition of arousal level, but EMG amplitude and neocortical EEG are commonly used heuristic measures: EMG amplitude is higher in the well-characterized waking states than the well-characterized sleep states (Gottesmann, 1992), and neocortical desynchronization is often interpreted as an indication of arousal (Pravdich-Neminsky, 1913; Berger, 1929; Moruzzi and Magoun, 1949; Green and Arduini, 1954; Pickenhain and Klingberg, 1967; O'Keefe and Nadel, 1978; Vanderwolf, 1969; Whishaw, 1972; Gottesmann, 1992). Thus, we recorded and characterized the neocortical EEG and EMG, in addition to hippocampal EEG and CA1 ensemble activity, of spontaneous SIA and of SIA elicited by auditory stimuli during sleep and waking, and compared them to the other well-characterized sleep and waking states.

Table 3.1. Global physiological states in the rat.

State	Hippocampal EEG	Neocortical EEG	Hippocampal population activity
Active waking[1]	Theta	Desynchronized	Place-related
Quiet waking[2]	LIA	Desynchronized	Place-related activity strongly degraded; mostly diffuse, with increases in activity during sharp waves
Slow-wave sleep[3]	LIA	Slow waves, spindles	Diffuse, increase in activity during sharp waves
Intermediate sleep[4]	Theta	Slow waves, spindles	Diffuse, begins to resemble active waking
REM[5]	Theta	Desynchronized	Resembles active waking
SIA[6]	SIA	Desynchronized	Place-related

For reviews, see O'Keefe and Nadel, 1978; Gottesmann, 1992; Skaggs and McNaughton, 1998.
[1] Green and Arduini, 1954; Gottesmann, 1964; Vanderwolf, 1969; Vanderwolf et al., 1975; O'Keefe and Dostrovsky, 1971; O'Keefe, 1976.
[2] Kubie et al., 1985; Buzsáki et al., 1986, 1992; Foster et al., 1989.
[3] Buzsáki et al., 1986, 1992; Gottesmann, 1964; Steriade et al., 1993; McCormick and Bal, 1997; Siapas and Wilson, 1998.
[4] EEGs: Gottesmann, 1973; Hippocampal population activity: B. Jarosiewicz, unpublished observations.
[5] Rapid eye movement sleep, corresponding in humans to dream sleep (Dement and Kleitman, 1957a,b); Louie and Wilson, 2001.
[6] Pickenhain and Klingberg, 1967; Vanderwolf, 1971; Whishaw, 1972; Roldán et al., 1963; Bergmann et al., 1987; Jarosiewicz and Skaggs, 1999, 2001, 2002; Jarosiewicz et al., 2002.

3.3. MATERIALS AND METHODS

3.3.1. Subjects

Data were collected from 8 male Sprague Dawley rats, weighing between 350 and 500 gm at the time of surgery. Each rat was housed individually in a 12 hr light/dark cycle in a temperature-controlled room with food and water available *ad libitum*. For 1-2 weeks before surgery, each rat was handled and gradually accustomed to the recording room environment for several hours a day, and food-deprived to about 95% of its *ad libitum* weight to motivate it to forage for randomly scattered sweetened food pellets so that recordings could be tracked between sleep and waking behavior. Recordings were made during the light phase of the cycle.

3.3.2. Behavioral Apparatus

Recordings were performed while rats slept or foraged for randomly scattered food pellets. Both behaviors took place on a circular vinyl-covered platform arena (~1.5 m dia.) with a 40 cm tall transparent border around the edge. The arena was located inside a sound-attenuated room with visual cues on the walls, and a computer speaker was placed underneath the arena for administering auditory stimuli. To prevent habituation, variable auditory stimuli were chosen from a set of 102 different computer game and Microsoft Windows OS audio files, varying in duration (1-2 sec) and amplitudes, and each played only once for a given rat. The speaker volume was generally held constant across rats, but if on any given recording day a rat was repeatedly awakened by the stimuli to the point of walking around, the volume was turned down and the sleep session was restarted. During active foraging ("run") sessions, the volume was set higher but still within a range comfortable to the human ear; the rats rarely showed any responses to these stimuli. Stimuli were played at pseudorandom intervals averaging 2 minutes apart, typically yielding 15 stimuli per sleep or run session. Stimuli during the sleep session were postponed as necessary to ensure they occurred following at least 10 seconds of continuous sleep (SWS or REM). The onsets and offsets of these stimuli were automatically flagged by the data acquisition software. We found that computer-generated stimuli were ineffective in causing rats to freeze during the run session, so in later rats, we manually generated auditory/visual stimuli that were known to make rats freeze. These included tearing a piece of paper, opening an

umbrella, crinkling a can, nudging the wastebasket along the floor, dropping a pen, etc. These events were flagged manually, and thus not as precisely as the computer-generated auditory stimuli.

3.3.3. Surgery

All surgery was performed under sterile conditions. Rats were anesthetized with ketamine (60 mg/kg, i.p.) and xylazine (6 mg/kg, i.p.), and boosts of ketamine and xylazine were given during surgery as necessary. Once deeply anesthetized, the rats were secured in earbars in a Kopf stereotaxic frame (David Kopf Instruments, Tujunga, CA). A small (~1 cm) incision was made along the midline of the scalp to expose the cranium. The skin and connective tissue were retracted, and seven small holes were drilled into the cranium to accommodate jeweler's screws, one of which was later connected to a ground channel.

A small hole was drilled over the frontal cortex (~1 mm dia., centered on 2 mm anterior, 2 mm lateral from bregma) to accommodate a bipolar neocortical EEG recording electrode, consisting of a twisted pair of 0.0045" (coated) stainless steel wires with ends spaced 2 mm apart vertically. The EMG electrode, consisting of a twisted pair of 0.0045" (coated) stainless steel wires, each with 1mm exposed at the tip and bent 2 mm back to form a hook, was inserted into the dorsal neck musculature by routing it under the skin from the incision. A few square 10 mA pulses of 1 ms duration were passed through the EMG electrodes at 1 Hz using a stimulus isolation unit and a Grass S88 stimulator to check for muscle twitch, to ensure proper placement of the wires. Another larger hole was drilled over the right hippocampus (~2 mm diameter, centered on 3.5 mm posterior, 2-3 mm lateral from bregma). The dura was retracted, and the exposed cortex was covered with sterilized petroleum jelly. The base of a "hyperdrive," which contained 12 individually drivable tetrodes and two single-channel reference/EEG electrodes all bundled to ~1.5 mm diameter at the base, was lowered toward the exposed cortex. In addition, a small hole was drilled at 0.5 mm anterior, 4.0 mm lateral from bregma to accommodate a 26 gauge guide cannula (Plastics One, Roanoke, VA), which entered the brain at a 30 degree angle ML, its tip inserted to within 1 mm of the medial septum/diagonal band of Broca. These cannulae were used for microinfusion studies not reported in this paper; no animal received infusions before or during data collection for the studies reported here. All implants were cemented in place with dental acrylic, which was anchored to the cranium by jeweler's screws.

Just after surgery, the tetrodes and reference electrodes were lowered ~680 μm toward the hippocampus, and the wound was covered with antibiotic ointment and a mild local anesthetic ointment. Over the next few days, the wound was cleaned and ointment was reapplied daily until the animal recovered. Tetrodes were gradually lowered over a few hours each day until they arrived at the hippocampal CA1 pyramidal cell layer (~2 mm deep), which was identified by its well-characterized EEG and spike waveform characteristics (Ranck, 1973; Fox and Ranck, 1975, 1981; O'Keefe, 1976; O'Keefe and Nadel, 1978; McNaughton et al., 1983a; Buzsáki et al., 1992; Skaggs et al., 1996).

3.3.4. Electrophysiology and Recording

For data acquisition, the top of the hyperdrive was connected to a headstage containing preamplifiers and a ring of light-emitting diodes used for position tracking by a camera mounted on the ceiling over the recording chamber. The headstage was attached to a pair of soft, flexible cables, partially suspended by a counterweight system to help ease the load on the rat's head. The cables ascended through the ceiling of the recording chamber into the adjoining room, where they connected to the Cheetah recording system (Neuralynx, Tucson, AZ), consisting of eight 8 channel amplifiers with software-configurable high- and low-pass filters, feeding their output to a custom-made controller and analog-to-digital processor. During recording, signals from each channel of each tetrode were filtered to 600-6000 Hz, sampled at 32 kHz per channel, formatted, and fed to a Windows NT system (Neuralynx, Inc., Tucson, AZ) running custom-written acquisition and control software. Each time the signal on any one of the tetrode channels crossed a specified threshold, a 1 msec sample of data from all four channels of that tetrode was written to disk, beginning 0.25 msec before the threshold was crossed, capturing the spike waveform on each channel along with its timestamp. Continuous recordings of EEG signals were also obtained from one channel on each tetrode, from an EEG electrode near the hippocampal fissure, from an EEG electrode in the prefrontal cortex, and from an EMG electrode in the dorsal neck musculature, at a bandwidth of 1-475 Hz (EEGs) or 100-475 Hz (EMG) and a sampling rate of 999 Hz. At the same time, position records containing information about the distribution of light across the video image were acquired at 60 Hz and written to disk. The rat's velocity was estimated as the change in position two timestamps before and two timestamps after the current

timestamp, divided by the elapsed time. The error of the tracker is approximately one-half the width of the ring of light-emitting diodes on the headstage, or 2.5 cm.

Once an adequate number of stable CA1 complex-spike cells were obtained and robust theta activity was visible on the hippocampal EEG electrode during locomotion, a recording session was performed. EEG and EMG signals, spike waveforms, and the position of the rat were recorded simultaneously while the rat slept, ran for randomly scattered food pellets, or performed some sequential combination of the two. Approximately 10-30 recording sessions ("data sets"), each on separate days, were performed for each animal, until damage from the tetrodes made cells difficult to find or until the animal otherwise became unusable, at which point the animal was humanely killed and its hyperdrive was removed for reuse.

3.3.5. Cell Isolation

Spike waveforms, EEG and EMG signals, and the rat's position data, along with their respective timestamps, were stored onto disk during the recording session for off-line analysis. Spikes were assigned to individual units by automated cluster-cutting software (Klustakwik, K. D. Harris), and clusters were then manually verified and cleaned using Mclust (A. D. Redish, current address, University of Minnesota, Minneapolis MN). Isolated units were then judged to be pyramidal cells or interneurons (Fox and Ranck, 1981), or artifact, according to their average waveforms, autocorrelograms, interspike interval histograms, etc.; only those units judged to be relatively clean, well-isolated pyramidal cells were included in further analysis.

3.3.6. Sleep State Delineation

Physiological states were delineated in 500 ms bins by a custom-written algorithm according to the following criteria:

• If total power (root-mean-square area under the curve) in the theta range (5-10 Hz) in the hippocampal EEG was at least 2 x the power in the LIA range (1-5 Hz), the bin was classified as “theta”; if LIA power was greater than theta power, it was classified as “LIA.”

• Theta whose EMG amplitude during the sleep session exceeded a set threshold was discarded as ambiguous; theta whose EMG amplitude during the sleep session fell below this threshold was classified as “REM”. The threshold was determined separately for each data set by inspection of

the EMG amplitude distribution, which was typically bimodal with a large sharp peak at the low end (corresponding to sleep) and a small, wide peak at the high end (corresponding to waking); the threshold was set at the local minimum between these peaks. All theta during the run session was classified as "run."

• If the hippocampal EEG amplitude was lower than a specified threshold, the bin was classified as "SIA", regardless of its power spectrum. The threshold was determined separately for each data set by calculating the 20^{th} percentile of the hippocampal EEG amplitude distribution from a continuous bout of sleep, since SIA was previously found to occupy approximately 20% of sleep (Jarosiewicz et al., 2002), and visually finding a local minimum near that amplitude in the distribution. All SIA beginning at stimulus onset and extending up to 10 seconds after was classified as "elicited SIA." All SIA occurring outside of the 10 seconds following a stimulus was classified as "spontaneous SIA." Although most elicited SIA episodes were shorter than 10 seconds, the 10-second time interval was chosen to minimize the misclassification of spontaneous SIA as elicited SIA. It was rare to observe multiple SIA episodes within a 10 second interval.

3.3.7. Data Analysis

Except where otherwise indicated, statistics were computed on data set means, and figures show grand means and SEMs. To construct mean power spectra, the power spectrum of each 500 ms bin during sleep was calculated using Welch's averaged, modified periodogram method, with a window size of 490 ms and a sampling frequency of 499.5 Hz. For each data set, bins were classified into physiological states as described above, and the mean power spectrum for a given state was the mean of the power spectra of the bins classified in that state. To compare power spectra across physiological states, mean powers of the specified frequency ranges were calculated for each data set, and statistics were done on these data set means. To quantify the similarity of power spectra in particular frequency ranges and EEG amplitudes between elicited and spontaneous SIA, linear regressions were done on the 8 data set means for elicited SIA and the 8 data set means for spontaneous SIA.

3.4. RESULTS

3.4.1. The Structure of Spontaneous and Elicited SIA during Sleep

Auditory stimuli that were played during sleep reliably elicited SIA episodes that were visually indistinguishable from spontaneous SIA episodes (Fig. 3.1). In both spontaneous and elicited SIA, the hippocampal and neocortical EEG abruptly flattened, and most hippocampal cells became quiet, except for a small subset of cells that abruptly became active at SIA onset and remained active through the duration of the SIA episode. These "SIA-active" cells were previously shown largely to be place cells whose place fields span the location in which the rat is sleeping (Jarosiewicz et al., 2002). The same cells were active during elicited SIA as during spontaneous SIA. The EMG amplitude of both elicited and spontaneous SIA remained as low as in the sleep period just before them, but longer SIA episodes were sometimes followed by movement, accompanied by an increase in muscle tone and the appearance of small-amplitude theta activity in the hippocampal EEG (Fig. 3.1*A*,*B*).

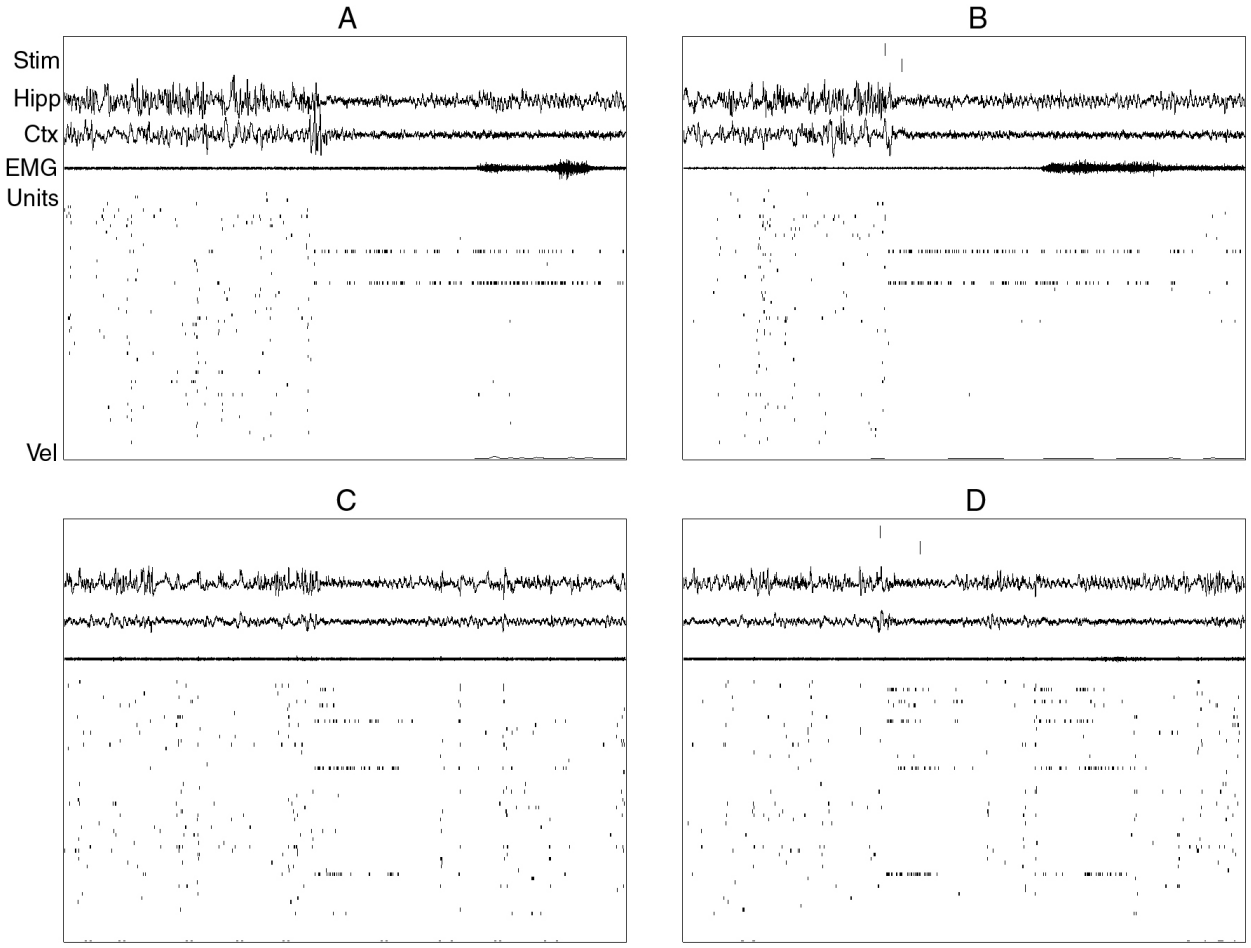

Figure 3.1. Spontaneous and elicited SIA.

Each panel contains a 20 second sample of simultaneously-recorded hippocampal EEG (Hipp), neocortical EEG (Ctx), EMG recorded from the dorsal neck musculature (EMG), spikes from ensembles of simultaneously-recorded CA1 pyramidal cells (Units), and the rat's velocity (vel, with zero aligned at the bottom of the panel) from a single sleep epoch. The tick marks at the top of panels B and D represent auditory stimulus onset and offset (Stim). A, Spontaneous SIA episode. The hippocampal and neocortical EEG abruptly flattened, and most hippocampal CA1 pyramidal cells became quiet, except for a small subset of cells whose place fields were in the current location of the rat. B, Example of an SIA episode elicited by an auditory stimulus from the same sleep session as A. Again, the neocortical and hippocampal EEGs flattened, and the same cells were active as during spontaneous SIA episodes. C, D, Examples of spontaneous (C) and elicited (D) SIA episodes from a different rat. Again, elicited SIA strongly resembled spontaneous SIA in hippocampal and neocortical EEG and population activity. SIA episodes usually evolved back into LIA, as in C and D; in these cases, the EMG remained the same amplitude as the preceding sleep period. Longer episodes, such as those in A and B, were sometimes followed by small movements or posture changes, accompanied by an increase in muscle tone and the appearance of small-amplitude theta activity in the hippocampal EEG.

Effect of auditory stimuli on EEG and EMG amplitudes. Figure 3.2 illustrates the relative consistency and robustness of the effect of auditory stimuli administered during sleep vs. during run. To construct this plot, the mean amplitudes of hippocampal EEG, neocortical EEG, and

EMG, normalized by their mean amplitudes during LIA, were calculated for each 500 ms bin around stimulus onset for each data set, and the grand mean and SEM of the 8 data set means are plotted. When an auditory stimulus was played during sleep (SWS or REM), the hippocampal and neocortical EEG abruptly flattened, and EMG amplitude sometimes increased after a few seconds when movement occurred. The mean amplitude of the hippocampal EEG in the period 1 to 5 seconds following stimulus onset (0.66 ± 0.03) was significantly reduced compared to the period 1 to 5 seconds prior to stimulus onset (1.06 ± 0.02; paired 1-tailed t-test; $p < 0.00001$). The mean amplitude of the neocortical EEG after stimulus onset (0.72 ± 0.07) was also significantly lower than the amplitude before stimulus onset (1.16 ± 0.07; $p = 0.0005$). The same auditory stimuli played during run, even at a louder volume, had no obvious effect on either behavior or physiology (based on 2 data sets). To test whether freezing behavior is critical for SIA, we caused the rat to freeze by various methods (e.g. tearing a piece of paper, opening an umbrella, etc.) and repeated the analysis. We still did not observe any robust SIA in response to these stimuli; a slight decrease in hippocampal EEG amplitude was sometimes observed, but never as dramatic as during sleep. Constructing the event-triggered average using only cases in which the rat displayed freezing responses (3 data sets), we found that the hippocampal EEG amplitude decreased slightly at stimulus onset (0.82 ± 0.02 before and 0.74 ± 0.02 after; $p = 0.01$), but much less than during sleep. The neocortical EEG amplitude did not change significantly, as it was already desynchronized during run. The EMG amplitude also did not change significantly. The transient increases at stimulus onset may be attributable in part to electrical artifact and/or volume-conducted field potentials from the neck EMG accompanying the occasional jerks of the head as the rat oriented to the stimulus. They might also correspond to the "evoked potentials" sometimes observed in the hippocampus and neocortex in response to sensory stimuli (Pickenhain and Klingberg, 1965; Brankack and Buzsáki, 1986; Deadwyler et al., 1981; Jirsa et al., 1992), or they may be a rat analogue of the evoked "K-complexes" observed in humans (Davis et al., 1939; Loomis et al., 1939; Roth et al., 1956; Ehrhart et al., 1981). Since we were unable to elicit robust SIA during run, no further analysis was done on the data in which stimuli were administered during run; all subsequent analysis was done on the 8 data sets in which stimuli were administered during sleep.

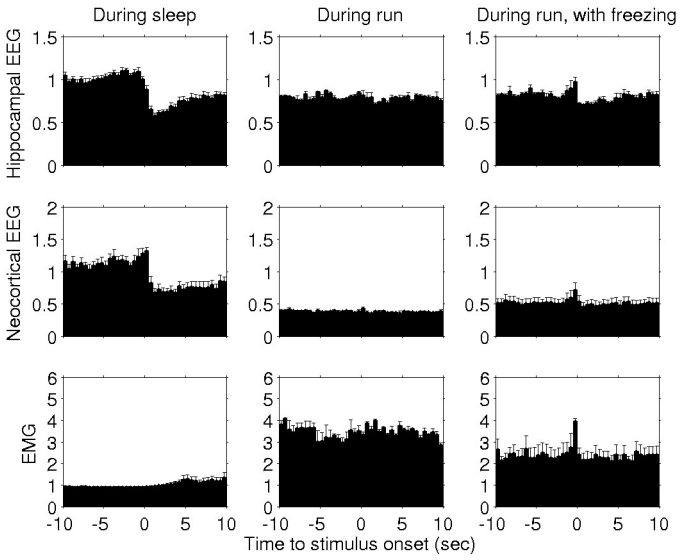

Figure 3.2. Effect of auditory stimuli on EEG and EMG amplitude.

The event-triggered average of the amplitudes of hippocampal EEG, neocortical EEG, and EMG are plotted around stimulus onset, after normalizing by their means during LIA. Bin size = 500 msec. When the auditory stimulus was played during sleep, the hippocampal and neocortical EEG abruptly flattened, and EMG amplitude often increased after a few seconds. The same auditory stimuli played during run, even at a louder volume, had no obvious effect on behavior or physiology. When sounds were generated manually that caused the rat to freeze, the hippocampal EEG amplitude decreased slightly, although much less consistently and robustly than during sleep. The neocortical EEG amplitude did not change significantly, as it was already desynchronized during run. The EMG amplitude also did not change significantly. The transient increases at stimulus onset are probably attributable to electrical artifact accompanying the occasional jerks of the head as the rat orients to the auditory stimulus, evoked potentials, and/or K-complexes.

Comparison of EEG and EMG amplitudes across physiological states. As described in Methods, physiological states were classified as "theta (REM)," "theta (run)," "LIA," "SIA," or "other" using an automated algorithm based on hippocampal EEG amplitude and power spectrum; all SIA occurring within 10 seconds after the onset of an auditory stimulus was classified as "elicited SIA"; the rest of SIA was classified as "spontaneous SIA." The RMS amplitudes of hippocampal EEG, neocortical EEG, and EMG, normalized by their respective means during LIA, were calculated for elicited SIA, spontaneous SIA, LIA, REM, and run in each data set (Fig. 3.3*A*). To compare the mean amplitudes of neocortical EEG and EMG between elicited and spontaneous SIA, a linear regression was done on the mean amplitudes from each data set; a high correlation signifies that the mean amplitude of elicited SIA is similar to the mean amplitude of spontaneous SIA in each data set. The correlation between the mean neocortical EEG amplitudes of elicited SIA (0.57 ± 0.04) and spontaneous SIA (0.59 ± 0.04) was 0.70 (Fig. 3.3*B*), and the correlation between the mean EMG amplitudes of elicited SIA (1.15 ± 0.11) and spontaneous

SIA (1.21 ± 0.10) was 0.89 (Fig. 3.3*C*). Thus, elicited and spontaneous SIA have similar neocortical EEG and EMG amplitudes.

Both elicited and spontaneous SIA had a significantly lower mean neocortical EEG amplitude than LIA (1-tailed paired t-test; $p < 0.00001$ for both elicited and spontaneous SIA) and REM ($p < 0.00001$ and $p = 0.0001$, respectively). The fact that the neocortical EEG amplitude during REM was not as low as during run is attributable to the fact that our sleep state delineation only considered hippocampal EEG; intermediate sleep (Gottesmann, 1973, 1992), the period of transition from SWS to REM during which the neocortical EEG still exhibits large-amplitude slow waves but theta activity already appears in the hippocampus, was grouped with REM in this study. Both elicited and spontaneous SIA had significantly lower EMG amplitude than run ($p = 0.0083$ and 0.0094, respectively), but slightly higher amplitude than REM ($p = 0.041$ and 0.017). They were roughly comparable in EMG amplitude to LIA. Thus, the neocortical EEG of SIA is desynchronized, and the EMG amplitude is higher than in REM but lower than in run, and comparable to that of LIA.

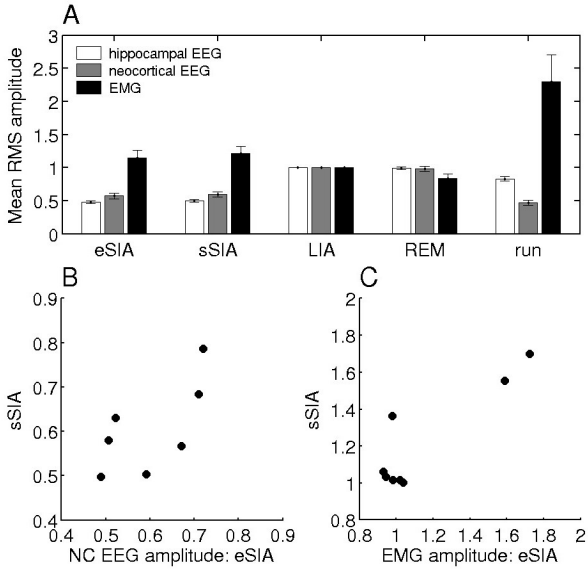

Figure 3.3. Comparison of hippocampal and neocortical EEG and EMG amplitudes.

The root-mean-square amplitude of hippocampal EEG, neocortical EEG, and EMG was calculated for elicited SIA ("eSIA"), spontaneous SIA ("sSIA"), LIA, REM, and run in each data set. (*A*) Elicited SIA was comparable to spontaneous SIA in hippocampal EEG (by definition), neocortical EEG, and EMG amplitudes. The neocortical EEG amplitude of both eSIA and sSIA was lower than LIA and REM, and the EMG amplitude was comparable to that of LIA. Each data set's elicited SIA was similar to its spontaneous SIA (*B*) in mean neocortical EEG amplitude ($r = 0.70$) and (*C*) in mean EMG amplitude ($r = 0.89$).

Comparison of hippocampal and neocortical EEG power spectra across physiological states. Average EEG amplitudes can appear very similar between EEG states even if their structure is very different; that is, even if two EEG states have similar amplitude, their component frequencies might have a different power distribution. For example, LIA and REM have very different hippocampal EEG structure, but as shown in Figure 3.3, their mean hippocampal EEG amplitudes are very similar. Thus, it was also important to compare the power spectra of elicited and spontaneous SIA to check whether this revealed any differences between them. Mean power spectra were constructed of hippocampal EEG (Fig. 3.4*A,B*) and neocortical EEG (Fig. 3.4*C,D*) for elicited and spontaneous SIA, LIA, REM, and run. By definition, in the hippocampal EEG power spectrum, REM and run have high power at theta frequency (5-10 Hz), LIA has high power between 1-5 Hz, and elicited and spontaneous SIA have low total power. The shapes of the power spectra of elicited and spontaneous SIA, however, were not predefined. They were found to have almost identical grand mean hippocampal power spectra ($r = 0.999$), with comparable levels of total power in both the low frequencies (1-10 Hz; regression across data sets: $r = 0.998$) and the high frequencies (80-160 Hz, chosen to exclude the artifact at 60 and 180 Hz; regression across data sets: $r = 0.999$).

There were significant differences across physiological states in the mean power in the low frequency range (two-way ANOVA with 4 and 7 df; $F = 28.44$; $p < 10^{-8}$) and the high frequency range ($F = 8.26$; $p = 0.00016$); *post-hoc* paired t-tests revealed that both elicited and spontaneous SIA had significantly less mean power than any of the other physiological states in both the low frequency range (for elicited SIA vs. LIA, REM, and run: $p = 0.0003$, 0.0005, and 0.0001, respectively; for spontaneous SIA vs. LIA, REM, and run: $p = 0.0003$, 0.0006, and 0.0001, respectively) and the high frequency range (for elicited SIA: $p = 0.0176$, 0.0173, and 0.0008; for spontaneous SIA: $p = 0.019$, 0.018, and 0.0006). Both elicited and spontaneous SIA were also found to have a small peak in the low-frequency (type 2) theta range (mean across data sets = 6.21 ± 0.20 and 6.12 ± 0.16 Hz, respectively), which is significantly lower than the peak frequency of theta during run (8.10 ± 0.08 Hz; $p < 0.00001$ for both elicited and spontaneous SIA) and REM (7.34 ± 0.07 Hz; $p < 0.00001$ for both elicited and spontaneous SIA). Thus, the power spectra of the hippocampal EEG are quite similar between spontaneous and elicited SIA.

The grand mean neocortical EEG power spectra of elicited and spontaneous SIA were also highly correlated ($r = 0.984$). Spontaneous SIA appeared slightly higher in amplitude in low

frequencies (1-10 Hz) than elicited SIA, but this difference varied across data sets and was not significant. It is probably attributable to the sleep state delineation method, which was more likely to allow 500 msec segments classified as spontaneous SIA than 500 msec segments classified as elicited SIA to contain small amounts of SWS, because auditory stimuli almost always elicited SIA (see Figure 3.2, left column). Interestingly, the power spectra also revealed that the neocortical desynchronization present during run differed from the neocortical desynchronization present during SIA; run had significantly higher power in the high frequencies (80-160 Hz) than elicited SIA and spontaneous SIA ($p = 0.00006$ and 0.0002, respectively). It also has significantly higher power in this range than REM ($p = 0.0004$), whose neocortical EEG is also desynchronized; REM and SIA were not significantly different from one another in this range. This unexpected difference between the desynchronization present during run and SIA/REM was present in all 8 rats.

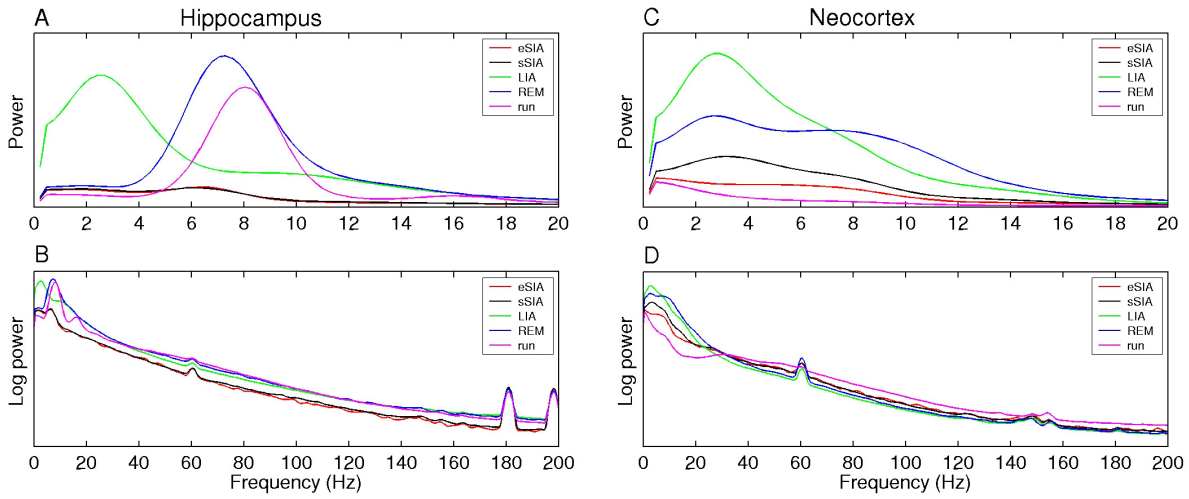

Figure 3.4. Comparison of hippocampal and neocortical EEG power spectra.

Power spectra were constructed using Welch's averaged, modified periodogram method, with a window size of 490 ms and a sampling frequency of 499.5 Hz. *A, B,* By definition, REM and run have peaks at theta frequency (5-10 Hz) in the hippocampal EEG, and LIA has a peak between 1-5 Hz. Elicited and spontaneous SIA had almost identical hippocampal power spectra ($r = 0.999$); both had low total power across the frequency spectrum and a small peak in the low-frequency (type 2) theta range (mean across data sets = 6.2 and 6.1 Hz, respectively). *B,* The same data as in *A* are plotted against log power to reveal detail in the high frequencies. *C, D,* Elicited and spontaneous SIA were also similar in neocortical EEG ($r = 0.98$). Spontaneous SIA appeared slightly higher in amplitude in low frequencies (1 – 10 Hz) than elicited SIA, but this difference was not significant; it was probably attributable to the sleep state delineation method, which was more likely to allow SWS to contaminate segments classified as spontaneous SIA than elicited SIA (i.e. it was unlikely for SWS to occur within the 10 seconds following an auditory stimulus). Interestingly, the neocortical "desynchronization" present during SIA was different from that of run; eSIA and sSIA had significantly lower power in the high frequencies (80-160 Hz) than run ($p = 0.00006$ and $p = 0.0002$, respectively). The sharp peaks at 60, 180, and 200 Hz are attributable to artifact.

Comparison of hippocampal unit activity between elicited and spontaneous SIA. To quantify the similarity of the CA1 ensemble spike activity between elicited and spontaneous SIA, the mean firing rate of each cell from each data set (total = 383 cells) was calculated for elicited SIA and for spontaneous SIA. Those cells that were active in spontaneous SIA were also found to be active in elicited SIA (Fig. 3.5*A*). Furthermore, the cells that were not very active in SIA (mean < ~1 Hz; about 95% of cells) still had similar mean firing rates in elicited and spontaneous SIA (Fig. 3.5*B*). The correlation between the population activity in elicited and spontaneous SIA when all cells were taken together was 0.975. The mean and SEM of each data set's population activity correlation coefficient was 0.88 ± 0.04. The very similar population activity between elicited and spontaneous SIA provides strong evidence that they are a single physiological state.

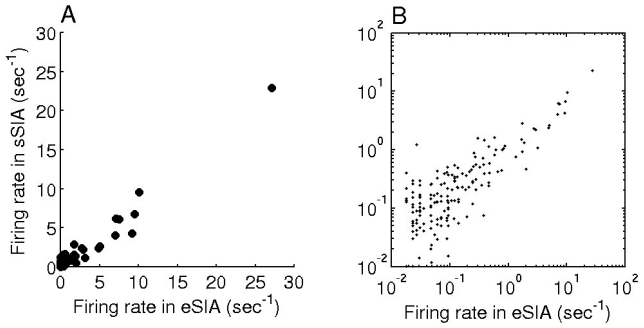

Figure 3.5. Hippocampal population activity during elicited vs. spontaneous SIA.

Hippocampal population activity during elicited vs. spontaneous SIA. Each cell's mean firing rate in elicited vs. spontaneous SIA is plotted for all cells from all data sets (total = 383 cells). *A,* Standard plot, showing that cells that were active in spontaneous SIA were also active in elicited SIA. *B,* Log-log plot, revealing that a linear relationship also existed for the firing rates of cells that were relatively quiet (< ~1 Hz) during elicited and spontaneous SIA. The correlation across all cells taken together was 0.98. The mean ± SEM correlation coefficient for each data set was 0.88 ± 0.04.

3.5. DISCUSSION

This study aimed to compare the level of arousal during the spontaneous sleep-SIA state whose hippocampal physiology was characterized previously (Jarosiewicz et al., 2002) with the other well-characterized physiological states of theta and LIA, and to test whether it corresponds to the SIA elicited by auditory stimuli (Pickenhain and Klingberg, 1967; Vanderwolf, 1971; Whishaw, 1972; Roldán et al., 1963; Bergmann et al., 1987). Hippocampal and neocortical EEG, neck

EMG, and hippocampal ensemble activity were recorded simultaneously from behaving rats presented with auditory stimuli. Results showed that (1) auditory stimuli presented during sleep reliably elicited SIA episodes very similar to spontaneous SIA episodes in EEG amplitude and power spectra, EMG amplitude, and hippocampal CA1 population activity; (2) the EMG amplitude, a measure of muscle tonus and therefore commonly used to judge behavioral arousal level, is significantly lower in elicited and spontaneous SIA than in run, slightly but significantly higher than in REM, and comparable to LIA; and (3) the neocortical EEG, which is commonly used to judge the level of cognitive arousal, is desynchronized in spontaneous and elicited SIA. Thus, what we call "spontaneous" SIA is probably also elicited by a stimulus, but one that is uncontrolled or unobserved by the experimenter. This appears to be the case in the probable human analogue of SIA, "micro-arousals," which occur spontaneously during sleep but can also be elicited by auditory stimuli (Schieber et al., 1968, 1971; Ehrhart and Muzet, 1974; Halász et al., 1979; for review, see Terzano et al., 1991).

The finding that the hippocampal EEG during SIA has a small peak in the low frequency theta range suggests a possible relationship between SIA and "type 2" theta (also called "atropine-sensitive," "sensory-elicited", or "immobility" theta), whose frequency is lower than the typical movement-associated "type 1" theta, is present under urethane or ether anesthesia, and has a different pharmacological and laminar profile than type 1 theta (Kramis et al., 1975; Bland, 1986). Type 2 theta is rarely observed in awake behaving rats, but is common in rabbits and guinea pigs, in whom it can readily be elicited by auditory stimuli during immobility (Kramis et al., 1975; Sainsbury and Montoya, 1984; for review, see Bland, 1986). The fact that SIA can be elicited similarly, and that it has a small power peak in the low-frequency theta range, suggests that SIA might simply be the rat analogue of type 2 theta. However, robust type 2 theta, comparable in amplitude to LIA, is present in urethane-anesthetized rats at the same recording site as baseline SIA (unpublished observations), and robust type 2 theta can be elicited by auditory stimuli in immobile rats in the presence of cats or ferrets (Sainsbury et al., 1987). Thus, either SIA is not simply the rat analogue of type 2 theta, or the amplitude of type 2 theta can vary significantly in different circumstances. Some studies report a positive correlation between theta frequency and/or amplitude and movement speed (Whishaw and Vanderwolf, 1973; McFarland et al., 1975; Rivas et al., 1996; Slawinska and Kasicki, 1998; but see Shin and Talnov, 2001); thus, another possibility is that the low frequency, low amplitude theta visible in

the SIA power spectrum is a low-amplitude, low-frequency type 1 theta emerging at the end of longer SIA episodes when the rat makes small movements.

Examination of the neocortical EEG power spectra unexpectedly reveals that run has more power across the high frequency range than SIA. This finding has several interesting implications, among them that what appears to be "desynchronization" in the raw EEG is not actually a homogeneous state, and thus, that its use as a measure of cognitive arousal should be made with discretion. In fact, run also has higher power across the high frequencies than REM, which also exhibits desynchronized neocortical EEG (although in this study, intermediate sleep periods were also classified as REM, so its desynchronization was not apparent in the graphs). Thus, it is possible that the power in the high frequency range of the neocortical EEG increases when the rat is actively moving around and/or engaged in associated behaviors such as whisking. Evidence for the latter comes from the finding that stimulating whiskers in an anesthetized rat produces an increase in high frequency oscillations (> 200 Hz) in the EEG of the barrel cortex (Jones and Barth, 1999). If the presence or absence of movement is really the sole determinant of the power in the high frequencies of the neocortical EEG, then the difference in desynchronization between SIA and active waking is trivial.

Despite our efforts, we were unable to elicit robust SIA during active waking. One possible explanation is that inducing freezing by external stimuli is somehow not adequate to produce SIA during waking; it might be necessary for the freezing to be somehow initiated by the rat without influence from external cues. Another possibility is that waking SIA is simply much less robust than SIA occurring during sleep; indeed, upon closer inspection of the two articles in which SIA was described to occur in rats that abruptly suppress ongoing movement (Bergmann et al., 1987; Vanderwolf, 1971; Whishaw, 1972), we found that the only examples shown of SIA in rats were in response to auditory stimuli administered during sleep; the two examples of SIA during waking (both in Whishaw, 1972) were actually taken from a Mongolian gerbil. Thus, it is likely that the SIA that occurs in rats during waking is simply not as robust as it is during sleep, or as it is in other species. It is also possible that differences exist between strains of rats; Bergmann et al. (1987) used Sprague-Dawley rats like we did but Vanderwolf (1971) and Whishaw (1972) used hooded rats.

In summary, the neocortical EEG provides provisional evidence that SIA is a state of heightened neocortical arousal, and the EMG provides evidence that SIA is a state of low

behavioral arousal. Taken with the finding that spontaneous SIA and elicited SIA elicited so strongly resemble one another, and with the finding that the SIA population activity reflects the rat's awareness of its current location in space (Jarosiewicz et al., 2002), this study provides compelling evidence that the rat's arousal level during SIA is heightened relative to the other well-characterized sleep states, but it is not as high as in active waking. Further support for the latter comes from unpublished observations in our laboratory that the population activity in SIA reflects a memory for the location in which the rat fell asleep, rather than an assessment of the rat's current location based on current sensory information: when the rat is moved to a new location while asleep, the population activity during subsequent SIA episodes continues to reflect the rat's old location in the room, although the rat's spatial representation reverts to room coordinates in subsequent active waking periods. We conclude that the level of arousal during SIA lies somewhere between sleep and active waking, sharing features with both.

Chapter 4. HIPPOCAMPAL PLACE-RELATED ACTIVITY DURING THE SMALL IRREGULAR ACTIVITY STATE DOES NOT REFLECT THE PROCESSING OF CURRENT VISUAL INFORMATION

4.1. PREFACE

This Chapter is based on a publication to be submitted to the Journal of Neuroscience. I would like to thank Bruce McNaughton for useful comments on an earlier draft of this Chapter. The reported experiments show that the population activity during SIA does not arise from a real-time assessment of the rat's current location in space, but a reactivation of a memory for the location in which the rat fell asleep.

4.2. INTRODUCTION

In the actively foraging rat, hippocampal pyramidal cells have strong spatial correlates; each "place cell" fires rapidly only when the rat enters a particular delimited portion of its environment, called that cell's "place field" (O'Keefe and Dostrovsky, 1971; O'Keefe, 1976; O'Keefe and Nadel, 1978). Thus, the spiking activity across a population of simultaneously recorded place cells can be used to estimate the current location of the rat (Wilson and McNaughton, 1993; Zhang et al., 1998). Place fields are controlled by an interaction of visual and self-motion cues: if the visual cues in an environment are rotated, place fields rotate by an equal amount (O'Keefe and Conway, 1978; Muller and Kubie, 1987; Bostock et al., 1991), but only if the rat has previously learned that the cues are stable (Knierim et al., 1995; Jeffery and O'Keefe, 1999). The activity across the hippocampal population is thought to reflect the rat's internal representation of its location in space, as errors in the rat's behavior correspond to

misalignments in place cell firing (O'Keefe and Speakman, 1987; Lenck-Santini et al., 2002; Rosenweig et al., 2003).

As shown by Jarosiewicz et al. (2002), hippocampal pyramidal cells also exhibit place-specific firing during a physiological state that occurs during sleep, termed "small irregular activity" (SIA) after the appearance of the hippocampal EEG (Vanderwolf, 1971; Whishaw, 1972). Each SIA episode, lasting on the order of a few seconds and occurring about twice a minute, is characterized by an abrupt flattening of the hippocampal EEG and a sudden change in hippocampal population activity: most CA1 pyramidal cells fall silent, except for a small subset of cells that become very active. These active cells largely correspond to place cells whose place fields are in the location in which the rat is sleeping (Jarosiewicz et al., 2002).

This finding raises the question of whether the rat determines its location in space during SIA using current sensory information, or whether it recalls the location in which it fell asleep. To disentangle these possibilities, in the experiment reported here, rats were allowed to fall asleep along the edge of a circular recording arena with minimal local features in a room with prominent distal visual cues. While the rat slept, the arena was slowly rotated about 90 degrees, moving the rat to a new location in the room without waking it. The population activity in SIA episodes after the rotation was found to reflect the location in which the rat fell asleep, rather than the rat's new location, even though the room coordinates governed the rat's spatial map alignment during active waking before and after the sleep session. Thus, the place-related activity in SIA reflects a memory for the location in which the rat fell asleep, rather than the processing of current visual information.

4.3. MATERIALS AND METHODS

To test whether the place-related CA1 population activity during SIA reflects the processing of current visual information, or whether it reflects a memory for the location in which the rat fell asleep, we recorded spikes from ensembles of CA1 pyramidal cells in rats that were moved to a new location while sleeping. We did this by allowing the rat to fall asleep along the edge of a large circular arena with minimal local cues in a room with prominent distal visual cues, and then rotating the arena by about 90 degrees over about 10 minutes. We then tested whether the cells active during SIA after the arena rotation had place fields in the location in which the rat

fell asleep or in the location to which the rat was moved. To verify that the distal cues controlled the alignment of the rat's spatial map during active waking, we mapped its place fields while it foraged for randomly scattered food pellets both before and after the sleep session.

4.3.1. Subjects

Data were collected from 6 male Sprague Dawley rats, weighing between 350 and 500 gm at the time of surgery. Each rat was housed individually in a 12 hr light/dark cycle in a temperature-controlled room with food and water available *ad libitum*. For 1-2 weeks before surgery, each rat was handled and placed in the recording arena for several hours a day to sleep and to forage for randomly scattered sweetened food pellets. Rats were food-deprived to about 95% of their *ad libitum* weight to motivate them to forage for food pellets when they were available. All handling and recording was done during the light phase of the cycle.

4.3.2. Surgery

All surgery was performed under sterile conditions. Rats were anesthetized with ketamine (60 mg/kg, i.p.) and xylazine (6 mg/kg, i.p.), and boosts of ketamine and xylazine were given during surgery as necessary. Once deeply anesthetized, rats were secured in earbars in a Kopf stereotaxic frame (David Kopf Instruments, Tujunga, CA). A small (~1 cm) incision was made along the midline of the scalp to expose the cranium. Skin and connective tissue were retracted, and seven small holes were drilled into the cranium to accommodate jeweler's screws, one of which was later connected to a ground channel.

A small hole was drilled over the frontal cortex (~1 mm dia., centered on 2 mm anterior, 2 mm lateral from bregma) to accommodate a bipolar neocortical EEG recording electrode, consisting of a twisted pair of 0.0045" (coated) stainless steel wires with ends spaced 2 mm apart vertically. An EMG electrode, consisting of a twisted pair of 0.0045" (coated) stainless steel wires, each with 1mm exposed at the tip and bent 2 mm back to form a hook, was inserted into the dorsal neck musculature by routing it under the skin from the incision. A few square 10 mA pulses of 1 ms duration were passed through the EMG wires at 1 Hz using a stimulus isolation unit and a Grass S88 stimulator to check for muscle twitch, to ensure proper placement of the wires. Another larger hole was drilled over the right hippocampus (~2 mm diameter, centered on

3.5 mm posterior, 2-3 mm lateral from bregma). The dura was retracted, and the exposed cortex was covered with sterilized petroleum jelly. The base of a Kopf "hyperdrive," which contained 12 individually drivable tetrodes (McNaughton et al., 1983b; Recce and O'Keefe, 1989) and two single-channel reference/EEG electrodes all bundled to ~1.5 mm diameter at the base, was lowered toward the exposed cortex. In addition, a small hole was drilled at 0.5 mm anterior, 4.0 mm lateral from bregma to accommodate a 26 gauge guide cannula (Plastics One, Roanoke, VA), which entered the brain at a 30 degree angle mediolaterally, its tip inserted to within 1 mm of the medial septum/diagonal band of Broca. These cannulas were used for microinfusion studies not reported in this paper; no animal received microinfusions before or during data collection for the studies reported here. All implants were cemented in place with dental acrylic, which was anchored to the cranium by jeweler's screws.

Just after surgery, the tetrodes and reference electrodes were lowered ~680 μm toward the hippocampus, and the wound was covered with antibiotic ointment and a mild local anesthetic ointment. Over the next few days, the wound was cleaned and ointment was reapplied daily until the animal recovered. Tetrodes were gradually lowered over a few hours each day until they arrived at the hippocampal CA1 pyramidal cell layer (~2 mm deep), which was identified by its well-characterized EEG and spike waveform characteristics (Ranck, 1973; Fox and Ranck, 1975, 1981; O'Keefe, 1976; O'Keefe and Nadel, 1978; McNaughton et al., 1983a; Buzsáki et al., 1992; Skaggs et al., 1996).

4.3.3. Behavioral Apparatus

Once stable cells and good EEG signals were obtained, recordings were performed while rats foraged for randomly scattered food pellets ("run 1"), slept, and then foraged again ("run 2") on a circular elevated arena (~1.5 m dia.) with a 40 cm tall transparent border around the edge. In order to minimize local cues and maximize distal cues, uniformly colored and textured vinyl flooring was installed in the recording arena, and the arena was placed in a soundproof room with large visual cues on the walls. Before each pretraining and recording session, the arena was cleaned and rotated to a new random orientation, but the distal cues always remained stable. Any local cues the rat deposited before the rotation were promptly removed.

Run sessions began when a ceiling-mounted feeder was turned on, dropping sweetened food pellets onto the arena every 28 sec. After 20-30 min of run 1, the feeder was turned off, and

the rats usually fell asleep spontaneously somewhere along the wall of the arena. The rat was allowed to sleep in this location for about ~10-15 min, and then the arena was rotated ~90 degrees over ~10-15 min via a silent motor-driven wheel abutting the edge of the arena, controlled from the adjoining room, moving the rat to a new location in the room. The rat was allowed to continue sleeping in this new location for another ~10-15 min. The food pellets were then turned back for about 20-30 minutes of run 2. Arena rotations during which the rat woke up and started walking around were terminated; if the rat subsequently went back to sleep, another arena rotation was attempted. Each rotation was carefully documented and the total amount of rotation could be deduced from the position records.

4.3.4. Electrophysiology and Recording

For data acquisition, the top of the hyperdrive was connected to a headstage containing preamplifiers and a ring of light-emitting diodes used for position tracking by a camera mounted on the ceiling over the recording chamber. The headstage was attached to a pair of soft, flexible cables, partially suspended by a counterweight system to help ease the load on the rat's head. The cables ascended through the ceiling of the recording chamber into the adjoining room, where they connected to the Cheetah recording system (Neuralynx, Tucson, AZ), consisting of eight 8 channel amplifiers with software-configurable high- and low-pass filters, feeding their output to a custom made controller and analog-to-digital processor. During recording, signals from each channel of each tetrode were filtered to 600-6000 Hz, sampled at 32 kHz per channel, formatted, and fed to a Windows NT system (Neuralynx, Inc., Tucson, AZ) running custom written acquisition and control software. Each time the signal on any one of the tetrode channels crossed a specified threshold, a 1 msec sample of data from all four channels of that tetrode was written to disk, beginning 0.25 msec before the threshold was crossed, capturing the spike waveform on each channel along with its timestamp. Continuous recordings were also obtained of EEG signals from one channel on each tetrode, from an EEG electrode near the hippocampal fissure, from an EEG electrode in the prefrontal cortex, and from an EMG electrode in the dorsal neck musculature, at a bandwidth of 1-475 Hz (EEGs) or 100-475 Hz (EMG) and a sampling rate of 999 Hz. At the same time, position records containing information about the distribution of light across the video image were acquired at 60 Hz and written to disk. The rat's velocity was estimated as the change in position two timestamps before and two timestamps after the current

timestamp, divided by the elapsed time. The error of the tracker was approximately one-half the width of the ring of light-emitting diodes on the headstage, or 2.5 cm.

Once an adequate number of stable CA1 complex-spike cells were obtained and robust theta activity was visible on the hippocampal EEG electrode during locomotion, a recording session was performed. EEG and EMG signals, spike waveforms, and the position of the rat were recorded simultaneously while the rat slept and/or ran for randomly scattered food pellets. Before the rotation experiments began, each rat underwent 1-3 recording sessions, each on separate days, in which auditory stimuli were played to it during sleep; this was part of a different experiment whose results are not presented here. The rotation experiment began after these experiments. As many rotation experiments were performed for each rat as possible, until good cells could no longer be obtained, the rat stopped sleeping well, or until the rat otherwise became unusable, at which point it was humanely killed and its hyperdrive was removed for reuse.

4.3.5. Cell Isolation

Spike waveforms, EEG and EMG signals, and the rat's position data, along with their respective timestamps, were stored onto disk during the recording session for off-line analysis. Spikes were assigned to individual units by automated cluster-cutting software (Klustakwik, K. D. Harris), and clusters were then manually verified and cleaned using Mclust (A. D. Redish). Isolated units were judged to be pyramidal cells or interneurons (Fox and Ranck, 1981), or artifact, according to their average waveforms, autocorrelograms, interspike interval histograms, etc.; only those units judged to be relatively clean, well-isolated pyramidal cells were included in further analysis.

4.3.6. Data Analysis

To delineate SIA episodes, the hippocampal EEG was divided into 500 ms bins, and if the hippocampal EEG amplitude was lower than a specified threshold, the bin was classified as SIA. This threshold was determined separately for each data set by calculating the 20^{th} percentile of the hippocampal EEG amplitude distribution from a continuous bout of sleep and visually finding a local minimum near that value in the amplitude distribution, since SIA was previously found to occupy approximately 20% of sleep (Jarosiewicz et al., 2002).

To construct "correlation maps," a mean SIA population activity vector was constructed by calculating each cell's mean firing rate during all SIA episodes occurring before the arena rotation ("pre-rotation SIA"), and another mean SIA population vector was calculated for the group of SIA episodes occurring after the arena rotation ("post-rotation SIA"). A mean population activity vector was also calculated for each pixel of the environment by determining each cell's mean firing rate across the entire run session in that pixel using the adaptive binning method of Skaggs et al. (1996). One such set of vectors was made for run 1 and one for run 2. Then, for each pixel in the environment, the correlation coefficient was calculated between the SIA population activity vector and the mean run population activity vector in that pixel, and the result was a correlation map reflecting the similarity between the population activity during SIA and the population activity in each location in the environment. Thus, four correlation maps were created for each data set, one for each combination of pre-rotation SIA and post-rotation SIA with run 1 and run 2. Peaks in these maps represent a reconstruction of the rat's internal representation of its current location in space during SIA, as determined by the relative activity of its hippocampal place cells.

4.4. RESULTS

Of 19 recording sessions from the 6 rats, 10 were successful, in that the rat remained asleep during the rotation and for at least 10 minutes afterwards, and robustly SIA-active cells were present both before and after the rotation. It was difficult to obtain multiple successful experiments from a single rat, since rats were less willing to sleep soundly in the arena on days subsequent to a successful rotation. Only 1 successful data set was obtained from each of 4 of the rats (p158-05, p163-14, p169-08, and p175-08); however, 5 successful data sets were obtained from one particularly sound sleeper (p181-02, -06, -07, -10, and -13). Results did not differ between p181 and the other 4 rats, or across data sets from rat p181, so all 9 of the above data sets were included as independent samples in the analysis. In one data set (p159-09), the cell activity profile during run 2 was distinctly different from that of the other data sets, in that the place fields rotated with the arena rather than remaining aligned with the room cues. Although the results from this data set are consistent with the other data sets, the fact that its control

condition was not satisfied precluded the rest of its analysis. Thus, its case is discussed separately below.

4.4.1. SIA Population Activity Reflects Memory Reactivation

Correlation maps peak in old location of rat. Figure 4.1*A* shows an example of EEG and cell ensemble activity during SIA before and after the rotation during sleep for one data set (p181-10). In this example, two of the three cells that were active during SIA before the rotation were also active during SIA after the rotation. Slight changes in the SIA population activity sometimes occurred over time even in the absence of arena rotations; thus, correlation maps were also constructed to show that even when the SIA population activity changed, it still represented the location in which the rat fell asleep, not the location to which it was rotated. Figure 4.1*B* shows the set of correlation maps from this data set. Consistent with previous findings (Jarosiewicz et al., 2002), during SIA before the arena rotation, the rat's representation of its current location closely matched its actual location (Fig. 4.1*B*, left 2 panels). However, after the arena was rotated, moving the rat to a new location in the room, the population activity during subsequent SIA episodes continued to reflect the location in which the rat fell asleep, rather than its new location (Fig. 4.1*B*, right 2 panels). This was true whether the run population activity vectors being compared to the mean SIA population activity vectors were taken from run 1 or run 2, verifying that the distal room cues governed the hippocampal place fields during the run sessions. Thus, this rat did not update its current spatial representation on the basis of current sensory input during SIA, but rather recalled the location in which it fell asleep.

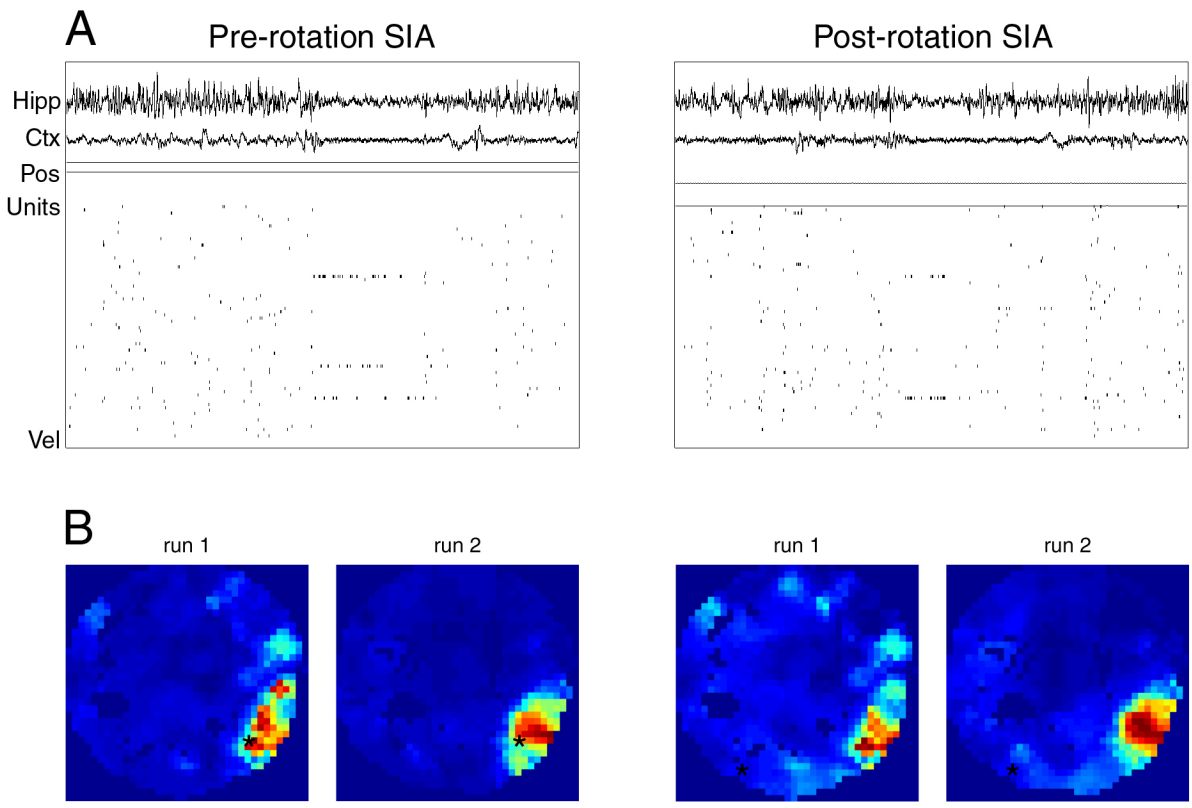

Figure 4.1. Effect of arena rotation on place representation during SIA, results from one recording session (p181-10).

A, Each panel contains a 20 second sample of simultaneously-recorded hippocampal EEG (*Hipp*), neocortical EEG (*Ctx*), spikes from 73 simultaneously-recorded CA1 pyramidal cells (*Units*), and the rat's velocity (*Vel*, arbitrary scale, with zero aligned at the bottom of the panel) from a single sleep epoch. The left panel shows an SIA episode occurring before the rotation (*Pre-rotation SIA*). During SIA, the hippocampal and neocortical EEG abruptly flatten, and most hippocampal CA1 pyramidal cells become quiet, except for a small subset of cells whose place fields generally encompass the location in which the rat is sleeping. The right panel shows an SIA episode occurring after the rotation (*Post-rotation SIA*). In this example, 2 of the 3 cells that were active in pre-rotation SIA were also active in post-rotation SIA. *B*, In each "correlation map," the correlation coefficient between the mean population activity vector across all pre-rotation SIA episodes (*left 2 panels*) or all post-rotation SIA episodes (*right 2 panels*) and the mean population activity vector during run before the sleep session (*run 1*) or during run after the sleep session (*run 2*) was plotted for each pixel of the arena. *Blue areas* correspond to low correlation values and *red areas* correspond to high correlation values. Peaks in the correlation maps correspond to areas in the arena where the population activity during run most strongly resembles the population activity during SIA, and thus presumably reflects the rat's internal representation of its location. The *black asterisk* represents the rat's actual location. The rat's representation of its current location during SIA before the rotation closely matched its actual location, but after the arena was rotated, moving the rat to a new location, the population activity during subsequent SIA episodes continued to reflect the rat's original location in the room rather than its new location. This was true whether the run firing rate vectors were taken from run 1 or from run 2, indicating that the distal room cues did in fact drive the hippocampal place fields during active foraging. Thus, this rat did not update its current spatial representation on the basis of current sensory input during SIA, but rather recalled the location in which it fell asleep. In this recording session, the correlation coefficient between the values in the correlation maps before and after the rotation was 0.906 when using the population activity from run 1, and 0.965 when using the population activity from run 2. For comparison, the grand mean and SEM of the correlation coefficient across data sets was 0.744 ± 0.096 using run 1 and 0.808 ± 0.068 using run 2.

To show that this finding was consistent across data sets, the correlation maps from all data sets were rotationally aligned on the actual location of the rat and averaged together (Fig. 4.2). The peak in the mean aligned correlation map occurred in the location in which the rats fell asleep (Fig. 4.2, left 2 panels), not in the location to which they were rotated (Fig. 4.2, right 2 panels), supporting the hypothesis that the population activity during SIA reflects a memory for the location in which the rat fell asleep rather than an updated spatial representation based on current sensory input. Again, all of the data sets in this analysis fit the above pattern whether the run population activity vectors being compared to the mean SIA population activity vectors were taken from run 1 (Fig. 4.2, top 2 panels) or run 2 (Fig. 4.2, bottom 2 panels), verifying that the distal cues governed the rat's spatial representation during run.

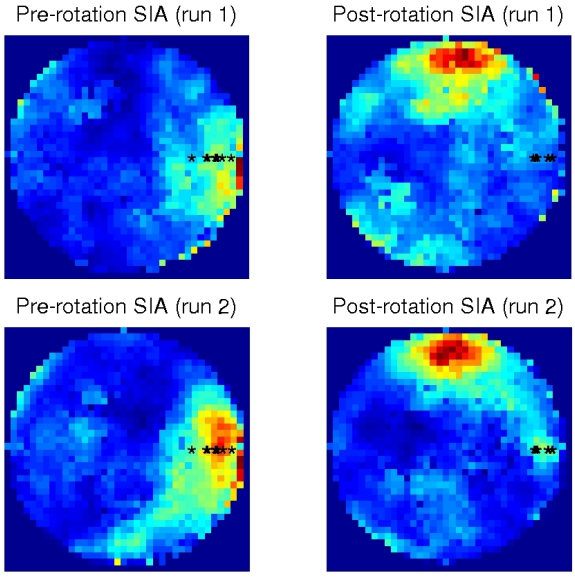

Figure 4.2. Effect of arena rotation on place representation during SIA, average results across data sets.

Correlation maps from 9 data sets from 5 different rats were rotationally aligned on the actual location of the rat (denoted by the *black asterisks*) and averaged together. Consistent with the data from the example recording session shown in Figure 4.1, on average, the peak in the mean aligned correlation map occurred in the location in which the rat fell asleep (*left 2 panels*), not in the location to which the rat was rotated (*right 2 panels*). Thus, the population activity during SIA reflects a memory for the location in which the rat fell asleep, rather than an updated spatial representation based on current sensory input.

Population activity is similar in pre-rotation SIA and post-rotation SIA. Figure 4.3*A*,*B* shows each cell's mean firing rate during SIA before the rotation against its mean firing rate during SIA after the rotation, using all 631 cells from the 9 data sets. In general, cells that were active in SIA before the rotation were also active in SIA after the rotation. Using all cells from all data sets, the correlation between the mean pre-rotation SIA and mean post-rotation SIA population activity vectors was 0.808. The grand mean and SEM of the correlation coefficients from each data set was 0.747 ± 0.095.

Post-rotation SIA activity is more similar to rat's old than new location. Because SIA-active cells sometimes change over time during sleep, and because place cells can have multiple place fields, a more decisive analysis than the correlation between the pre-rotation and post-rotation SIA population activity vectors is the correlation between the post-rotation SIA population activity vector on the one hand and the run population activity vector in the rat's original or new location on the other (Fig. 4.3*C*,*D*). If the population activity during SIA reflects a memory for the location in which the rat fell asleep, then the correlation between the post-rotation SIA population activity vector and the run population activity in the spot in which the rat fell asleep ("*post,1*") should be higher than the correlation between post-rotation SIA vector and the run population activity vector in the spot to which the rat was moved ("*post,2*"). Indeed, *post,1* (grand mean ± SEM = 0.301 ± 0.093 for run 1; 0.424 ± 0.072 for run 2) was significantly higher than *post,2* (0.023 ± 0.012 for run 1; 0.115 ± 0.032 for run 2) when using the population activity vectors from either run 1 ($p = 0.01$; Fig. 4.3*C*) or from run 2 ($p = 0.001$; Fig. 4.3*D*).

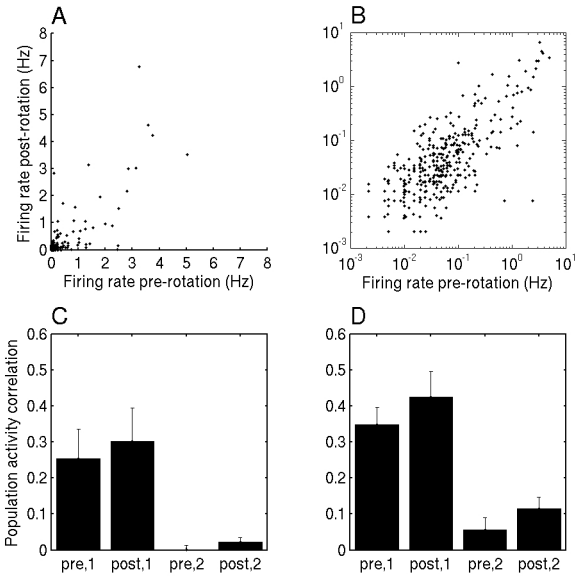

Figure 4.3. Quantification of results.

A,B, Hippocampal population activity during SIA before and after the arena rotation. Each cell's mean firing rate during SIA before the rotation was plotted against its mean firing rate during SIA after the rotation, using all 631 cells from the 9 data sets. *A,* In general, cells that were active in SIA before the rotation were also active in SIA after the rotation. *B,* The same data as in *A* are plotted on a log-log scale to show that even the firing rates of cells that were not very active during SIA (< ~1 Hz) were also similar in pre-rotation and post-rotation SIA. Using all cells from all data sets, the correlation between the mean pre-rotation SIA and mean post-rotation SIA population activity vectors was 0.808. The mean ± SEM of the correlation for each data set was 0.747 ± 0.095. *C, D,* For each data set, mean population activity vectors were constructed for pre-rotation SIA, post-rotation SIA, active foraging in the pixel of the arena in which the rat fell asleep, and active foraging in the pixel of the arena to which the rat was rotated, and the correlation coefficient was calculated for each combination of vectors from SIA and active foraging. The means and SEMs of these correlations are plotted for run 1 (*C*) and run 2 (*D*). If the population activity during SIA reflects a memory for the location in which the rat fell asleep, then the correlation between the post-rotation SIA vector and the population activity in the location in which the rat fell asleep (*post,1*) should be higher than the correlation between post-rotation SIA and the population activity in the location to which the rat was rotated (*post,2*). Indeed, *post,1* was significantly higher than *post,2* using either run 1 ($p = 0.01$) or run 2 ($p = 0.001$).

4.4.2. Case of an Anomalous Rat Whose Run 2 Spatial Map Rotated with the Arena

In one anomalous data set (p159-09), not included in the rest of the analysis, the place fields remained rotated with the arena during run 2. That is, the place fields obtained from run 2 were rotated ~150 degrees from their locations in run 1 (Fig. 4.4*A*,*B*), corresponding to the amount by which the arena had been rotated during sleep. Thus, even though the cells active during SIA continued to code for the location in which the rat fell asleep, these cells had place fields in the rat's new location during run 2, so it was impossible to distinguish whether this rat was recalling where it fell asleep during SIA, or whether it was determining its location based on current sensory information from local arena cues that we did not manage to eliminate. Although this data set is consistent with the other data sets, it could not be analyzed in the same way, because in run 2, "spot 1" was equivalent to "spot 2."

To test whether this rat always aligned its spatial map with the arena frame rather than the room frame, it underwent an additional manipulation with three rotations in a single recording session, two during run and one during sleep. The rat was allowed to run on the stable arena for at least 5 minutes before and after each rotation to allow place fields to be mapped. Figure 4.4*C* shows 8 representative place field maps from each of the stable periods. When the arena was rotated during run, the place fields remained aligned with the room coordinates, but when the arena was rotated during sleep, the place fields rotated with the arena. Thus, this rat did not always align its spatial map with the arena; it only did so when the arena had been rotated during sleep. Possible implications of these results are considered in the discussion.

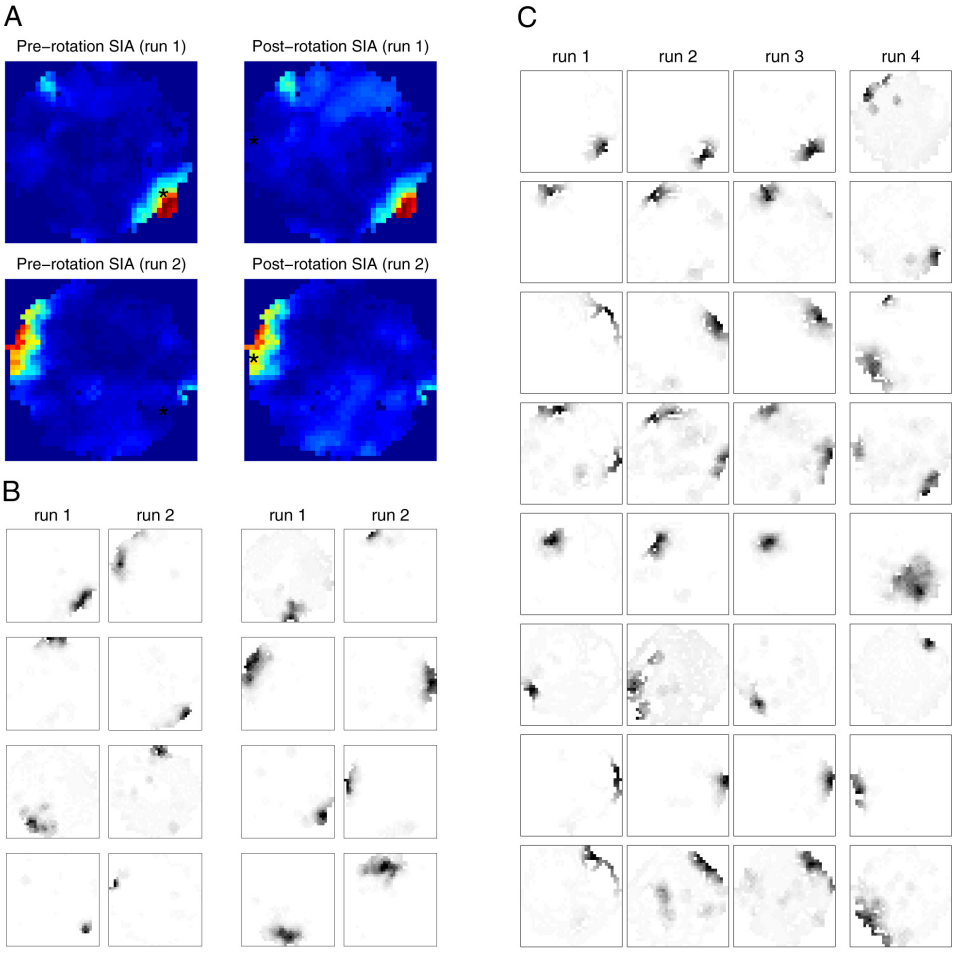

Figure 4.4. Results from an anomalous rat whose place fields remained rotated with the arena in run 2.

A, Correlation maps from data set p159-09. Same format as Fig. 4.1*B*, except that the arena in this data set was rotated about 150 degrees instead of 90. *B,* Representative place field maps from 8 of the simultaneously recorded CA1 pyramidal cells from run 1 (total of 20 minutes) and run 2 (total of 23 minutes). Consistent with the other rats, the post-rotation SIA population activity continued to reflect the rat's original location; however, unlike all other rats, the place fields remained aligned with the arena coordinates in run 2, rather than realigning with the room coordinates. Thus, the fact that its hippocampal population activity during post-rotation SIA continued to code for the location in which it fell asleep does not address the issue of whether the rat was recalling where it fell asleep or determining its new position based on current sensory information during SIA. *C,* To test whether this rat always aligned its spatial map with the arena frame rather than the room frame, we rotated the arena while this rat ran and slept in the same recording session (data set p159-10). Three 180 degree rotations were performed, two during run and one during sleep, with at least 5 minutes of run in the stable arena before and after each rotation to map out place fields. Representative place field maps from 8 of the simultaneously recorded cells are shown for each of the stable run periods. Two rotations occurred during run: one between run 1 and run 2, and the other between run 2 and run 3. A third rotation occurred during sleep, between run 3 and run 4. When the arena was rotated during run, place fields remained with the room coordinates, but when the arena was rotated during sleep, place fields rotated with the arena as they did in data set p159-09. Thus, when the arena was rotated during run, this rat's spatial map was aligned to the reference frame of the room; but when the arena was rotated during sleep, the rat's spatial map in subsequent waking periods was aligned with the reference frame of the arena. Possible implications of this finding are explored in the discussion. Data from this anomalous rat were not used in the other analyses.

4.5. DISCUSSION

When rats were moved to a new location in the room during sleep, the population activity in subsequent SIA episodes was found to reflect the location in which the rats fell asleep, rather than the location to which they were moved, even though the place fields were controlled by room cues during active waking. The simplest interpretation is that the place-related activity in SIA does not arise from the processing of current sensory information, as does the place-related activity in active waking, but from a reactivation of the memory for where the rat fell asleep.

Another possibility is that rats used current sensory information to determine their position during SIA, but that instead of using the prominent distal visual cues, the rats used whatever minimal local arena cues were still available to them despite our efforts to eliminate them. It is likely that some local arena cues were available to the rats, because one rat was able to keep its spatial map aligned with the rotated arena for 23 minutes in run 2, despite the conflict between the orientation of the arena and the orientation of the distal visual room cues. The appearance and texture of the arena was rotationally uniform, so it is unlikely that this rat was able to use visual or texture cues to maintain the alignment of its spatial map with the arena, but it might have been able to deposit and use local olfactory cues. In support of this possibility, there is evidence that rats can use local olfactory cues to guide navigation when visual information is absent (Lavenex and Schenk, 1998; Maaswinkel and Whishaw, 1999; Wallace et al, 2002), and rats are more impaired at navigating in the dark when local olfactory cues are shuffled than when they are stable (Stuchlik et al, 2001; but see Stuchlik and Bures, 2002). However, rats are more likely to use visual information than olfactory information if both are available and the two sets of cues are in conflict (Lavenex and Schenk, 1995; Maaswinkel and Whishaw, 1999), as was the case for most of the rats in the present study. In a follow-up experiment, the anomalous rat was found to align its spatial map with the arena in subsequent run periods only when the arena had been rotated during sleep, but not when the arena was rotated during active foraging. It is not known why this rat used local cues to align its spatial map in the subsequent run session after the arena had been rotated during sleep.

Nevertheless, if rats are able to use local olfactory cues to determine their current location in space during active waking, it is possible that rats were able to use local olfactory cues to determine their current location during SIA. Under this conception, rats' perception, or perceptual attention, would have been altered during SIA, such that nearby cues became more salient than distal cues, and they aligned their maps with local cues in SIA but distal cues (in most cases) during active waking. This possibility would still require the reactivation of a memory during SIA for the association between the deposited olfactory cues and the particular location in which they were deposited; thus, even if rats do use local olfactory cues to determine their current location in space during SIA, they must also be using memory. The issue that distinguishes this possibility from the above possibility, then, is whether the cues used to reactivate the memory for the location in which the rat fell asleep are external (e.g. distal visual cues or local olfactory cues) or internal. The present study has eliminated the possibility that rats are using distal visual cues. One way to eliminate the possibility that the rats are using local olfactory cues is by repeating this study in anosmic rats. If the SIA-active cells following the rotation still reflect the location in which the rat fell asleep, rather than the location to which it was rotated, then the rats are not using olfactory cues to determine their current location in space during SIA, but are rather recalling the location in which they fell asleep.

If sleeping rats maintain a working memory for their current location in space, where is this working memory stored? The hippocampal population activity does not contain any obvious information about the rat's sleeping location during REM and SWS. However, patterns of hippocampal activity during REM and SWS resemble patterns present during the immediately preceding waking period more than expected by chance (Wilson and McNaughton, 1994; Skaggs and McNaughton, 1996; Louie and Wilson, 2001); thus, it is possible that the information about the rat's spatial history contained in these reactivated patterns is enough to reconstruct its current location at SIA onset. This hypothesis would predict that, if the path represented by the population activity just before SIA onset were reconstructed with a small enough temporal grain, it would reflect a trajectory to the rat's current location. Another possibility is that the rat's current spatial location is stored within the hippocampus as a "latent attractor" (Doboli et al., 2000), not evident in the patterns of neural activity but available in the short-term synaptic structure of the network, that can be reactivated when the animal is aroused. This memory reactivation could be aided by local sensory cues that had been associated with that location

before the rat fell asleep, such as the rat's sleeping position and the resulting pressure of the floor on various parts of the its body, local olfactory cues, etc. It is important for a sleeping animal to maintain in memory the context in which it is sleeping. For example, a person needs to sleep differently on the top bunk of a narrow bunk bed than on a king-size bed, and a rat needs to maintain a memory for its location relative to nearby passages through which a potential predator can enter or by which the rat can escape if necessary. SIA might provide the neural substrate for such context sensitivity during sleep.

Chapter 5. SEROTONIN MICROINFUSION INTO THE MEDIAL SEPTUM INDUCES HIPPOCAMPAL SMALL IRREGULAR ACTIVITY

5.1. PREFACE

The focus of previous Chapters has been to characterize the physiology, behavioral and neural correlates, and level of arousal of naturally occurring SIA. This Chapter investigates possible mechanisms by which SIA is generated.

5.2. INTRODUCTION

As discussed in Section 1.3, evidence has accumulated over the last 50 years in support of the existence of an "ascending brainstem synchronizing system" that induces theta activity in various limbic structures via its influence on the MSDB. Briefly, the pathways originate in the nucleus recticularis pontis oralis and the peduncolopontine tegmental nucleus and ascend to the MSDB via the posterior hypothalamus and supramammillary nuclei (Green and Arduini, 1954; McNaughton et al., 1995; Bland and Oddie, 1998; for a review, see Bland and Colom, 1993). The theta rhythm is thought to reflect intrinsic oscillations in postsynaptic potentials of hippocampal pyramidal cells and/or interneurons, entrained by direct input from rhythmically-bursting cholinergic and/or GABAergic septohippocampal projection cells (for reviews, see Stewart and Fox, 1990; Smythe et al., 1992; Vertes and Kocsis, 1997; and Buzsáki, 2002.)

The bulk of research on the generation mechanisms of LIA has focused on the cellular mechanisms of its more prominent subcomponents – sharp waves, ripples, and the fast (~100-140 Hz) oscillations that occur between sharp waves (O'Keefe and Nadel, 1978; Buzsáki, 1986; Buzsáki et al., 1992; Ylinen et al., 1995a; Csicsvari et al., 1999a,b). All of these subcomponents are thought to arise within the hippocampus, suggesting that LIA might be the "default" EEG state in the absence of external theta drive. However, the existence of a third hippocampal EEG state, SIA, complicates matters; something has to determine whether the hippocampus goes into

LIA or SIA in the absence of theta drive. Thus, either SIA or LIA, or both, must have a driving mechanism (or at least a trigger) that is external to the hippocampus.

The mechanism by which SIA is generated is not addressed in the few studies characterizing its behavioral correlates. However, a hippocampal "desynchronization" visually resembling SIA has been reported under three sets of experimental conditions: (1) when theta activity would normally be expected but the MSDB has been lesioned or temporarily inactivated (Winson, 1978; Givens and Olton, 1990; Mizumori et al., 1989; Lawson and Bland, 1993; Kirk and McNaughton, 1993; Oddie et al., 1996); (2) when the MSDB is stimulated at frequencies beyond physiological theta range (Brücke et al., 1959; Ball and Gray, 1971; Klemm and Dreyfus, 1975); (3) and when the median raphe nucleus (MnR) is stimulated (Macadar et al., 1974; Assaf and Miller, 1978; Vertes, 1981). This effect appears to be mediated by serotonergic projections from the MnR to the MSDB, as continuous theta activity results under manipulations that suppress the activity of MnR serotonergic neurons (for review, see Vertes and Kocsis, 1997); MnR serotonergic fibers directly inhibit a subset of septohippocampal cholinergic projection cells via 5HT-1A receptors (Milner and Veznedaroglu, 1993; Kia et al., 1996) and directly excite septohippocampal GABAergic projection cells via 5-HT-2A and possibly other receptor subtypes (Alreja, 1996; Leranth and Vertes, 1999); and MnR stimulation inhibits irregularly firing septal neurons and disrupts the rhythmicity of regularly bursting septal neurons (Assaf and Miller, 1978). Together, the first two sets of results suggest the hypothesis that SIA might occur when both theta activity and LIA are somehow precluded. The third set of results suggests a second hypothesis, consistent with the first hypothesis but more specific: that the factor that determines whether the hippocampus goes into SIA or LIA in the absence of external theta drive might be the level of serotonin in the MSDB. In support of this second hypothesis, the activity of the MnR appears to be related to level of arousal: serotonergic raphe cell activity is highest during active waking, lower in LIA, lower yet in SWS, and almost entirely absent in REM (McGinty and Harper, 1976; Trulson and Jacobs, 1979; Lydic et al., 1983; Rasmussen et al., 1984; Shima et al., 1986; Sakai and Crochet, 2001), and serotonergic MnR neurons increase their firing at the offset of REM episodes and in response to visual or auditory stimuli during waking and sleep (Rasmussen et al., 1984), when SIA would be expected. Thus, if SIA is really a state of heightened arousal, perhaps the factor that triggers the appearance of SIA in the hippocampus is a sudden increase of serotonin levels in the MSDB.

To test the more general hypothesis of whether SIA is simply the state that occurs in the absence of both theta activity and LIA, theta activity was transiently abolished by MSDB inactivation, and LIA was precluded by allowing the rats to forage for randomly-scattered food pellets. To test the more specific hypothesis of whether serotonin in the MSDB is the agent of hippocampal EEG desynchronization in SIA, serotonin was microinfused into the MSDB. The amplitudes and power spectra of the resulting hippocampal and neocortical EEG, and the hippocampal CA1 population activity, were compared to those of naturally occurring SIA obtained from baseline sleep. This is the first study to directly test the hypothesis that the presence of serotonin in the MSDB induces hippocampal desynchronization, and to test whether this and/or MSDB inactivation-induced desynchronization has a profile of hippocampal EEG, neocortical EEG, and hippocampal CA1 population activity similar to naturally occurring SIA.

5.3. MATERIALS AND METHODS

Details of the surgical procedure, behavioral apparatus, and electrophysiology were reported in Chapters 3 and 4. All rats in this study also underwent the auditory stimulation (Chapter 3) and maze rotation (Chapter 4) protocols prior to the microinfusions reported here.

5.3.1. Subjects

Data were collected from 9 male Sprague Dawley rats, weighing between 350 and 500 gm at the time of surgery. Each rat was housed individually in a 12 hr light/dark cycle in a temperature controlled room with food and water available *ad libitum*. For 1-2 weeks before surgery, each rat was handled and gradually accustomed to the recording room environment for several hours a day, and food-deprived to about 95% of its *ad libitum* weight to motivate it to forage for randomly scattered sweetened food pellets so that recordings could be tracked between sleep and waking behavior. All handling and recording was done during the light phase of the cycle.

5.3.2. Surgery

In addition to the hyperdrive, neocortical EEG electrode, and EMG electrode, each rat was implanted with a 26 gauge guide cannula (Plastics One, Roanoke, VA) via a small hole that was drilled at 0.5 mm anterior, 3.5 mm lateral to bregma. The cannula entered the brain at a 30 degree angle from the left in the coronal plane, its tip aimed 1 mm outside the center of the MSDB so that the internal cannula (Plastics One, Roanoke, VA), which extended an extra 1 mm, reached the center of the MSDB when inserted for microinfusion.

5.3.3. Microinfusion

Rats were placed in the arena and at least 15 min of baseline run and 15 min of baseline sleep were recorded. For microinfusion, the rat was placed in a towel-lined bowl on a small platform in the arena, and drug was administered into the MSDB via a microinfusion cannula connected by PE-10 tubing to a 10 μL Hamilton syringe. The syringe was fixed in a constant rate microinfusion pump and 1.5 μL of phosphate-buffered saline (PBS) (Sigma-Aldrich, St. Louis, MO), 2% lidocaine hydrochloride stock solution (American Pharmaceutical Partners, Inc., Los Angeles, CA), or 15-30 μg 5-HT (serotonin) hydrochloride (Sigma-Aldrich, St. Louis, MO) freshly dissolved in PBS was infused over 3 min. The internal cannula was left in place for another minute before removal.

The rat was then placed back on the arena for another 45-60 min (or until drug effects wore off), during which it foraged and rested as it chose. The food dispenser was turned on and off periodically in an attempt to capture periods of both activity and inactivity so that drug effects on both theta and LIA could be assessed, but this was sometimes difficult, as discussed in Results. Each rat was infused with each of the drug solutions and PBS, with infusions spaced at least 2 days apart to allow for recovery between infusions. Lidocaine was infused first as a preliminary test for correct cannula placement, as inactivation of the MSDB is known to suppress hippocampal theta activity (Mizumori et al., 1989; Lawson and Bland, 1993), and then the order of 5-HT and control infusions were counterbalanced across animals. If no response was observed to the lower dose of 5-HT in a given animal, an extra microinfusion was administered after 2 days of recovery, using the larger dose.

5.3.4. Physiological State Delineation

Physiological states were classified in 500 ms bins according to the following criteria:

- If the hippocampal EEG amplitude was lower than a specified threshold, the bin was classified as SIA. This threshold was determined separately for each data set by calculating the 20th percentile of the hippocampal EEG amplitude distribution from a continuous bout of sleep and visually finding the nearest local minimum below that value in the amplitude distribution, since SIA was previously found to occupy approximately 20% of sleep (Jarosiewicz et al., 2002).
- "Baseline SIA" was defined as periods of SIA during the baseline sleep session.
- All "Run" was taken from the baseline run period, using only bins whose power in the theta range (5-10 Hz) in the hippocampal EEG was at least 2 x the power in the LIA range (1-5 Hz).
- All "LIA" was taken from the baseline sleep period, using only bins whose LIA power was greater than theta power.
- "Lidocaine SIA" was defined as periods in the 10 min after lidocaine infusion whose mean hippocampal EEG amplitude fell below the amplitude threshold for baseline SIA; and "Serotonin SIA" was defined as periods in the 15 min after serotonin infusion whose mean hippocampal EEG amplitude fell below the amplitude threshold for baseline SIA.

5.4. RESULTS

Of the 9 rats used in this study, 6 exhibited effects of lidocaine infusions that were obvious by visual inspection of the raw data. Histology revealed that these 6 rats had fairly good cannula placements, and that the remaining 3 rats did not (Fig. 5.1). Of these 6 rats that showed an effect of lidocaine infusions, 5 also showed an effect of serotonin infusions. Only those data sets in which effects of infusions were obvious in the raw data were used in subsequent analysis.

A

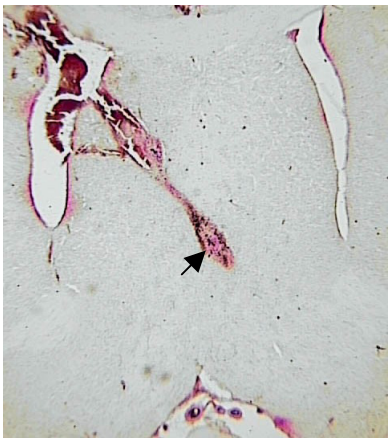

B

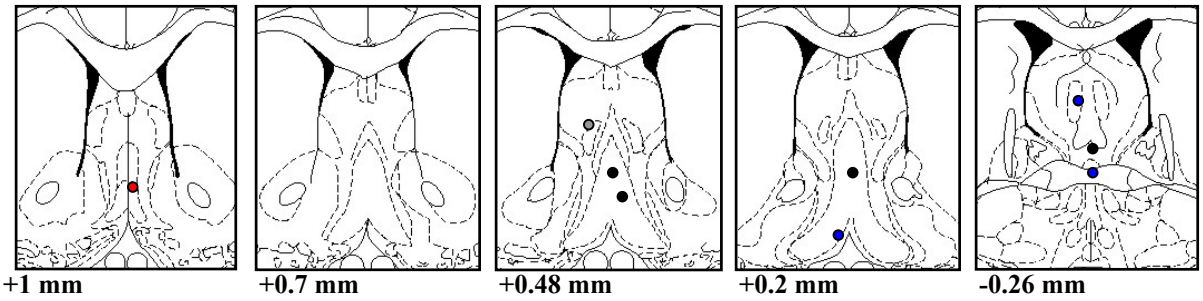

Figure 5.1 Cannula placement.

A, Example of good cannula placement (p175). Coronal section approximately 0.5 mm anterior to bregma. The arrow marks the location of the gliosis resulting from the infusions, in the middle of the MSDB. *B*, Infusion sites from all rats. The sites from the 4 animals in which the lidocaine and serotonin infusions had consistent effects across rats are shown in *black*; the site from the rat that showed an effect of both serotonin and lidocaine but whose serotonin infusion results were inconsistent with the others (p180) is shown in *red*; the site from the rat that showed an effect of lidocaine but not serotonin infusion (p178) is shown in *gray*; and the sites from the 3 rats in which neither infusion had an effect on hippocampal EEG are shown in *blue*. Brain atlas line drawings and coordinates are reprinted from Paxinos and Watson, Copyright 1997, The Rat Brain in Stereotaxic Coordinates on CD ROM, 3rd Ed., with permission from Elsevier.

5.4.1. Lidocaine Infusions

Lidocaine infusions into the MSDB had no noticeable effect on behavior. The mean movement speed during the run session before the infusion (grand mean and SEM = 19.0 ± 1.3 cm/sec) was not significantly different from the mean movement speed in the 10 min after rats were placed back on the arena after the infusion (18.2 ± 1.8 cm/sec). Hippocampal theta amplitude was markedly suppressed for approximately 5 min after the infusion (although some small-amplitude theta was still visible in most rats), and slowly recovered to near baseline levels over

approximately 20 min. Figure 5.2 shows an example of raw data at various times before and after the lidocaine infusion from one recording session. In this example, theta activity was almost completely suppressed for the first 3 min following the infusion. During this period of almost complete theta suppression, despite the fact that the rat was as active as during the run session before the infusion, the CA1 population activity appeared similar to baseline LIA: cells were diffusely active, with transient increases during sharp waves, and did not show any obvious place-related activity. Place-related cell activity reappeared before theta amplitude completely recovered (Fig. 5.2C). In the rest of the rats in this study, the initial suppression of the CA1 place-related activity did not occur, possibly because their cannula placements were not as accurate and their lidocaine infusions did not suppress theta activity as completely. This was likely to have also been the case in Mizumori et al. (1989), who found that CA1 pyramidal cells showed normal place-related activity following inactivation of the MSDB.

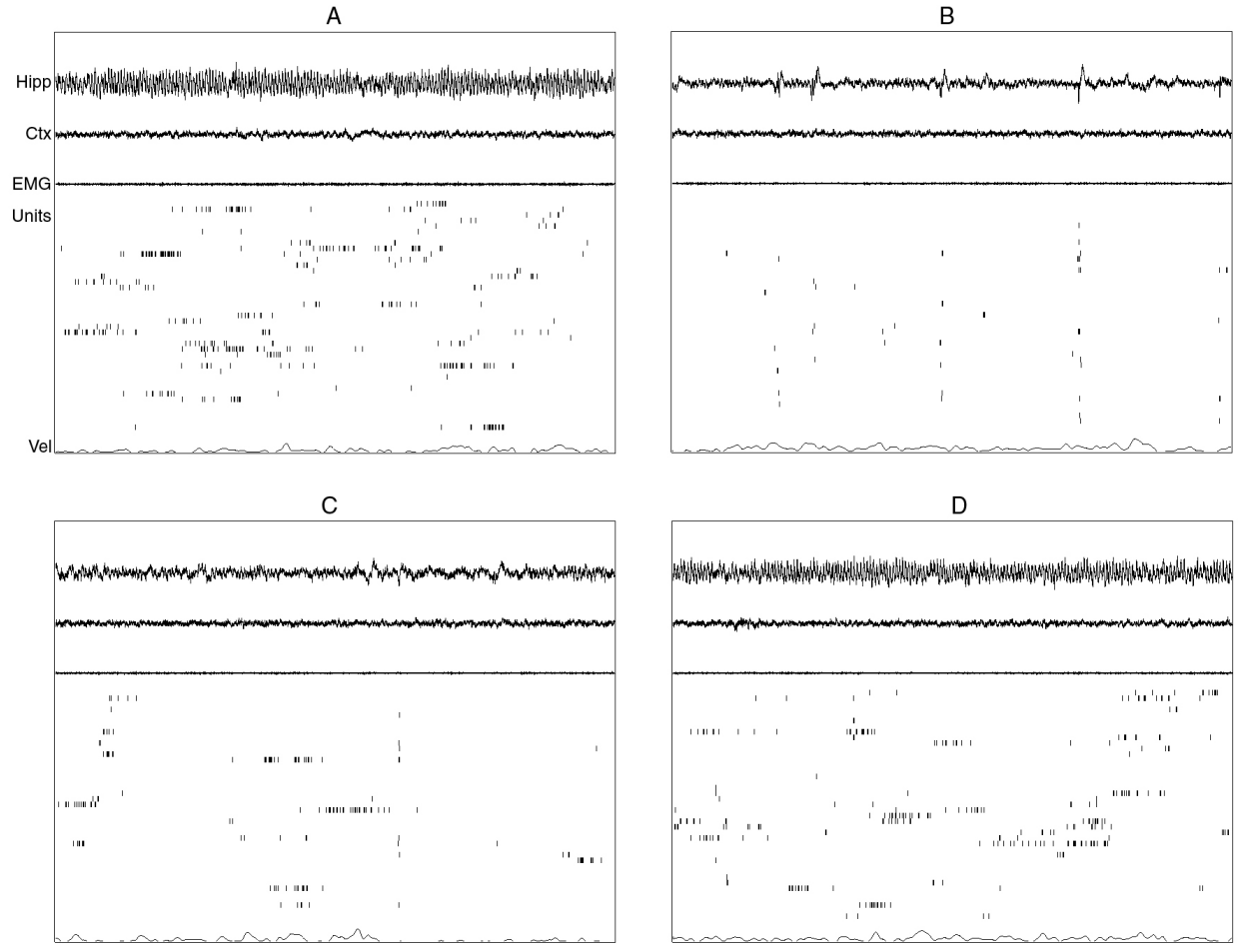

Figure 5.2. Example of raw data before and after lidocaine infusion into the MSDB.

Each panel contains a 20 second sample of simultaneously-recorded hippocampal EEG (*Hipp*), neocortical EEG (*Ctx*), EMG recorded from the dorsal neck musculature (*EMG*), spikes from ensembles of simultaneously-recorded CA1 pyramidal cells (*Units*), and the rat's velocity (*Vel*, arbitrary scale, with zero aligned at the bottom of the panel) from rat p175. *A* occurred about 20 min before the infusion. *B*, *C*, and *D* occurred about 3, 7, and 13 min after the infusion, respectively. The temporary suppression of theta amplitude after the lidocaine infusion, even at movement speeds comparable to baseline run, was clearly visible in the raw data. In this rat, during the initial, almost complete suppression of theta (*B*), the cell ensemble activity appeared more similar to that of baseline LIA than baseline theta, even when the rat was actively exploring the environment. Normal place-related activity resumed within a few minutes, accompanied by the appearance of small-amplitude theta (*C*). This initial change in population activity was not observed in the other rats, probably because their cannula placements were not as accurate and their lidocaine infusions did not completely suppress theta activity. LIA, briefly present during moments in which the rat stopped actively exploring the environment, was not visibly affected by lidocaine infusions (not shown).

To capture as much post-infusion data as possible without including too much of the recovery period, the first 10 min after rats were placed back on the arena was used as the post-infusion period for data analysis. For each data set, the effect of lidocaine infusions on the hippocampal EEG amplitude was quantified in two ways: 1) by calculating the mean amplitude of the hippocampal EEG averaged over the entire run session before the infusion and the mean amplitude of the hippocampal EEG averaged over the 10 min after the infusion, normalized by the mean baseline LIA amplitude, and 2) by the total time spent in SIA, defined as having a hippocampal EEG amplitude below a given threshold, during sleep before the infusion and during the whole 10 minute post-infusion period, to make sure the amount of SIA increased beyond what would be expected if the rat simply fell asleep after the infusion. All statistics were performed on the data set means. The hippocampal EEG amplitude in the post-infusion period (grand mean and SEM = 0.62 ± 0.04) was significantly lower than in the run session preceding the infusion (0.90 ± 0.05; 2-tailed paired t-test, $p = 0.0006$), and the percent time spent in "SIA" (as defined by hippocampal EEG amplitude alone) was significantly higher in the post-infusion period (57.1 ± 10.3 %) than in baseline sleep (16.7 ± 3.3 %; $p = 0.0061$). Thus, both indices show that lidocaine significantly suppressed hippocampal EEG amplitude.

Although the hippocampal desynchronization resulting from MSDB inactivation appears similar in the raw data to the SIA observed in baseline sleep, power spectral analysis revealed consistent and striking differences between them in both the hippocampal EEG (Fig. 5.3) and the neocortical EEG (Fig. 5.4). In the hippocampal EEG, the peak frequency of baseline SIA (6.46 ± 0.31 Hz) was significantly lower than that of baseline run (8.12 ± 0.10 Hz; $p = 0.0024$), consistent with Figures 2.2*C* and 3.4*A*. However, the peak frequency of lidocaine-induced desynchronization (8.12 ± 0.12 Hz) remained close to that of baseline run, and was significantly

higher than baseline SIA ($p = 0.0010$). These results are consistent with those of Kirk and McNaughton (1993), who showed that inactivation of the MSDB suppresses the amplitude, but not the frequency, of hippocampal theta activity.

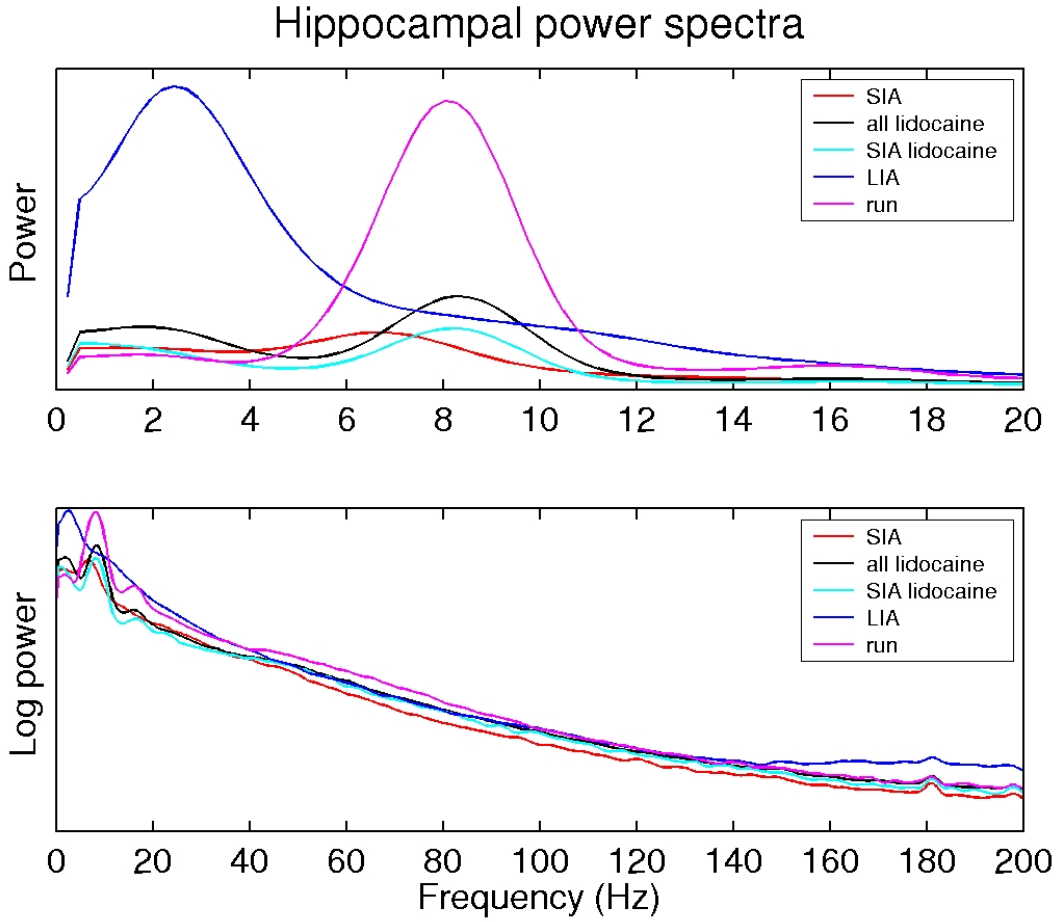

Figure 5.3. Hippocampal power spectra: lidocaine infusion.

Power spectra were constructed for baseline SIA and LIA from the baseline sleep period, for run from the baseline run period, for post-infusion periods of desynchronization (*SIA lidocaine*, those periods whose hippocampal EEG amplitude was lower than the amplitude threshold used for delineating baseline SIA), and for the EEG from the entire 10 min post-infusion period (*all lidocaine*). This plot shows the grand mean of the 6 data sets' mean power spectra. MSDB inactivation suppressed theta activity, but the peak of theta power remained at the same frequency as in baseline run rather than decreasing to levels near baseline SIA. The bottom plot shows log power as a function of frequency, revealing detail in the high frequency range. The peak at 180 Hz is attributable to artifact.

In the neocortical EEG, the mean power in the high frequencies (defined as 70 - 140 Hz, chosen to avoid the electrical artifact near 60 Hz and the chewing artifact at 140-160 Hz) during baseline SIA was significantly lower than it was during run ($p < 0.0001$), consistent with Figure 3.4*D*. However, the mean power in the high frequencies of the neocortical EEG during lidocaine-induced desynchronization was similar to run, and significantly higher than baseline SIA ($p =$

0.0018). Thus, although the hippocampal and neocortical EEG induced by lidocaine inactivation appeared similar to SIA in the raw data, the power spectra of these EEG signals revealed differences in both.

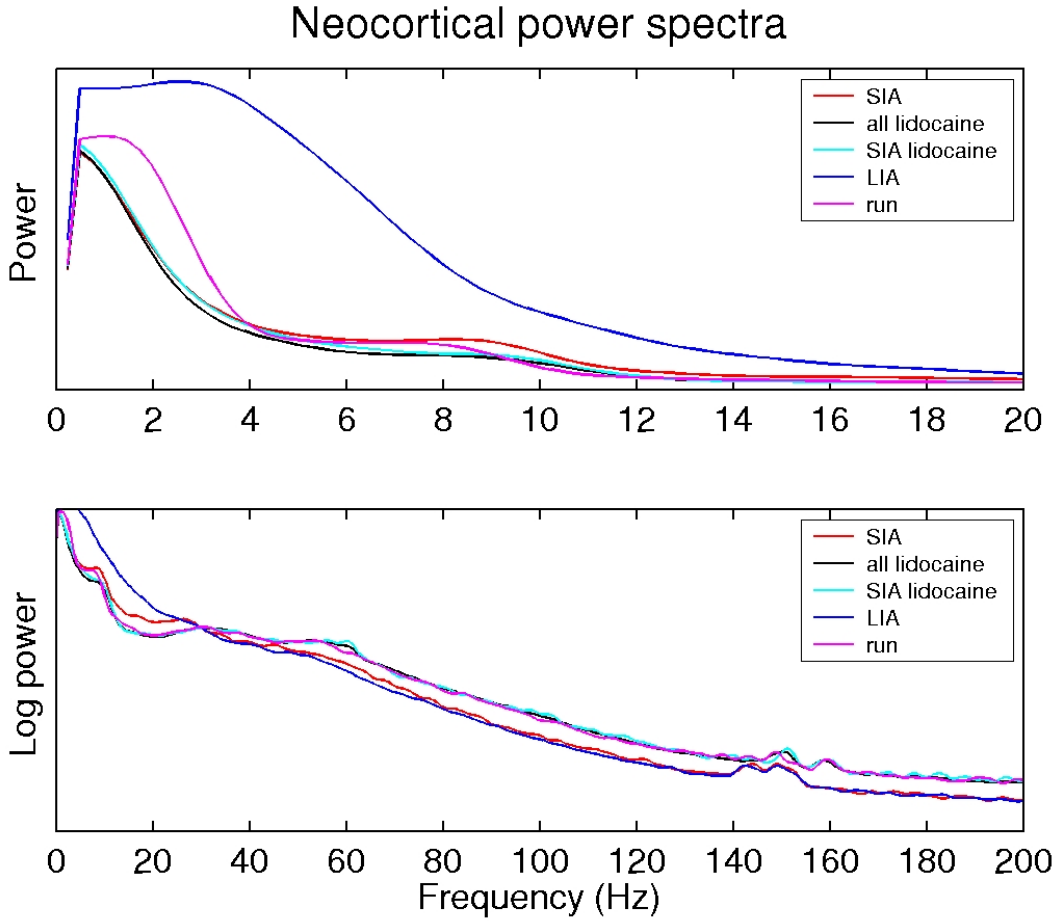

Figure 5.4. Neocortical EEG power spectra: lidocaine infusion.

The bottom plot reveals that the power in the high frequencies of the neocortical EEG following lidocaine inactivation of the MSDB was more similar to baseline run than to baseline SIA.

5.4.2. Serotonin Infusions

In 5 of the 6 rats whose lidocaine infusions suppressed hippocampal EEG amplitude, serotonin also suppressed hippocampal EEG amplitude. There was one exception rat (p178) in whom lidocaine infusions strongly suppressed the amplitude of hippocampal EEG but, for unknown reasons, serotonin had no obvious effect. This rat's serotonin data were excluded from subsequent analysis.

Unlike lidocaine infusions, serotonin infusions into the MSDB had a striking effect on behavior: for about 20 minutes after the infusion, most rats (4 of the 5 that showed an effect of serotonin) tended to lay on their abdomens with their eyes open, barely responsive to external stimuli, and it was difficult to induce them to move around. The mean movement speed across these 4 rats decreased from 22.0 ± 0.9 cm/s in the run session before the infusion to 6.2 ± 1.3 cm/s in the first 15 min after the infusion ($p = 0.0003$). During this "flopping" behavior, both the hippocampal EEG and population activity appeared similar to SIA, interrupted every few seconds by sharp waves (Fig. 5.5*A*,*B*). The hippocampal and neocortical EEG were low in amplitude, and the CA1 pyramidal cells showed the sparse activity that characterizes baseline SIA, with the cells active during flopping representing the rat's current location in space, and changing when the rat changed its position. When we did manage to induce the rats to move around by waving a paper towel for them to chase, theta activity appeared reduced in amplitude (Fig. 5.5*C*,*D*), but since the movement of these rats was not as robust as in baseline run, it was difficult to determine whether this was due to the serotonin infusion or simply the rats' slower and smaller movements.

One of the 5 rats that showed an effect of serotonin infusion on hippocampal EEG did *not* exhibit this flopping behavior (p180). This rat's mean movement speed during the run session before the infusion was 20.8 cm/s, and after the infusion it was 16.1 cm/s (its mean decreased slightly only because the food dispenser was periodically turned off to assess the effects of the serotonin infusion on LIA). In this rat, hippocampal theta amplitude was clearly suppressed (but not absent) during active exploration (Fig. 5.8), but the place-related activity of the CA1 pyramidal cells appeared normal. Because this rat's results differed slightly from the others, its data are presented separately below. The statistics that follow are based on the data set means from the 4 rats whose results were consistent.

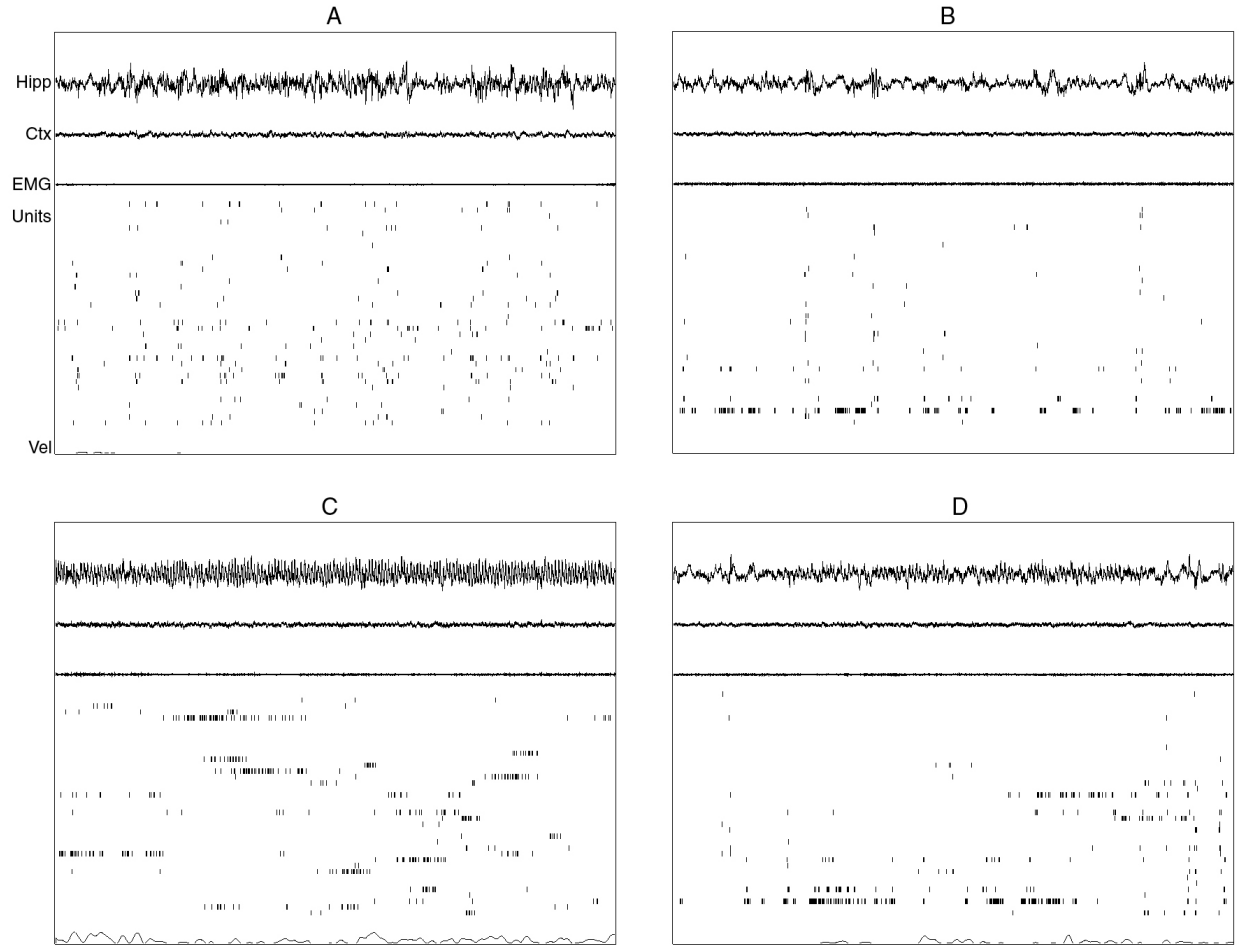

Figure 5.5. Example of raw data before and after serotonin infusion into the MSDB.

Each panel contains a 20 second sample of simultaneously-recorded hippocampal EEG (*Hipp*), neocortical EEG (*Ctx*), EMG recorded from the dorsal neck musculature (*EMG*), spikes from ensembles of simultaneously-recorded CA1 pyramidal cells (*Units*), and the rat's velocity (*Vel*, arbitrary scale, with zero aligned at the bottom of the panel), from rat p175. *A*, An example of baseline LIA, which normally occurs during periods when the rat is awake but sitting quietly. *B*, The dominant state following serotonin infusion, accompanied by "flopping" behavior. Both the EEG and population activity appeared very similar to SIA instead of LIA. *C*, An example of baseline theta. *D*, During the rare, brief periods of movement following the serotonin infusion (this sample was taken from about 5 min after the infusion), theta activity was still visible in the EEG, but appeared diminished in amplitude.

The effects of serotonin infusions on hippocampal EEG usually lasted much longer than the effects of lidocaine infusions; in some cases, the EEG suppression was usually visible for up to an hour after the serotonin infusion. The behavioral effects of serotonin usually lasted ~20 min. For analysis of the serotonin infusion data, we used the first 15 min after the rat was placed back on the arena as the post-infusion period. The mean hippocampal EEG amplitude in the post-infusion period (0.72 ± 0.05) was significantly lower than in the run session preceding the infusion (0.97 ± 0.06; $p = 0.02$). This measure underestimates the robustness of the EEG

suppression because large-amplitude sharp waves still occurred frequently, intermixed with the hippocampal EEG suppression, during the flopping following serotonin infusions. The percent time spent in "SIA" (as defined by hippocampal EEG amplitude alone) was significantly higher in the post-infusion period (41.7 ± 11.0%) than it was in baseline sleep (9.3 ± 0.7%; p = 0.018); thus, the time spent in SIA increased beyond what would be expected if the serotonin infusion had simply induced sleep.

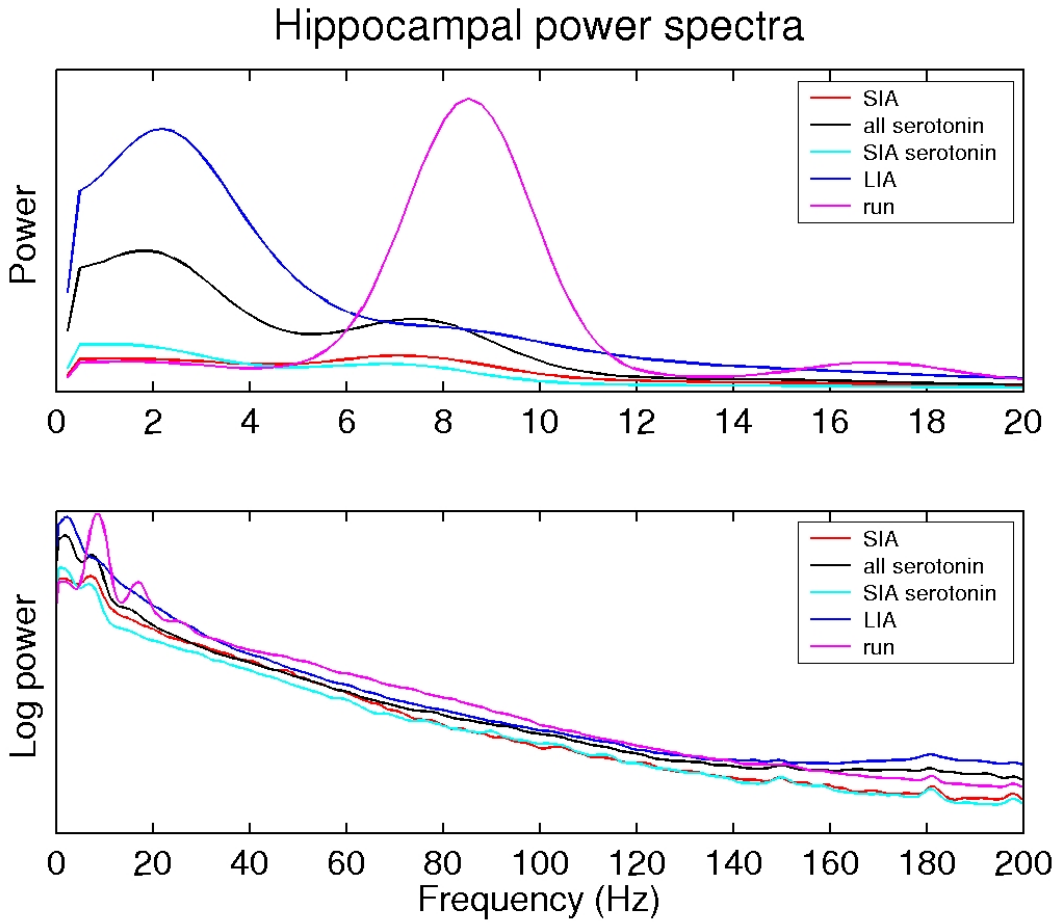

Figure 5.6. Hippocampal power spectra: serotonin infusion.

Power spectra were constructed for baseline SIA and LIA from the pre-infusion sleep period, for run from the pre-infusion run period, for post-infusion periods of desynchronization (*SIA serotonin*, those periods whose hippocampal EEG amplitude was lower than the amplitude threshold used for delineating baseline SIA), and for EEG from the entire 15 min post-infusion period (*all serotonin*). This plot shows the grand mean of the 4 consistent data sets. Like lidocaine infusions, serotonin infusions suppressed hippocampal EEG amplitude, but unlike lidocaine infusions, the peak frequency of the EEG following serotonin infusions was similar to the peak frequency of baseline SIA.

Serotonin-induced desynchronization, unlike lidocaine-induced desynchronization, was found to be similar to baseline SIA not only in the appearance of the raw hippocampal EEG, but also in its power spectrum (Fig. 5.6). In the hippocampal EEG, the peak frequency of baseline SIA (7.07 ± 0.15 Hz) was again significantly lower than that of baseline run (8.48 ± 0.09 Hz; p = 0.0013); the peak frequency of serotonin-induced SIA (6.63 ± 0.45 Hz) was also significantly lower than baseline run (p = 0.0106), and comparable to baseline SIA.

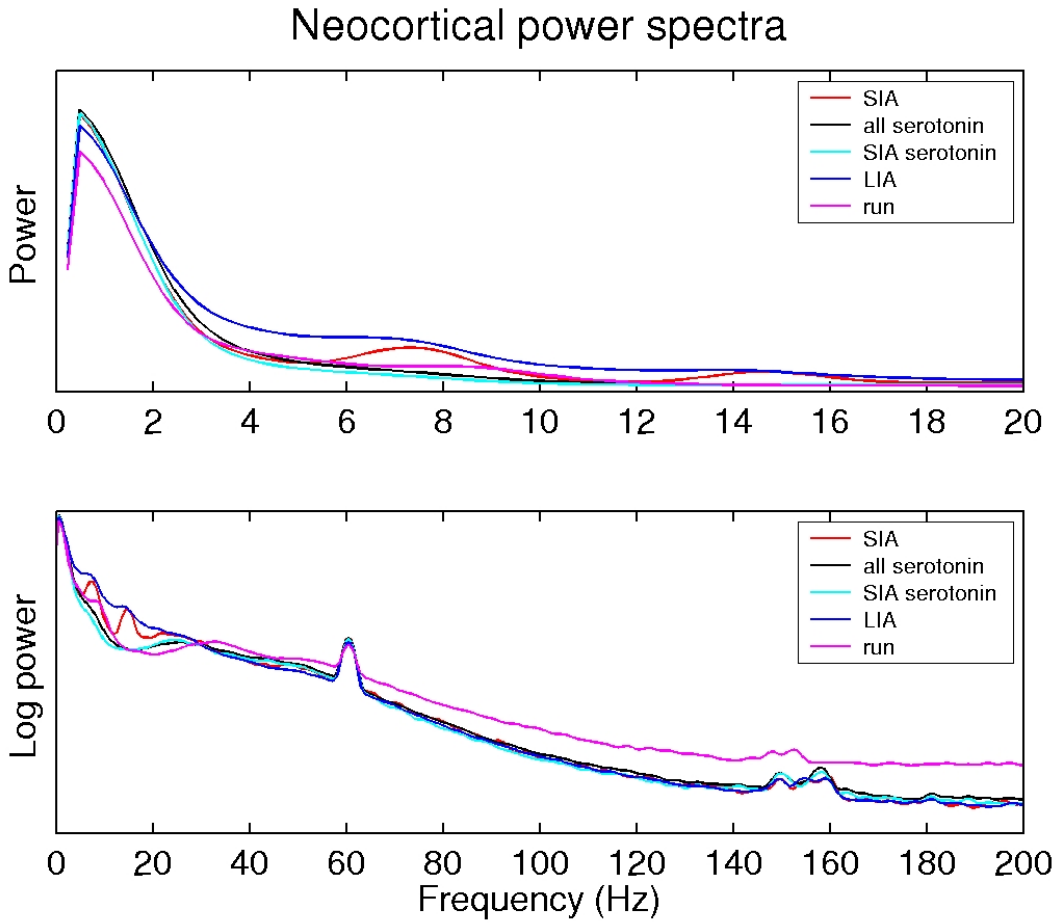

Figure 5.7. Neocortical power spectra: serotonin infusion.

Grand mean of 4 consistent data sets. Unlike lidocaine-induced SIA (*Fig. 5.4*), serotonin-induced desynchronization resembled baseline SIA in its low neocortical EEG power in the high frequency range (70-140 Hz).

The power spectrum of the neocortical EEG following serotonin infusion was also similar to that of baseline SIA (Fig. 5.7). Again, the power in the high frequencies of baseline SIA was significantly lower than that of run (p = 0.0131). Serotonin-induced desynchronization was also

accompanied by significantly lower power in the high frequencies of the neocortical EEG than run ($p = 0.0044$).

Thus, serotonin-induced desynchronization resembled baseline SIA not only in the appearance of its raw hippocampal and neocortical EEG, but also in the peak frequency of the hippocampal EEG and in the power in the high frequencies of the neocortical EEG. Figure 5.8 summarizes the effects of lidocaine and serotonin infusions from the consistent data sets.

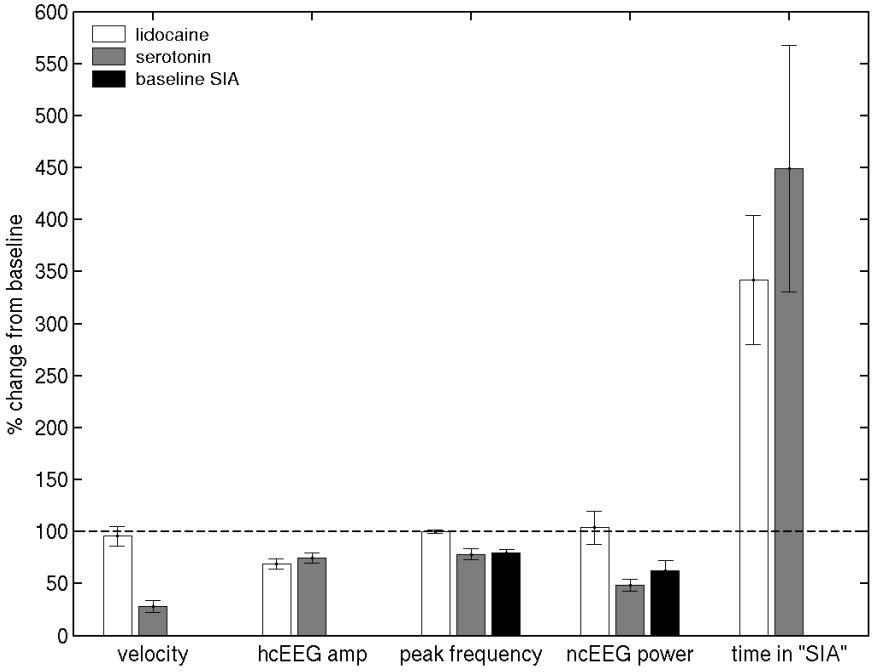

Figure 5.8. Summary of infusion results.

All *velocity*, *hcEEGamp*, *peak frequency*, and *ncEEG power* values are calculated separately for each data set, normalized by their mean values during baseline run in that data set, and then averaged. For *time in "SIA"*, the baseline was normalized by the time spent in baseline SIA.

• Lidocaine infusions into the MSDB had no noticeable effects on the rats' behavior, and their velocity (*velocity*) remained similar to baseline run. Serotonin infusions, on the other hand, produced a striking cessation of activity.

• Both serotonin and lidocaine infusions into the MSDB suppressed hippocampal EEG amplitude (*hcEEG amp*) relative to baseline run.

• Following lidocaine infusions, the peak frequency in the theta range of the hippocampal EEG (*peak frequency*) and the power in the high frequencies of the neocortical EEG (*ncEEG power*) were more similar to baseline run than to baseline SIA.

• The rats spent more time in "SIA," as defined by EEG amplitude alone (*time in "SIA"*), following serotonin or lidocaine infusions, than they spent in SIA during baseline sleep.

In the rat that did not flop after the serotonin infusion (p180), the serotonin infusion still suppressed hippocampal EEG amplitude (Fig. 5.8) and induced a shift in peak theta frequency to that of baseline SIA (Fig. 5.9). While this rat was actively foraging following the serotonin

infusion, theta activity was present but greatly suppressed in amplitude, and CA1 pyramidal cells exhibited normal place-related activity (Fig. 5.9*D*). Unlike the other rats, this rat showed high power in the high frequencies of the neocortical EEG following the serotonin infusion, similar to baseline run (Fig. 5.9). Its infusion site was found to be about 0.5 mm anterior and 0.5 mm ventral to the center of the MSDB, centered in the anterior part of the vertical limb of the diagonal band of Broca (Fig. 5.1). It is likely that this rat's anomalous effects were attributable to its somewhat anomalous cannula placement.

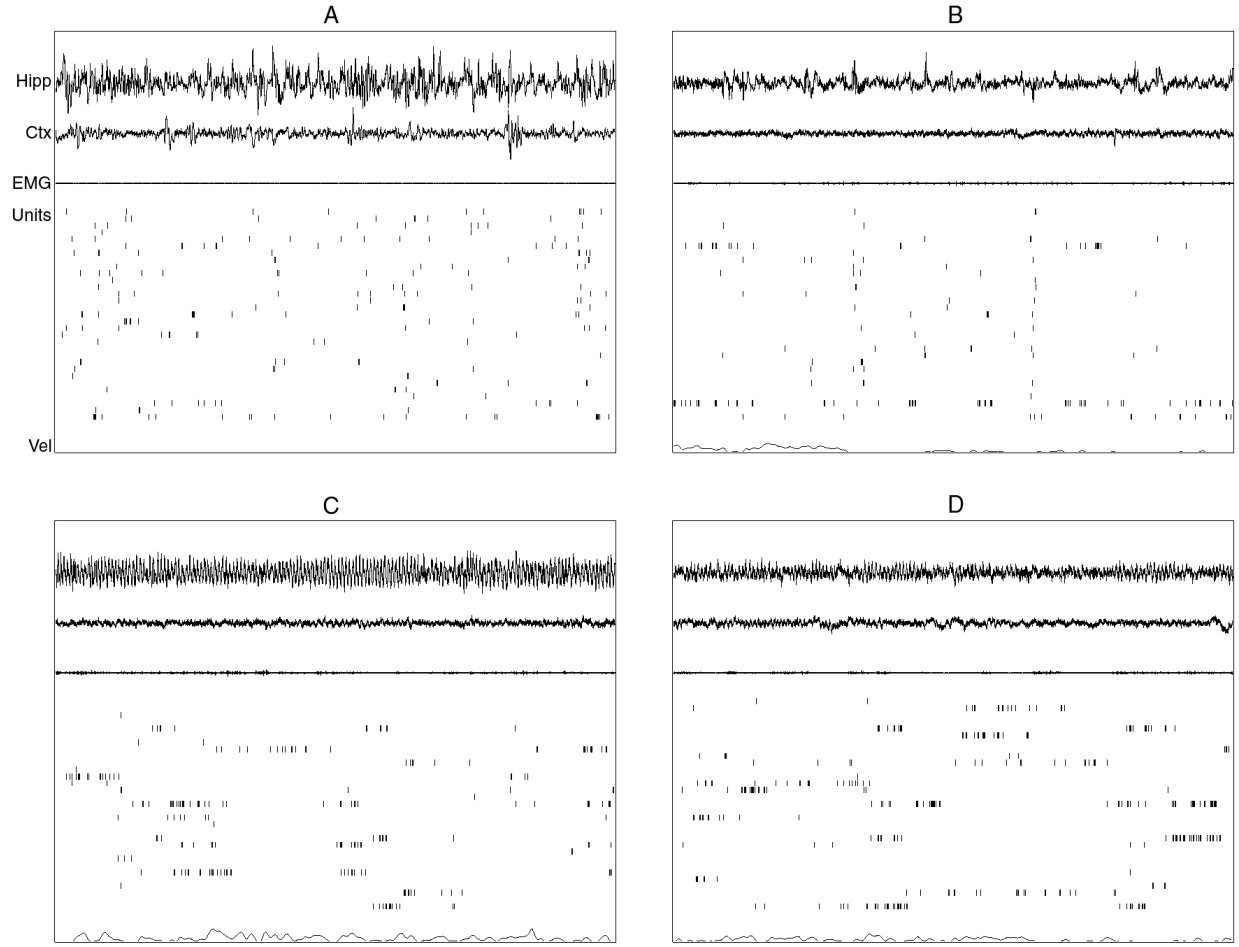

Figure 5.9. Example of raw data from p180, an anomalous rat in which the serotonin infusion did not induce flopping.

A, An example of baseline LIA. *B*, The hippocampal physiology accompanying periods of quiet waking, which were much less frequent in this rat than the others, following serotonin infusion. Nevertheless, during these periods when LIA would normally be expected, both the EEG and population activity appeared very similar to SIA. *C*, An example of baseline theta. *D*, During active exploration, the predominant behavioral state in this rat following serotonin infusion, theta activity was still visible in the EEG, but it was reduced in amplitude. Place-related activity of the CA1 pyramidal cells was normal.

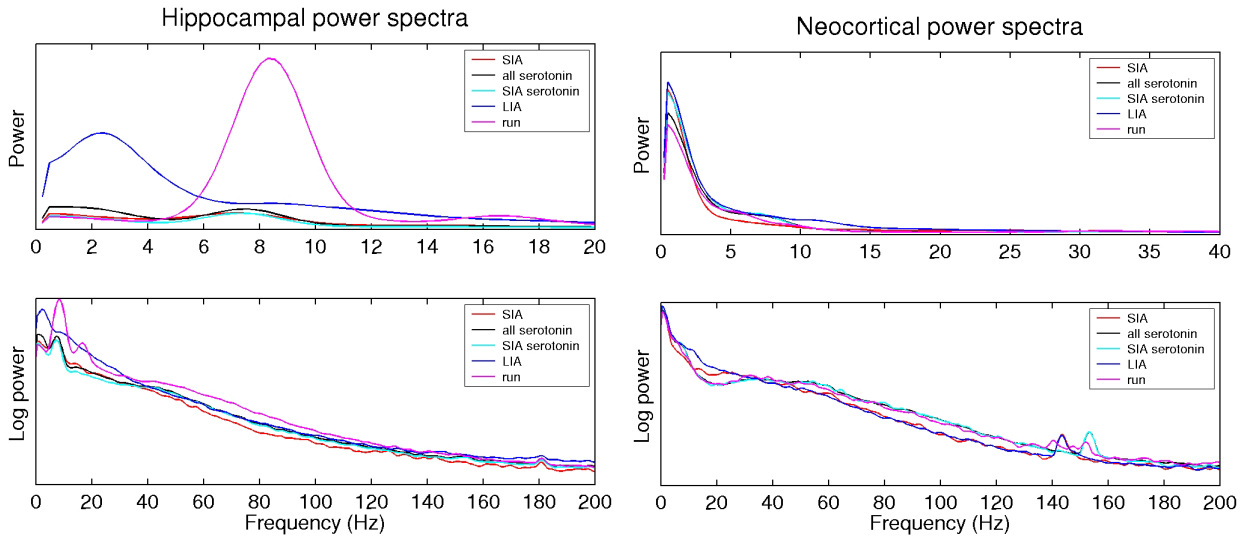

Figure 5.10. Hippocampal and neocortical power spectra from the anomalous rat.

The hippocampal EEG power spectrum of the rat that did not flop following serotonin infusion (p180) was consistent with the other data sets: serotonin infusions suppressed EEG amplitude and shifted the peak frequency near that of baseline SIA. However, the neocortical EEG power spectrum was inconsistent with the other rats: the power in the high frequencies during serotonin-induced desynchronization remained similar to run, rather than reducing to levels near baseline SIA.

5.5. DISCUSSION

These studies showed that (1) when the MSDB was inactivated by lidocaine microinfusion, the resulting "desynchronization" of the hippocampal EEG consistently differed from baseline SIA in its hippocampal and neocortical power spectra: the peak frequency in the theta range of the hippocampal EEG and the amplitude in the high frequencies of the neocortical EEG were more similar to run than to baseline SIA. (2) When serotonin was microinfused into the MSDB, inter-sharp wave periods of LIA and theta activity were suppressed in amplitude, and the peak frequency in the theta range of the hippocampal EEG and, in all but 1 rat, the power in the high frequencies of the neocortical EEG actually matched those of baseline SIA. The sparse, place-related hippocampal population activity that characterizes baseline SIA was also present in the periods of suppressed LIA during the typical "flopping" behavior following serotonin infusion.

The rat that did not flop also did not show a suppression of power in the high frequencies of the neocortical EEG. Taken in combination with the finding that SIA is similar to the other

sleep states in neocortical EEG power in the high frequencies (see Fig. 3.4), the most parsimonious explanation for these results is that the power in the high frequency range of the neocortical EEG is low when the rat is still, but high when the rat is actively moving around and/or engaged in associated behaviors such as whisking. Evidence for the latter comes from the finding that stimulating whiskers in an anesthetized rat produces an increase in high frequency oscillations (> 200 Hz) in the EEG of the barrel cortex (Jones and Barth, 1999). If the rat's behavior is really the sole determinant of the amount of power in the high frequencies of the neocortical EEG, then our finding that the desynchronization in the rats that flopped following the serotonin infusion resembles baseline SIA in neocortical EEG, but that the desynchronization following lidocaine infusion does not, should not be taken as evidence that serotonin but not lidocaine induces SIA. However, the frequency of the peak in the theta range was reduced in all rats that showed any effect of serotonin infusions, including the anomalous rat whose behavior did not change during the post-infusion period. This effect would need to be confirmed in more rats, but it suggests that the hippocampal desynchronization elicited by serotonin infusions in the MSDB matches that of baseline SIA in at least one non-trivial way in which the hippocampal desynchronization elicited by lidocaine inactivation of the MSDB does not.

The finding that serotonin infusions into the MSDB result in a hippocampal EEG pattern that has a peak in the low-frequency theta range provides evidence that the MSDB can affect the frequency of the hippocampal theta rhythm. This finding contradicts the hypothesis put forth by Kirk and McNaughton (1993) that the SuM, not the MSDB, is the pacemaker of the hippocampal theta rhythm, based on their finding that inactivation of various points along the ascending brainstem synchronizing system from the reticular nucleus pontis oralis (PnO) to the supramammillary nucleus (SuM), but not of pathways from the SuM to the MSDB or of the MSDB itself, reduced the frequency of hippocampal theta rhythm. However, Kirk and McNaughton (1993) were assessing effects on the frequency of theta elicited by PnO stimulation in urethane-anesthetized rats; it is possible that slightly different mechanisms underlie the generation of naturally occurring theta activity in freely moving rats. This possibility is supported by the finding that in awake, behaving rats, SuM lesion or inactivation does not suppress the frequency of hippocampal theta activity nearly as much as it does in urethane-anesthetized rats (McNaughton et al., 1995; Thinschmidt et al., 1995). Another possibility is that, under normal conditions, the MSDB relays the frequency of theta drive that has already been

established in the SuM, but that increases in serotonin levels in the MSDB can reduce the firing frequency of its cells in a way that simple inactivation of the MSDB, or of afferents to the MSDB, cannot.

The finding that serotonin, but not lidocaine, in the MSDB produces a desynchronization that closely resembles SIA, taken with the evidence that stimulation of the MnR produces hippocampal desynchronization (Macadar et al., 1974; Assaf and Miller, 1978; Vertes, 1981), probably via serotonergic input to the MSDB (Vertes and Kocsis, 1997; Milner and Veznedaroglu, 1993; Kia et al., 1996; Alreja, 1996; Leranth and Vertes, 1999; Assaf and Miller, 1978), and that serotonergic MnR cells increase their firing at the offset of REM episodes and in response to visual or auditory stimuli (Rasmussen et al., 1984), leads us to propose the following model for the generation of SIA. During active awake behaviors, serotonin levels are high and steady, and rhythmic input from the MSDB induces theta activity in the hippocampus. In quiet waking and SWS, serotonin levels are low and theta drive is absent, and the hippocampus spontaneously produces LIA. If the animal is suddenly aroused, there is a sudden increase in MnR activity, resulting in a sudden increase in brain serotonin levels. The effect of the sudden increase in serotonin levels in the MSDB is a simultaneous inhibition of cholinergic septohippocampal projection cells (Milner and Veznedaroglu, 1993; Kia et al., 1996) and excitation of GABAergic septohippocampal projection cells (Alreja, 1996; Leranth and Vertes, 1999), sending a sudden stream of predominantly non-rhythmic input into the hippocampus. This input shuts down the intrinsic mechanisms producing LIA without driving theta activity, resulting in hippocampal SIA. This model predicts that SIA in the hippocampal EEG occurs concomitantly with increases in MnR cell activity, which could be tested by simultaneous recording of MnR cell activity and hippocampal EEG.

Chapter 6. SUMMARY AND CONCLUSIONS

This dissertation was motivated by the finding that, when rasters of spikes from simultaneously recorded hippocampal CA1 pyramidal cells are viewed simultaneously with hippocampal EEG from a sleeping rat, a third physiological state, strikingly different from both REM and SWS, is revealed (Skaggs, 1995). This state is likely to correspond to "low-amplitude irregular activity" (Pickenhain and Klingberg, 1967), also called "small-amplitude irregular activity" or SIA (Vanderwolf, 1971; Whishaw, 1972; see O'Keefe and Nadel, 1978, for a review), which has been reported to occur when a rat is startled out of sleep. The following is a summary and discussion of the findings that each chapter in this dissertation has added to our understanding of the SIA state.

6.1. HIPPOCAMPAL POPULATION ACTIVITY DURING THE SMALL-AMPLITUDE IRREGULAR ACTIVITY STATE IN THE RAT (CHAPTER 2)

This study was aimed at more carefully characterizing the hippocampal EEG and population activity of the SIA state observed spontaneously during sleep. We recorded ensembles of hippocampal CA1 pyramidal cells and hippocampal EEG in rats foraging for randomly scattered food pellets in an open arena and sleeping in a designated "nest," a towel-lined bowl, on the floor of the open arena. It was found that:

1) **SIA occurs frequently during sleep in the rat.**
2) **Hippocampal CA1 pyramidal cell activity during SIA is sparse, with the same subset of cells (3-5% of the total recorded population) active across long sequences of episodes.**
3) **SIA episodes are irregularly intermixed with LIA during periods of SWS, occupying ~33% of SWS and 20% of total sleep, usually lasting ~2 seconds but occasionally much longer, and occurring on average 30-44 seconds apart.**
4) **The population activity during SIA statistically resembled the population activity during waking states while the rat was in its sleeping-nest, and SIA-active cells**

sometimes changed when the rat changed its position in the nest; i.e. the cells active during SIA are place cells with place fields in the location in which the rat is sleeping.

A major contribution of this study was the finding that hippocampal CA1 pyramidal cells show place-related activity during SIA. Subsequent autocorrelation analysis revealed that SIA-active cells show little or no residual theta modulation during SIA. These are novel and important findings in light of the growing confidence among hippocampal physiologists that place-related activity and the theta rhythm are functionally intertwined. For example, the findings that pyramidal cell spike times are modulated by the theta rhythm (Buzsáki et al., 1983; Fox et al., 1986), and that spikes advance to earlier phases of the theta cycle as the rat passes through a place field, a phenomenon termed "phase precession" (O'Keefe and Recce, 1993; Skaggs et al., 1996), have inspired numerous computational models of how the phase relationship of place cell spike timing might influence the properties of place-related activity and underlie the various forms of learning and memory that have been attributed to the hippocampus (e.g. Skaggs, 1995; Skaggs et al., 1996; Tsodyks et al., 1996; Wallenstein and Hasselmo, 1997; Sohal and Hasselmo, 1998; Jensen and Lisman, 2000; Huxter et al., 2003; Sato and Yamaguchi, 2003). Our finding that place-related CA1 cell activity also occurs during SIA demonstrates that place selectivity is not dependent on theta activity or theta modulation, which should be taken into account in future models of hippocampal function.

Our observations that SIA occurs so frequently within LIA during SWS (often within minutes of REM onset), that it consistently occurs just after REM, and that its occurrence during sleep is consistent across animals suggest that SIA is a sleep state. Conversely, the fact that the spontaneous SIA state we observe during sleep (at least superficially) resembles the waking SIA state reported in the literature, the finding that SIA rarely occurs immediately before or during REM, and the finding that the hippocampal population activity during SIA reflects the rat's awareness of its location in space suggest that SIA is a waking state. Thus, the issue is raised whether SIA is a sleep state whose physiology resembles that of waking SIA, in the same way that REM is a sleep state whose physiology resembles waking theta, or whether it is a waking state that repeatedly interrupts sleep. A third possibility is that both of these manifestations of SIA correspond to a single state that falls somewhere toward the middle of a continuum of levels of arousal. Such a continuum appears to exist, for instance, in humans, in whom the transition from waking to sleep is more accurately depicted as an interval of time rather than an instant,

when both EEG and behavioral responsiveness are taken into account (Ogilvie and Wilkinson, 1988). Furthermore, during normal sleep in humans, transitory states of heightened arousal exist, lasting on the order of seconds to tens of seconds and occurring every 4-5 minutes, called "phases d'activation transitoire" (Schieber et al., 1968, 1971; Ehrhart and Muzet, 1974) or "micro-arousals" (Halász et al., 1979; for review, see Terzano et al., 1991). These resemble arousal in EEG, EMG, and heart rate; they are often accompanied by shifts in posture or other movements; they occur more frequently during "lighter" stages of sleep than "deeper" stages; and they can be elicited by auditory stimuli, supporting the idea that they are states of increased arousal. Conversely, eliciting a large number of them seems to reduce the number of spontaneously occurring ones, so that their total incidence throughout the night is preserved (Ehrhart and Muzet, 1974); they do not reset the sleep cycle; and they are rarely recalled by the sleeper upon awakening, supporting the idea that they are nevertheless a natural part of sleep. These micro-arousals are likely to be the human analogue of SIA; like micro-arousals, perhaps SIA episodes are simply transient states of relatively heightened arousal that occur during normal sleep.

There is no consensus in the literature on an absolute definition of arousal level, but several characteristics are commonly used heuristically to assess arousal level: motion, EEG, EMG, etc. During LIA and theta activity, whether a rat is awake or asleep can be determined by whether or not it is moving. In the case of SIA, such an assessment is inconclusive, because rats are reported to be motionless during waking SIA as well. Neocortical EEG desynchronization is taken as a sign of cortical arousal because it is present during active waking (Pravdich-Neminsky 1913; Berger 1929; Moruzzi and Magoun 1949; Green and Arduini, 1954; Pickenhain and Klingberg, 1967; O'Keefe and Nadel, 1978; Vanderwolf, 1969; Whishaw, 1972; Gottesmann, 1992). However, EEG-based criteria were developed as a secondary, post hoc measure of behavioral state transitions; EMG, a measure of muscle tone, more directly measures behavioral phenomena that originally motivated the conception of this dichotomy. EMG amplitude is highest in active waking (during theta activity), decreases in quiet waking (during LIA), and decreases further during SWS, reaching a minimum during REM (Timo-Iaria et al., 1970; Kohn et al., 1974; Johns et al., 1977). Thus, the findings reported in Chapter 2 led us to characterize the level of arousal during SIA by recording EMG and neocortical EEG and comparing SIA to the other well-characterized physiological states in these standard measures of arousal level.

Additionally, we directly tested whether spontaneous SIA and SIA elicited by auditory stimuli during sleep correspond to a single state by playing controlled auditory stimuli to the rats during sleep, in the spirit of Pickenhain and Klingberg (1967), and comparing the profile of hippocampal EEG and population activity, neocortical EEG, and EMG between elicited and spontaneous SIA.

6.2. LEVEL OF AROUSAL DURING THE SMALL IRREGULAR ACTIVITY STATE IN THE RAT (CHAPTER 3)

To answer the questions raised by Chapter 2, hippocampal and neocortical EEG, neck EMG, and hippocampal ensemble activity were recorded simultaneously from behaving rats presented with auditory stimuli. This study showed that:

1) **Auditory stimuli presented during sleep reliably elicited SIA episodes very similar to spontaneous SIA episodes in hippocampal and neocortical EEG amplitude and power spectra, EMG amplitude, and hippocampal CA1 population activity.**
2) **The EMG amplitude, a measure of muscle tonus and therefore commonly used to judge behavioral arousal level, is significantly lower in elicited and spontaneous SIA than in run, slightly but significantly higher than in REM, and comparable to LIA.**
3) **The neocortical EEG, which is commonly used to judge the level of cognitive arousal, is desynchronized in spontaneous and elicited SIA.**
4) **The hippocampal EEG during SIA has a small peak in the low frequency theta range.**
5) **In the neocortical EEG, there is more power across the high frequency range during run than during SIA.**

The finding that spontaneous and elicited SIA appear so similar across all these measures that are found to vary systematically across the other physiological states suggests that what we call "spontaneous" SIA might also be SIA elicited by a stimulus, but one that is uncontrolled or unobserved by the experimenter. This appears to be the case in the probable human analogue of SIA, "micro-arousals," which appear to occur spontaneously during sleep but can also be elicited by auditory stimuli (Schieber et al., 1968, 1971; Ehrhart and Muzet, 1974; Halász et al., 1979; for review, see Terzano et al., 1991). The neocortical EEG provides provisional evidence that

SIA is a state of heightened neocortical arousal, and the EMG provides evidence that SIA is a state of low behavioral arousal. Taken with the finding that spontaneous SIA and elicited SIA elicited so strongly resemble one another, and with the finding that the SIA population activity reflects the rat's awareness of its current location in space (Jarosiewicz et al., 2002), this study provides compelling evidence that the rat's arousal level during SIA is higher than the other well-characterized sleep states, but it is not as high as in active waking.

This study also showed that the hippocampal EEG during SIA has a small peak in the low frequency theta range. This finding suggests a possible relationship between SIA and "type 2" theta (Kramis et al., 1975; Bland, 1986). Type 2 theta is rarely observed in awake behaving rats, but is common in rabbits and guinea pigs, in whom it can readily be elicited by auditory stimuli during immobility (Kramis et al., 1975; Sainsbury and Montoya, 1984; for review, see Bland, 1986). The fact that SIA can be elicited similarly, and that it has a small power peak in the low-frequency theta range, suggests that SIA might simply be the rat analogue of type 2 theta. However, robust type 2 theta, comparable in amplitude to LIA, is present in urethane-anesthetized rats at the same recording site as baseline SIA (unpublished observations), and robust type 2 theta can be elicited by auditory stimuli in immobile rats in the presence of cats or ferrets (Sainsbury et al., 1987). Thus, either SIA is not simply the rat analogue of type 2 theta, or the amplitude of type 2 theta can vary significantly in different circumstances. Some studies report a positive correlation between theta frequency and/or amplitude and movement speed (Whishaw and Vanderwolf, 1973; McFarland et al., 1975; Rivas et al., 1996; Slawinska and Kasicki, 1998; but see Shin and Talnov, 2001); thus, another possibility is that the low frequency, low amplitude theta visible in the SIA power spectrum is attributable to type 1 theta emerging at the end of longer SIA episodes when the rat makes small, slow movements.

Examination of the neocortical EEG power spectra unexpectedly reveals that run has more power across the high frequency range than SIA. This finding has several interesting implications, among them that what appears to be "desynchronization" in the raw EEG is not a homogeneous state, and thus, that its use as a measure of cognitive arousal should be made with discretion. It is possible that the amount of power in the high frequency range of the neocortical EEG is simply attributable to whether or not the rat is moving, because it is also low during REM and SWS.

Despite our efforts, we were unable to elicit robust SIA during active waking. One possible explanation is that inducing freezing by external stimuli is somehow not adequate to produce SIA during waking; it might be necessary for the freezing to be somehow initiated by the rat without influence from external cues. Another possibility is that waking SIA is simply much less robust than SIA occurring during sleep. Upon closer inspection of the two articles in which SIA was described to occur in rats that abruptly suppress ongoing movement (Bergmann et al., 1987; Vanderwolf, 1971; Whishaw, 1972), we found that the only examples shown of SIA in rats were in response to auditory stimuli administered during sleep; the two examples of SIA during waking (both in Whishaw, 1972) were actually taken from a Mongolian gerbil. Thus, it is likely that the SIA that occurs in rats during waking is simply not as robust as it is during sleep, or as it is in other species.

Besides recording EMG and neocortical EEG, a third common way to assess an animal's arousal level is by testing its responsiveness to sensory stimuli. One difficulty with this approach is in finding a satisfactory definition of an "arousal response." If one uses a physiological measure to axiomatically define an arousal response, one begs the question. For example, in some studies, neocortical desynchronization is considered a sufficient arousal response (Neckelmann and Ursin, 1993); the problem arises when one desires to test the level of arousal of a state that is already accompanied by neocortical desynchronization. If one instead uses a behavioral definition of arousal response, for example by requiring the rat to make an overt orienting movement or by training the rat to respond in a particular way to avoid a punishment or obtain a reward, it takes a long time (~5-10 minutes) for the rat to fall back asleep. This makes it difficult to obtain good sampling in a recording session of a reasonable duration. The other difficulty with this approach is in choosing an appropriate stimulus to which to test the animal's responsiveness. If the stimulus is meaningless, the animal rapidly habituates to it with repeated exposure and ceases to respond in any physiological state. For example, Dillon and Webb (1965) reported that "on some occasions the animal would awaken from either type of sleep as a chair creaked or a pencil fell, and on other occasions they would sleep through our maximum stimulus (approximately 100 db)" (p. 447). Habituation can be avoided by varying the stimuli, but then it would become difficult to distinguish whether differences in the animal's responsiveness are attributable to the animal's arousal level or to the stimulus parameters. Habituation can also be avoided by using a single but meaningful stimulus, for example by training the animal to respond

to the stimulus in a certain way to obtain a reward or to avoid a punishment. But this is again subject to the issue of poor sampling in a limited recording time.

Instead of attempting to overcome these hurdles, we took advantage of the finding that the hippocampal population activity during SIA reflects the rat's current location in space to test the rat's "cognitive responsiveness" during SIA. Namely, we wanted to test whether the place-related activity during SIA arises as a result of active processing of current sensory information during SIA, or whether it reflects a memory for the location in which the rat fell asleep. This issue was addressed in Chapter 4.

6.3. HIPPOCAMPAL PLACE-RELATED ACTIVITY DURING THE SMALL IRREGULAR ACTIVITY STATE DOES NOT REFLECT THE PROCESSING OF CURRENT VISUAL INFORMATION (CHAPTER 4)

To test whether the place-related CA1 population activity during SIA reflects the processing of current visual information, or whether it reflects a memory for the location in which the rat fell asleep, we recorded spikes from ensembles of CA1 pyramidal cells in rats that were moved to a new location while sleeping. We did this by allowing the rat to fall asleep along the edge of a large circular arena with minimal local cues in a room with prominent distal visual cues, and then rotating the arena by about 90 degrees over about 10 minutes. We then tested whether the cells active during SIA after the arena rotation had place fields in the location in which the rat fell asleep or in the location to which the rat was moved. To verify that the distal cues controlled the alignment of the rat's spatial map during active waking, we mapped its place fields while it foraged for randomly scattered food pellets both before and after the sleep session. We found that:

1) **When rats were moved to a new location in the room during sleep, the population activity in subsequent SIA episodes was found to reflect the location in which the rats fell asleep, rather than the location to which they were moved, even though the place fields were controlled by room cues during active waking.**

The simplest interpretation is that the place-related activity in SIA does not arise from the processing of current sensory information, as does the place-related activity in active waking, but from a reactivation of the memory for where the rat fell asleep. This suggests that the level of

arousal during SIA is not as high as in active waking. Another possibility is that rats used current sensory information to determine their position during SIA, but that instead of using the prominent distal visual cues, the rats used whatever minimal local arena cues were still available to them despite our efforts to eliminate them. It is likely that some local arena cues were available to the rats, because one rat was able to keep its spatial map aligned with the rotated arena for 23 minutes in run 2, despite the conflict between the orientation of the arena and the orientation of the distal visual room cues. The appearance and texture of the arena was rotationally uniform, so it is unlikely that this rat was able to use visual or texture cues to maintain the alignment of its spatial map with the arena, but it might have been able to deposit and use local olfactory cues. If rats are able to use local olfactory cues to determine their current location in space during active waking, it is possible that rats were also able to use local olfactory cues to determine their current location during SIA. Under this conception, rats' perception, or perceptual attention, were altered during SIA, such that nearby cues became more salient than distal cues, and they aligned their maps with local cues in SIA but distal cues (in most cases) during active waking. The present study has eliminated the possibility that rats use visual cues to determine their location during SIA; one could eliminate the possibility that rats use local olfactory cues by repeating this study in anosmic rats. Nevertheless, if rats are using local but not distal cues to determine their location in space during SIA, their sphere of attention (so to speak) must be smaller in SIA than it is in active waking, which is still consistent with the conclusion that the level of arousal during SIA is not as high as in active waking.

If sleeping rats maintain a working memory for their current location in space, where is this working memory stored? The hippocampal population activity does not contain any obvious information about the rat's sleeping location during REM and SWS. However, patterns of hippocampal activity during REM and SWS resemble patterns present during the immediately preceding waking period more than expected by chance (Wilson and McNaughton, 1994; Skaggs and McNaughton, 1996; Louie and Wilson, 2001); thus, it is possible that the information about the rat's spatial history contained in these reactivated patterns is enough to reconstruct its current location at SIA onset. This hypothesis would predict that, if the path represented by the population activity just before SIA onset were reconstructed with a small enough temporal grain, it would reflect a trajectory to the rat's current location. Another possibility is that the rat's current spatial location is stored within the hippocampus as a "latent attractor" (Doboli et al.,

2000), not evident in the patterns of neural activity but available in the short-term synaptic structure of the network, that can be reactivated when the animal is aroused. This memory reactivation could be aided by local sensory cues that had been associated with that location before the rat fell asleep, such as the rat's sleeping position and the resulting pressure of the floor on various parts of the its body and local olfactory cues.

6.4. SEROTONIN MICROINFUSION INTO THE MEDIAL SEPTUM INDUCES HIPPOCAMPAL SMALL IRREGULAR ACTIVITY (CHAPTER 5)

The theta rhythm is triggered by activity in the "ascending brainstem synchronizing system" via its influence on the MSDB (Green and Arduini, 1954; Stewart and Fox, 1990; Smythe et al., 1992; Bland and Colom, 1993; McNaughton et al., 1995; Vertes and Kocsis, 1997; Bland and Oddie, 1998; Buzsáki, 2002.) LIA appears to arise within the hippocampus in the absence of external theta drive (O'Keefe and Nadel, 1978; Buzsáki, 1986; Buzsáki et al., 1992; Ylinen et al., 1995a; Csicsvari et al., 1999a,b). The existence of SIA complicates matters, because some factor has to determine whether the hippocampus goes into LIA or SIA in the absence of theta drive.

The mechanism by which SIA is generated is not addressed in the few studies characterizing its behavioral correlates, but a hippocampal "desynchronization" visually resembling SIA has been reported under three sets of experimental conditions: (1) when theta activity would normally be expected but the MSDB has been lesioned or temporarily inactivated (Winson, 1978; Givens and Olton, 1990; Mizumori et al., 1989; Lawson and Bland, 1993; Kirk and McNaughton, 1993; Oddie et al., 1996); (2) when the MSDB is stimulated at frequencies beyond physiological theta range (Brücke et al., 1959; Ball and Gray, 1971; Klemm and Dreyfus, 1975); (3) and when the median raphe nucleus (MnR) is stimulated (Macadar et al., 1974; Assaf and Miller, 1978; Vertes, 1981). This effect appears to be mediated by serotonergic projections from the MnR to the MSDB, as continuous theta activity results under manipulations that suppress the activity of MnR serotonergic neurons (for review, see Vertes and Kocsis, 1997); MnR serotonergic fibers directly inhibit a subset of septohippocampal cholinergic projection cells via 5HT-1A receptors (Milner and Veznedaroglu, 1993; Kia et al., 1996) and directly excite septohippocampal GABAergic projection cells via 5-HT-2A and possibly other receptor

subtypes (Alreja, 1996; Leranth and Vertes, 1999); and MnR stimulation inhibits irregularly firing septal neurons and disrupts the rhythmicity of regularly bursting septal neurons (Assaf and Miller, 1978). Together, the first two sets of results suggest the hypothesis that SIA might occur when both theta activity and LIA are somehow precluded. The third set of results suggests a second hypothesis, consistent with the first hypothesis but more specific: that the factor that determines whether the hippocampus goes into SIA or LIA in the absence of external theta drive might be the level of serotonin in the MSDB.

To test the more general hypothesis of whether SIA is simply the state that occurs in the absence of both theta activity and LIA, theta activity was transiently abolished by MSDB inactivation, and LIA was precluded by allowing the rats to forage for randomly-scattered food pellets. To test the more specific hypothesis of whether serotonin in the MSDB is the agent of hippocampal EEG desynchronization in SIA, serotonin was microinfused into the MSDB. The amplitudes and power spectra of the resulting hippocampal and neocortical EEG, and the hippocampal CA1 population activity, were compared to those of naturally occurring SIA obtained from baseline sleep. This is the first study to directly test the hypothesis that the presence of serotonin in the MSDB induces hippocampal desynchronization, and to test whether this and/or MSDB inactivation-induced desynchronization has a profile of hippocampal EEG, neocortical EEG, and hippocampal CA1 population activity similar to naturally occurring SIA. It was found that:

1) **When the MSDB was inactivated by lidocaine microinfusion, the resulting "desynchronization" of the hippocampal EEG consistently differed from baseline SIA in its hippocampal and neocortical power spectra: the peak frequency in the theta range of the hippocampal EEG and the amplitude in the high frequencies of the neocortical EEG were more similar to run than to baseline SIA.**
2) **When serotonin was microinfused into the MSDB, inter-sharp wave periods of LIA and theta activity were suppressed in amplitude, and the peak frequency in the theta range of the hippocampal EEG and, in all but 1 rat, the power in the high frequencies of the neocortical EEG actually matched those of baseline SIA. The sparse, place-related hippocampal population activity that characterizes baseline SIA was also present in the periods of suppressed LIA during the typical "flopping" behavior following serotonin infusion.**

The finding that serotonin, but not lidocaine, in the MSDB produces a desynchronization that closely resembles SIA, taken with the evidence that stimulation of the MnR produces hippocampal desynchronization (Macadar et al., 1974; Assaf and Miller, 1978; Vertes, 1981), probably via serotonergic input to the MSDB (Vertes and Kocsis, 1997; Milner and Veznedaroglu, 1993; Kia et al., 1996; Alreja, 1996; Leranth and Vertes, 1999; Assaf and Miller, 1978), and that serotonergic MnR cells increase their firing at the offset of REM episodes and in response to visual or auditory stimuli (Rasmussen et al., 1984), leads us to propose the following model for the generation of SIA. During active waking, serotonin levels are high and steady, and rhythmic input from the MSDB induces theta activity in the hippocampus. In quiet waking and SWS, serotonin levels are low and theta drive is absent, and the hippocampus spontaneously produces LIA. If the animal is suddenly aroused, there is a sudden increase in MnR activity, resulting in a sudden increase in brain serotonin levels. The effect of the sudden increase in serotonin levels in the MSDB is a simultaneous inhibition of cholinergic septohippocampal projection cells (Milner and Veznedaroglu, 1993; Kia et al., 1996) and excitation of GABAergic septohippocampal projection cells (Alreja, 1996; Leranth and Vertes, 1999), sending a sudden stream of predominantly non-rhythmic input into the hippocampus. This input shuts down the intrinsic mechanisms producing LIA without driving theta activity, resulting in hippocampal SIA. This model predicts that SIA in the hippocampal EEG occurs concomitantly with increases in MnR cell activity, which could be tested by simultaneous recording of MnR cell activity and hippocampal EEG.

The rat that did not flop also did not show a suppression of power in the high frequencies of the neocortical EEG. Taken in combination with the finding that SIA is similar to the other sleep states in neocortical EEG power in the high frequencies (see Fig. 3.4), the most parsimonious explanation for these results is that the power in the high frequency range of the neocortical EEG is low when the rat is still, but high when the rat is actively moving around. If the rat's behavior is really the sole determinant of the amount of power in the high frequencies of the neocortical EEG, then our finding that the desynchronization in the rats that flopped following the serotonin infusion resembles baseline SIA in neocortical EEG, but that the desynchronization following lidocaine infusion does not, is trivial and should not be taken as evidence that serotonin but not lidocaine induces SIA. However, the frequency of the peak in the theta range was reduced in all rats that showed effects of serotonin infusions, including the

anomalous rat that remained active during the post-infusion period. This effect would need to be confirmed in more rats, but it suggests that the hippocampal desynchronization elicited by serotonin infusions in the MSDB matches that of baseline SIA in at least one non-trivial way in which the hippocampal desynchronization elicited by lidocaine inactivation of the MSDB does not.

The finding that serotonin infusions into the MSDB result in a hippocampal EEG pattern that has a peak in the low-frequency theta range provides evidence that the MSDB can affect the frequency of the hippocampal theta rhythm. This finding contradicts the hypothesis put forth by Kirk and McNaughton (1993) that the SuM, not the MSDB, is the pacemaker of the hippocampal theta rhythm, which was based on their finding that inactivation of various points along the ascending brainstem synchronizing system from the reticular nucleus pontis oralis (PnO) to the supramammillary nucleus (SuM), but not of pathways from the SuM to the MSDB or of the MSDB itself, reduced the frequency of hippocampal theta rhythm. However, Kirk and McNaughton (1993) were assessing effects on the frequency of theta elicited by PnO stimulation in urethane-anesthetized rats; it is possible that slightly different mechanisms underlie the generation of naturally occurring theta activity in freely moving rats. This possibility is supported by the finding that in awake, behaving rats, SuM lesion or inactivation does not suppress the frequency of hippocampal theta activity nearly as much as it does in urethane-anesthetized rats (McNaughton et al., 1995; Thinschmidt et al., 1995). Another possibility is that, under normal conditions, the MSDB relays the frequency of theta drive that has already been established in the SuM, but that increases in serotonin levels in the MSDB can reduce the firing frequency of its cells in a way that simple inactivation of the MSDB, or of afferents to the MSDB, cannot.

6.5. CONCLUSIONS AND FUTURE DIRECTIONS

Based on the findings reported in this dissertation, we propose the following relationship between SIA and the other physiological states. During active awake behaviors and REM, rhythmic input from the MSDB induces theta activity in the hippocampus. During quiet waking and SWS, external theta drive is turned off, and the hippocampus spontaneously produces LIA.

SIA occurs when an external or internal stimulus induces a sudden arousal during sleep, triggered by an increase in the level of serotonin in the MSDB. SIA allows the rat to surface slightly without fully awakening, so that it can assess whether the stimulus warrants a behavioral response. It is important for an animal to remember the context in which it is sleeping, such as its location and immediate surroundings, when attempting to determine the significance of a stimulus and plan an appropriate behavioral response. The finding that the hippocampal cell activity reflects a memory for the location in which the rat fell asleep suggests that SIA might also provide the neural substrate for such context sensitivity during sleep. The following future studies would help to complete this picture:

1) Repeat the arena rotation experiment in anosmic rats. Does the SIA population activity also reflect the location in which rats fell asleep, rather than the location to which they were moved? If so, this would rule out the possibility that rats are using local olfactory information to determine their current location in space during SIA, strengthening the hypothesis that the population activity during SIA reflects a memory for the location in which the rat fell asleep.
2) Reconstruct with fine temporal grain the trajectory encoded by the hippocampal population activity immediately preceding SIA. Does the reconstructed path reflect a trajectory to the rat's current location? If so, this would support the hypothesis that the hippocampus stores a memory for the location in which the rat is sleeping during SIA.
3) Repeat the serotonin microinfusion studies using smaller volumes of drug solution to verify that serotonin in the MSDB induces an EEG state with a peak in the type 2 theta range even if the rat does not "flop." If so, this would strengthen the finding that the MSDB can affect hippocampal theta frequency and that increases in serotonin in the MSDB might underlie SIA generation.
4) Microinfuse serotonin agonists specific for the receptors present in the MSDB to test whether one or multiple receptor subtypes are responsible for the effect of serotonin in the MSDB inducing hippocampal SIA. Confirm their specificity by checking whether selective antagonists for those receptors prevent the effects of the agonists.
5) Record MnR cell activity simultaneously with hippocampal EEG to directly test whether hippocampal SIA is accompanied by sudden and dramatic increases in MnR cell activity. This would provide strong evidence that increases in serotonin underlie the generation of naturally occurring SIA.

An important objective in the field of neuroscience is to understand how the transformation takes place in an organism's brain between the various energies imposed upon the organism and its resulting behaviors. A large portion of neuroscience research has been devoted to the important intermediate step of mapping the relationship between various aspects of the organism's brain activity and the organism's various inputs and outputs. Hopefully, this dissertation has also demonstrated that, if we are trying to understand the brain, it is extremely important to understand its various physiological states, and to take them into account when attempting to interpret changes in neural activity. For example, in an early single-unit recording study in the hippocampus, Vinogradova and colleagues placed rabbits in small semi-dark boxes and exposed them to occasional noises and flashing lights. They found 2 classes of hippocampal neurons: those that are activated by all sensory stimuli tested, and those that are inactivated by all sensory stimuli tested. With repeated exposure to any particular stimulus, these responses eventually habituated, but were immediately reinstated when a novel stimulus was used. The interpretation was that hippocampal cells encode arousal level (Vinogradova, 1970; Vinogradova et al., 1970). Given our current knowledge of hippocampal population activity during LIA and SIA, a more likely interpretation is that the rabbits were probably in a state of LIA most of the time in the small semi-dark box. The stimuli elicited SIA, and the cells that were "activated" by them were probably place cells that had place fields in the box, and the ones that were inactivated were probably place cells that did not have place fields in the box. The habituation of the neurons was probably coincident with the habituation of the rabbit to the stimuli, at which point the stimuli were no longer effective in inducing SIA. O'Keefe and Nadel (1978) and Vanderwolf (1983) wisely emphasized the importance of permitting the widest possible range of behaviors and the most naturalistic possible setting when seeking correlates of brain activity; I would like to extend this advice by emphasizing the importance of also taking into account the effects of the animal's ongoing physiological state.

BIBLIOGRAPHY

Adey WR (1966) Neurophysiological correlates of information transaction and storage in brain tissue. In: Progress in physiological psychology (Stellar E, Sprague J, eds), 1:1-43. New York: Academic.

Adey WR (1977) The sensorium and the modulation of cerebral states: tonic environmental influences on limbic and related systems. Ann NY Acad Sci 290:396-420.

Alreja M (1996) Excitatory actions of serotonin on GABAergic neurons of the medial septum and diagonal band of Broca. Synapse 22:15-27.

Amaral DG, Kurz J. (1985) An analysis of the origins of the cholinergic and noncholinergic septal projections to the hippocampal formation of the rat. J Comp Neurol 240(1):37-59.

Amaral DG, Witter MP (1995) Hippocampal formation. In: The Rat Nervous System, 2nd ed.(Paxinos G, ed), 443-493. San Diego: Academic.

Anchel H, Lindsley DB (1972) Differentiation of two reticulohypothalamic systems regulating hippocampal activity. Electroenceph Clin Neurophysiol 32:209-226.

Andersen P, Bliss TV, Skrede KK (1971) Lamellar organization of hippocampal excitatory pathways. Exp Brain Res 13:222-238.

Aserinsky E, Kleitman N (1955) Two types of ocular motility occurring in sleep. J Appl Physiol 8:1-10.

Assaf SY, Miller JJ (1978) The role of a raphe serotonin system in the control of septal unit activity and hippocampal desynchronization. Neurosci 3:539-550.

Ball GG, Gray JA (1971) Septal self-stimulation and hippocampal activity. Physiol Behav 6:547-549.

Barnes CA, McNaughton BL, Mizumori SJY, Leonard BW, Lin LH (1990) Comparison of spatial and temporal characteristics of neuronal activity in sequential stages of hippocampal processing. Prog Brain Res 83:287-300.

Bennett TL (1969) Evidence against the theory that hippocampal theta is a correlate of voluntary movement. Commun Behav Biol, Part A 4:165-169.

Berger H (1929) Ueber des Electrenkephalogramm des Menschen. Arch f Psychiat 87:527-570.

Bergmann BM, Winter JB, Rosenberg RS, Rechtschaffen A (1987) NREM sleep with low-voltage EEG in the rat. Sleep 10(1):1-11.

Best PJ, Ranck JB Jr (1982) Reliability of the relationship between hippocampal until activity and sensory-behavioral events in the rat. Exp Neurol 75:652-664.

Bland BH (1986) The physiology and pharmacology of hippocampal formation theta rhythms. Prog Neurobiol 26:1-54.

Bland BH, Colom LV (1993) Extrinsic and intrinsic properties underlying oscillation and synchrony in limbic cortex. Prog Neurobiol 41:157-208.

Bland BH, Colom LV, Ford RD (1990) Responses of septal theta-on and theta-off cells to activation of the dorsomedial-posterior hypothalamic region. Brain Res Bull 24:71-79.

Bland BH, Konopacki J, Kirk IJ, Oddie SD, Dickson CT (1995) Discharge patterns of hippocampal theta-related cells in the caudal diencephalon of the urethan-anesthetized rat. J Neurophysiol 74:322-333.

Bland BH, Oddie SD (1998) Anatomical, electrophysiological and pharmacological studies of ascending brainstem hippocampal synchronizing pathways. Neurosci Biobehav Rev 22(2):259-273.

Bland BH, Oddie SD, Colom LV, Vertes RP (1994) Extrinsic modulation of medial septal cell discharges by the ascending brainstem hippocampal synchronizing pathway. Hippocampus 4:649-660.

Bland BH, Vanderwolf CH (1972) Diencephalic and hippocampal mechansisms of motor activity in the rat: effects of posterior hypothalamic stimulation on behavior and hippocampal slow wave activity. Brain Res 43:67-88.

Bostock E, Muller RU, Kubie JL (1991) Experience-dependent modifications of hippocampal place cell firing. Hippocampus 1:193-206.

Brankack J, Buzsáki G (1986) Hippocampal responses evoked by tooth pulp and acoustic stimulation: Depth profiles and effect of behavior. Brain Res 378:303-314.

Brankack J, Stewart M, Fox SE (1993) Current source density analysis of the hippocampal theta rhythm: Associated sustained potentials and candidate synaptic generators. Brain Res 615:310-327.

Brazhnik ES, Vinogradova OS, Karanov AM (1985) Frequency modulation of neuronal theta-bursts in rabbit's septum by low frequency repetitive stimulation of the afferent pathways. Neuroscience 14:501-508.

Brown BB (1968) Frequency and phase of hippocampal theta activity in the spontaneously behaving cat. Electroenceph Clin Neurophysiol 24:53-62.

Brown JE, Skaggs WE (2002) Concordant and discordant coding of spatial location in populations of hippocampal CA1 pyramidal cells. J Neurophysiol 88(4):1605-1613.

Brücke F, Petsche H, Pillat B, Deisenhammer E (1959) Die beeinflussung der "hippocampus-arousal-reaktion" beim kaninchen durch elektrische reizung im septum. Pflügers Archiv 269:319-338.

Buzsáki G (1986) Hippocampal sharp waves: Their origin and significance. Brain Res 298:242-252.

Buzsáki G (2002) Theta oscillations in the hippocampus. Neuron 33 (3):325-340.

Buzsáki G, Czopf J, Kondakor I, Kellenyi L (1986) Laminar distribution of hippocampal rhythmic slow activity (RSA) in the behaving rat: Current source density analysis, effects of urethane and atropine. Brain Res 365:125-137.

Buzsáki G, Horvath Z, Urioste R, Hetke J, Wise K (1992) High-frequency network oscillation in the hippocampus. Science 256:1025-1027.

Buzsáki G, Leung L, Vanderwolf CH (1983) Cellular bases of hippocampal EEG in the behaving rat. Brain Res Rev 6:139-171.

Caplan JB, Madsen JR, Schulze-Bonhage A, Aschenbrenner-Scheibe R, Newman EL, Kahana MJ (2003) Human theta oscillations related to sensorimotor integration and spatial learning. J Neurosci 23(11):4726-4736.

Chrobak JJ, Buzsaki G (1996) High-frequency oscillations in the output networks of the hippocampal-entorhinal axis of the freely behaving rat. J Neurosci 16:3056-3066.

Csicsvari J, Hirase H, Czurkó A, Mamiya A, Buzsáki G (1999a) Oscillatory coupling of hippocampal pyramidal cells and interneurons in the behaving rat. J Neurosci 19:274-287.

Csicsvari J, Hirase H, Czurkó A, Mamiya A, Buzsáki G (1999b) Fast network oscillations in the hippocampal CA1 region of the behaving rat. J Neurosci 19(RC20):1-4.

Czurkó A, Hirase H, Csicsvari J, Buzsáki G (1999) Sustained activation of hippocampal pyramidal cells by "space clamping" in a running wheel. Eur J Neurosci 11:344-352.

Davis H, Davis PA, Loomis AL, Harvey EN, Hobart G (1939) Electrical reactions of the human brain to auditory stimulation during sleep. J Neurophysiol 2:500-514.

Davis K, Heins E, Van Twyver H (1972) A study of paradoxical sleep depth in the rat. Psychon Sci 26(3):173-174.

Deadwyler SA, West MO, Robinson JH (1981) Entorhinal and septal inputs differentially control sensory-evoked responses in the rat dentate gyrus. Science 211:1181-1183.

Dement W, Kleitman N (1957a) Cyclic variations in EEG during sleep and their relation to eye movements, body motility, and dreaming. Electroenceph Clin Neurophysiol 9:673-690.

Dement W, Kleitman N (1957b) The relation of eye movements during sleep to dream activity: an objective method for the study of dreaming. J Exp Psych 53:339-346.

Dillon RF, Webb WB (1965) Threshold of arousal from "activated" sleep in the rat. J Comp Physiol Psych 59(3):446-447.

Doboli S, Minai A, Best PJ (2000) Latent attractors: A model for context-dependent place representations in the hippocampus. Neural Computation 12:1009-1043.

Douglas RJ (1967) The hippocampus and behavior. Psychol Bull 67:416-522.

Elazar A, Adey WR (1967a) Spectral analysis of low frequency components in the electrical activity of the hippocampus during learning. Electroenceph Clin Neurophysiol 23:225-240.

Elazar A, Adey WR (1967b) Electroencephalographic correlates of learning in subcortical and cortical structures. Electroenceph Clin Neurophysiol 23:306-319.

Ehrhart J, Muzet A. (1974) Fréquence et durée des phases d'activation transitoire au cours du sommeil normal ou perturbé chez l'homme. Arch Sci Physiol 28:213-260.

Ehrhart J, Ehrhart M, Muzet A, Shieber JP, Naitoh P (1981) K-complexes and sleep spindles before transient activation during sleep. Sleep 4:400-407.

Eichenbaum H, Dudchenko P, Wood E, Shapiro M, Tanila H (1999) The hippocampus: Is it spatial memory or a memory space? Neuron 23:209-226.

Fell J, Klaver P, Elfadil H, Schaller C, Elger CE, Fernandez G (2003) Rhinal-hippocampal theta coherence during declarative memory formation: interaction with gamma synchronization? Eur J Neurosci 17(5):1082-1088.

Foster TC, Castro CA, McNaughton BL (1989) Spatial selectivity of rat hippocampal neurons: Dependence on preparedness for movement. Science 244:1580-1582.

Fox SE, Ranck JB Jr. (1975) Localization and anatomical identification of theta and complex spike cells in dorsal hippocampal formation of rats. Exp Neurol 49:299-313.

Fox SE, Ranck JB Jr. (1981) Electrophysiological characteristics of hippocampal complex-spike cells and theta cells. Exp Brain Res 41:399-410.

Fox SE, Wolfson S, Ranck JB Jr. (1986) Hippocampal theta rhythm and the firing of neurons in walking and urethane anesthetized rats. Exp Brain Res 62:495-508.

Givens BS, Olton DS (1990) Cholinergic and GABAergic modulation of medial septal area: effect on working memory. Behav Neurosci 104(6):849-855.

Gottesmann C (1964) Données sur l'activité corticale au cours du sommeil profond chez le rat. C R Soc Biol (Paris) 158:1829-1834.

Gottesmann C (1973) Le stade intermédiaire du sommeil chez le rat. Rev Electroenceph Neurophysiol (Paris) 3:65-68.

Gottesmann C (1992) Detection of seven sleep-waking stages in the rat. Neurosci Biobehav Rev 16:31-38.

Grastyán E, Karmos G, Vereczkey L, Kellenyi L (1966) The hippocampal electrical correlates of the homeostatic regulation of motivation. Electroenceph Clin Neurophysiol 21:34-53.

Grastyán E, Lissak K, Madarász I, Donhoffer H (1959) Hippocampal electrical activity during the development of conditioned reflexes. Electroenceph Clin Neurophysiol 11:409-430.

Green JD, Arduini AA (1954) Hippocampal electrical activity in arousal. J Neurophysiol 15:533-557.

Halász P, Kundra O, Rajna P, Pál I, Vargha M (1979) Micro-arousals during nocturnal sleep. Acta Physiol Acad Sci Hung 54(1):1-12.

Harper RM (1971) Frequency changes in hippocampal electrical activity during movement and tonic immobility. Physiol Behav 7:55-58.

Hirase H, Czurkó A, Csicsvari J, Buzsáki G (1999) Firing rate and theta-phase coding by hippocampal neurons during 'space clamping.' Eur J Neurosci 11:4373-4380.

Huxter J, Burgess N, O'Keefe J (2003) Independent rate and temporal coding in hippocampal pyramidal cells. Nature 425 (6960): 828-832.

Ikonen S (2001) The role of the septohippocampal cholinergic system in cognitive functions. Doctoral dissertation, published electronically, University of Kuopio.

James DTD, McNaughton N, Rawlins JNP, Feldon J, Gray JA (1977) Septal driving of hippocampal theta rhythm as a function of frequency in the free-moving male rat. Neuroscience 2:1007-1017.

Jarosiewicz B, McNaughton BL, Skaggs WE (2002) Hippocampal population activity during the small-amplitude irregular activity state in the rat. J Neurosci 22:1373-1384.

Jarosiewicz B, Skaggs WE (1999) Complex structure of hippocampal population activity during slow-wave sleep in the rat. Soc Neurosci Abstr 25(2):556.7.

Jarosiewicz B, Skaggs WE (2001). Hippocampal place-related activity during the small-amplitude irregular activity state in the rat. Soc Neurosci Abstr 27:643.10.

Jarosiewicz B, Skaggs WE (2002). Level of arousal during the small irregular activity state in the rat. Soc Neurosci Abstr 28:584.16.

Jeffery KJ, O'Keefe JM (1999) Learned interaction of visual and idiothetic cues in the control of place field orientation. Exp Brain Res 127:151-161.

Jensen O, Lisman JE (2000) Position reconstruction from an ensemble of hippocampal place cells: Contribution of theta phase coding. J Neurophysiol 83(5):2602-2609.

Jensen O, Tesche CD (2002) Frontal theta activity in humans increases with memory load in a working memory task. Eur J Neurosci 15(8):1395-1399.

Jirsa R, Poc P, Radil T (1992) Hippocampal auditory evoked response threshold in the rat: behavioral modulation. Brain Res Bull 28:149-153.

Johns TG, Piper DC, James GWL, Birtley RDN, Fischer M (1977) Automated analysis of sleep in the rat. Electroenceph Clin Neurophysiol 43:103-105.

Jones MS, Barth DS (1999) Spatiotemporal organization of fast (>200 Hz) electrical oscillations in rat vibrissa/barrel cortex. J Neurophysiol 82:1599-1609.

Kahana MJ, Sekuler R, Caplan JB, Kirschen M, Madsen JR (1999) Human theta oscillations exhibit task dependence during virtual maze navigation. Nature 399:781-783.

Kamondi A, Acsády L, Wang, XJ, Buzsáki G (1998) Theta oscillations in somata and dendrites of hippocampal pyramidal cells in vivo: Activity dependent phase-precession of action potentials. Hippocampus 8:244-261.

Kia HK, Brisorgueil MJ, Daval G, Langlois X, Hamon M, Vergé D (1996) Serotonin$_{1A}$ receptors are expressed by a subpopulation of cholinergic neurons in the rat medial septum and diagonal band of Broca: a double immunocytochemical study. Neurosci 74(1):143-154.

Kimble DP (1968) The hippocampus and internal inhibition. Psychol Bull 70:285-295.

Kirk IJ, McNaughton N (1991) Supramammillary cell firing and hippocampal rhythmical slow activity. Neuroreport 2:723-725.

Kirk IJ, McNaughton N (1993) Mapping the differential effects of procaine on frequency and amplitude of reticularly elicited hippocampal rhythmical slow activity. Hippocampus 3(4):517-526.

Kirk IJ, Oddie SD, Konopacki J, Bland BH (1996) Evidence for differential control of posterior hypothalamic, supramammillary, and medial mammillary theta-related cellular discharge by ascending and descending pathways. J Neurosci 16:5547-5554.

Klemm WR (1971) EEG and multiple-unit activity in limbic and motor systems during movement and immobility. Physiol Behav 7:337-343.

Klemm WR (1972) Effects of electronic stimulation of brainstem reticular formation on hippocampal theta rhythm and muscle activity in unanesthetized, cervical and midbrain transected rats. Brain Res 41:331-344.

Klemm WR, Dreyfus LR (1975) Septal- and caudate-induced behavioral inhibition in relation to hippocampal EEG of rabbits. Physiol Behav 15:561-567.

Knierim JJ (2002) Dynamic interactions between local surface cues, distal landmarks, and intrinsic circuitry in hippocampal place cells. J Neurophysiol 88:1605-1613.

Knierim JJ, Kudrimoti HS, McNaughton BL (1995) Place cells, head direction cells, and the learning of landmark stability. J Neurosci 15:1648-1659.

Knierim JJ, Kudrimoti HS, McNaughton BL (1998) Interactions between idiothetic cues and external landmarks in the control of place cells and head direction cells. J Neurophysiol 80:425-446.

Kocsis B, Vertes RP (1994) Characterization of neurons in the supramammillary nucleus and mammillary body that discharge rhythmically with the hippocampal theta rhythm in the rat. J Neurosci 14:7040-7052.

Kohn M, Litchfield D, Branchey M, Brebbia DR (1974) An automatic hybrid analyzer of sleep stages in the rat. Electroenceph Clin Neurophysiol 37:518-520.

Kramis R, Vanderwolf CH, Bland BH (1975) Two types of hippocampal rhythmic slow activity in both the rabbit and the rat: relations to behavior and effects of atropine, diethyl ether, urethane, and pentobarbital. Exp Neurol 49:58-85.

Kubie JL, Muller RU, Fox SE (1985) Firing fields of hippocampal place cells: Interim report. In: Electrical Activity of the Archicortex (Buzsáki G, Vanderwolf CH. ed), 221-231. Budapest: Akadémiai Kiadó.

Kubie JL, Ranck JB Jr. (1983) Sensory-behavioral correlates in individual hippocampus neurons in three situations: space and context. In: Neurobiology of the Hippocampus (Seifert W, ed), 433–447. New York: Academic.

Lavenex P, Schenk F (1995) Influence of local environmental olfactory cues on place learning in rats. Physiol Behav 58(6):1059-1066.

Lavenex P, Schenk F (1998) Olfactory traces and spatial learning in rats. Animal Behav 56:1129-1136.

Lawson VH, Bland BH (1993) The role of the septohippocampal pathway in the regulation of hippocampal field activity and behavior: analysis by the intraseptal microinfusion of carbachol, atropine, and procaine. Exp Neurol 120:132-144.

Lenck-Santini P, Muller RU, Save E, Poucet B (2002) Relationships between place cell firing fields and navigational decisions by rats. J Neurosci 22:9035-9047.

Leranth C, Vertes RP (1999) Median raphe serotonergic innervation of medial septum/diagonal band of Broca (MSDB) parvalbumin-containing neurons: possible involvement of the MSDB in the desynchronization of the hippocampal EEG. J Comp Neurol 410:586-598.

Loomis AL, Harvey E, Hobart GA (1935a) Potential rhythms of the cerebral cortex during sleep. Science 81:597-598.

Loomis AL, Harvey E, Hobart GA (1935b) Further observations on the potential rhythms of the cerebral cortex during sleep. Science 82:198-199.

Loomis AL, Harvey EN, Hobart GA (1939) Distribution of disturbance patterns in the human encephalogram, with special reference to sleep. J Neurophysiol 2: 413-430.

Louie K, Wilson MA (2001) Temporally structured replay of awake hippocampal ensemble activity during rapid eye movement sleep. Neuron 29(1):145-156.

Lydic R, McCarley RW, Hobson JA (1983) The time-course of dorsal raphe discharge, PGO waves, and muscle tone averaged across multiple sleep cycles. Brain Res 274:365-370.

Maaswinkel H, Whishaw IQ (1999) Homing with locale, taxon, and dead reckoning strategies by foraging rats: Sensory hierarchy in spatial navigation. Behav Brain Res 99:143-152.

Macadar SW, Chalupa LM, Lindsley DB (1974) Differentiation of brainstem loci which affect hippocampal and neocortical activity. Exp Neurol 43:499-514.

Markus EJ, Barnes CA, McNaughton BL, Gladden VL, Skaggs WE (1994) Spatial information content and reliability of hippocampal CA1 neurons: effects of visual input. Hippocampus 4:410-421.

Markus EJ, Qin YL, Leonard B, Skaggs WE, McNaughton BL, Barnes CA (1995) Interactions between location and task affect the spatial and directional firing of hippocampal neurons. J Neurosci 15:7079-7094.

McClelland JL, McNaughton BL, O'Reilly RC (1995) Why there are complementary learning systems in the hippocampus and neocortex: Insights from the successes and failures of connectionist models of learning and memory. Phychol Rev 102(3):419-457.

McCormick DA, Bal T (1997) Sleep and arousal: Thalamocortical mechanisms. Annu Rev Neurosci 20:185-215.

McFarland WL, Teitelbaum H, Hedges EK (1975) Relationship between hippocampal theta activity and running speed in the rat. J Comp Physiol Psychol 88:324-328.

McGinty DJ, Harper RW (1976) Dorsal raphe neurons: depression of firing during sleep in cats. Brain Res 101:569-575.

McNaughton BL, Barnes CA, O'Keefe J (1983a) The contributions of position, direction, and velocity to single unit activity in the hippocampus of freely-moving rats. Exp Brain Res 52:41-49.

McNaughton BL, O'Keefe J, Barnes CA (1983b) The stereotrode: A new technique for simultaneous isolation of several single units in the central nervous system from multiple unit recordings. J Neurosci Methods 8:391-397.

McNaughton N, Logan B, Panickar KS, Kirk IJ, Pan W, Brown NT, Heenan A (1995) Contribution of synapses in the medial supramammillary nucleus to the frequency of hippocampal theta rhythm in freely moving rats. Hippocampus 5:534-545.

Milner TA, Veznedaroglu E (1993) Serotonin-containing terminals synapse on septo-hippocampal neurons in the rat. J Neurosci Res 36:260-271.

Mitzdorf U (1985) Current source-density method and application in cat cerebral cortex: Investigation of evoked potentials and EEG phenomena. Physiol Rev 65:37-100.

Mizumori SJY, McNaughton BL, Barnes CA, Fox KB (1989) Preserved spatial coding in hippocampal CA1 pyramidal cells during reversible suppression of CA3 output: Evidence for pattern completion in hippocampus. J Neurosci 9:3915-3928.

Moruzzi G, Magoun HW (1949) Brain stem reticular formation and activation of the EEG. Electroenceph Clin Neurophysiol 1:455-473.

Muller RU, Kubie JL (1987) The effects of changes in the environment on the spatial firing of hippocampal complex-spike cells. J Neurosci 7:1951-1968.

Nádasdy Z, Hirase H, Czurkó A, Csicsvari J, Buzsáki G (1999) Replay and time compression of recurring spike sequences in the hippocampus. J Neurosci 19:9497-9507.

Neckelmann D, Ursin R (1993) Sleep stages and EEG power spectrum in relation to acoustical stimulus arousal threshold in the rat. Sleep 16(5):467-477.

Oddie SD, Bland BH, Colom LV, Vertes RP (1994) The midline posterior hypothalamic region comprises a critical part of the ascending brainstem hippocampal synchronizing pathway. Hippocampus 4:454-473.

Oddie SD, Stefanek W, Kirk IJ, Bland BH (1996) Intraseptal procaine abolishes hypothalamic stimulation-induced wheel-running and hippocampal theta field activity in rats. J Neurosci 16:1948-1956.

Ogilvie RD, Wilkinson RT (1988) Behavioral versus EEG-based monitoring of all-night sleep/wake patterns. Sleep 11(2):139-155.

O'Keefe J (1976) Place units in the hippocampus of the freely moving rat. Exp Neurol 51:78-109.

O'Keefe J, Conway D (1978) Hippocampal place units in the freely moving rat: why they fire where they fire. Exp Brain Res 31:573-590.

O'Keefe J, Dostrovsky J (1971) The hippocampus as a spatial map: Preliminary evidence from unit activity in the freely moving rat. Brain Res 34:171-175.

O'Keefe J, Nadel L (1978) The hippocampus as a cognitive map. Oxford: Clarendon.

O'Keefe J, Speakman A (1987) Single unit activity in the rat hippocampus during a spatial memory task. Exp Brain Res 68:1-27.

O'Keefe J, Recce ML (1993) Phase relationship between hippocampal place units and the EEG theta rhythm. Hippocampus 3:317-330.

Olds J (1967) The limbic system and behavioural reinforcement. Prog Brain Res 27:144-164.

Olds J, Hirano T (1969) Conditioned responses of hippocampal and other neurons. Electroenceph Clin Neurophysiol 2:159-166.

Pavlides C, Winson J (1989) Influences of hippocampal place cell firing in the awake state on the activity of these cells during subsequent sleep episodes. J Neurosci 9:2907-2918.

Paxinos G, Watson C (1997) The rat brain in stereotaxic coordinates, compact 3rd ed. San Diego: Academic.

Petsche H, Gogolak G, Van Zweiten PA (1965) Rhythmicity of septal cell discharges at various levels of reticular excitation. Electroenceph Clin Neurophysiol 19:25-33.

Petsche H, Stumpf CH, Gogolak G (1962) The significance of the rabbit's septum as a relay station between the midbrain and the hippocampus. I. The control of hippocampus arousal activity by the septum cells. Electroenceph Clin Neurophysiol 14:202-211.

Pickenhain L, Klingberg F (1965) Behavioural and electrophysiological changes during avoidance conditioning to light flashes in the rat. Electroenceph Clin Neurophysiol 18:464-476.

Pickenhain L, Klingberg F (1967) Hippocampal slow wave activity as a correlate of basic behavioral mechanisms in the rat. In: Progress in brain research: Structure and function of the limbic system (Adey WR, Tokizane T, eds), 27:218-227. Amsterdam: Elsevier.

Pravdich-Neminsky VV (1913) Ein Versuch der Registrierung der elektrischen Gehirnerscheinungen. Zbl Physiol 27:951-960.

Quirk GJ, Muller RU, Kubie JL, Ranck JB Jr (1990) The firing of hippocampal place cells in the dark depends on the rat's recent experience. J Neurosci 10:2008-2017.

Ranck JB Jr (1973) Studies on single neurons in dorsal hippocampal formation and septum in unrestrained rats, Part I: Behavioral correlates and firing properties. Exp Neurol 41:461-531.

Rasmussen K, Heym J, Jacobs B (1984) Activity of serotonin-containing neurons in nucleus centralis superior of freely moving cats. Exp Neurol 83:302-317.

Rechtschaffen A, Hauri P, Zeitlin M (1966) Auditory awakening thresholds in REM and NREM sleep stages. Percept Mot Skills 22:927-942.

Rechtschaffen A, Kales A, Eds. (1968) A manual of standardized terminology, techniques and scoring system for sleep stages of human subjects. Los Angeles: UCLA, Brain Information Service/Brain Research Institute.

Redish AD (1999) Beyond the cognitive map. Cambridge: MIT.

Rivas J, Gaztelu JM, Garcia-Austt E (1996) Changes in hippocampal cell discharge patterns and theta rhythm spectral properties as a function of walking velocity in the guinea pig. Exp Brain Res 108:113-118.

Roldán E, Weiss T, Fifková E (1963) Excitability changes during the sleep cycle of the rat. Electroenceph Clin Neurophysiol 15:775-785.

Rosenweig ES, Redish AD, McNaughton BL, Barnes CA (2003) Hippocampal map realignment and spatial learning. Nature Neurosci 6(6):609-615.

Roth M, Shaw J, Green J (1956) The form voltage distribution and physiological significance of the K-Complex. Electroenceph Clin Neurophysiol 8:385–402.

Sainsbury RS, Montoya CP (1984) The relationship between type 2 theta and behavior. Physiol Behav 33:621-626.

Sainsbury RS, Heynen A, Montoya CP (1987) Behavioral correlates of hippocampal type 2 theta in the rat. Physiol Behav 39:513-519.

Sakai K, Crochet S (2001) Differentiation of presumed serotonergic dorsal raphe neurons in relation to behavior and wake-sleep states. Neurosci 104(4):1141-1155.

Sakai K, Sano K, Iwahara S (1973) Eye movements and hippocampal theta activity in cats. Electroenceph Clin Neurophysiol 34:547-549.

Sato N, Yamaguchi Y (2003) Memory encoding by theta phase precession in the hippocampal network. Neural Comput 15(10):2379-2397.

Schieber JP, Muzet A, Ferrière PJ (1968) Caractéristiques de l'activation transitoire spontanée au cours du sommeil lent et du sommeil rapide chez l'homme. J Phys (Paris) 60:542.

Schieber JP, Muzet A, Ferrière PJ (1971) Les phases d'activation transitoire spontanées au cours du sommeil normal chez l'homme. Arch Sci Physiol 25:443-465.

Scoville WB, Milner B (1957) Loss of recent memory after bilateral hippocampal lesions. J Neurol Neurosurg Psych 20:11-21.

Shapiro ML, Tanila H, Eichenbaum H (1997) Cues that hippocampal place cells encode: dynamic and hierarchical representation of local and distal stimuli. Hippocampus 7:624-642.

Sharp PE, Blair HT, Etkin D, Tzanetos DB (1995) Influences of vestibular and visual motion information on the spatial firing patterns of hippocampal place cells. J Neurosci 15:173-189.

Shima K, Nakahama H, Yamamoto M (1986) Firing properties of two types of nucleus raphe dorsalis neurons during the sleep-waking cycle and their responses to sensory stimuli. Brain Res 399:317-326.

Shin J, Talnov A (2001) A single trial analysis of hippocampal theta frequency during nonsteady wheel running in rats. Brain Res 897:217-221.

Siapas AG, Wilson MA (1998) Coordinated interactions between hippocampal ripples and cortical spindles during slow-wave sleep. Neuron 21:1123-1128.

Skaggs WE (1995) Relations between the theta rhythm and activity patterns of hippocampal neurons. PhD Dissertation, University of Arizona, Program in Neuroscience.

Skaggs WE, McNaughton BL (1996) Replay of neuronal firing sequences in the rat hippocampus during sleep following spatial experience. Science 271:1870-1873.

Skaggs WE, McNaughton BL (1998) Neuronal ensemble dynamics in hippocampus and neocortex during sleep and waking. In: Neuronal ensembles (Eichenbaum H, Davis JL, eds), 235-246. New York:Wiley-Liss.

Skaggs WE, McNaughton BL, Wilson MA, Barnes CA (1996) Theta phase precession in hippocampal neuronal populations and the compression of temporal sequences. Hippocampus 6:149-172.

Slawinska U, Kasicki S (1998) The frequency of rat's hippocampal theta rhythm is related to the speed of locomotion. Brain Res 796:327-331.

Smythe JW, Colom LV, Bland BH (1992) The extrinsic modulation of hippocampal theta depends on the coactivation of cholinergic and GABAergic medial septal inputs. Neurosci Biobeh Rev 16:289-308.

Sohal VS, Hasselmo ME (1998) $GABA_B$ modulation improves sequence disambiguation in computational models of hippocampal region CA3. Hippocampus 8:171-193.

Squire LR (1992) Memory and the hippocampus: a synthesis from findings in rats, monkeys, and humans. Physiol Rev 68:649-741.

Steriade M, McCormick DA, Sejnowski TJ (1993) Thalamocortical oscillations in the sleeping and aroused brain. Science 262:679-685.

Stewart M, Fox SE (1990) Do septal neurons pace the hippocampal theta rhythm? Trends Neurosci 13(5):163-168.

Stuchlik A, Fenton AA, Bures J (2001) Substratal idiothetic navigation of rats is impaired by removal or devaluation of extramaze and intramaze cues.

Stuchlik A, Bures J (2002) Relative contribution of allothetic and idiothetic navigation to place avoidance on stable and rotating arenas in darkness. Behav Brain Res 128:179-188.

Stumpf C (1965) The fast component in the electrical activity of rabbit's hippocampus. Electroenceph Clin Neurophysiol 18:477-486.

Stumpf CH, Petsche H, Gogolak G (1962) The significance of the rabbit's septum as a relay station between the midbrain and the hippocampus. II. The differential effects of drugs upon both the septal cell firing pattern and the hippocampus theta activity. Electroenceph Clin Neurophysiol 14:212-219.

Swisher JE (1962) Manifestation of "activated" sleep in the rat. Science 138:1110.

Tanila H, Shapiro ML, Eichenbaum H (1997) Discordance of spatial representations in ensembles of hippocampal place cells. Hippocampus 7:613-623.

Terzano MG, Halász P, Declerck AC (1991). Phasic events and dynamic organization of sleep. New York: Raven Press.

Thinschmidt JS, Kinney GG, Kocsis B. (1995) The supramammillary nucleus: is it necessary for the mediation of hippocampal theta rhythm? Neuroscience 67(2):301-312.

Thompson LT, Best PJ (1989) Place cells and silent cells in the hippocampus of freely-behaving rats. J Neurosci 9:2382-2390.

Timo-Iaria C, Negrão N, Schmidek WR, hoshino K, Lobato de Menezes CE, Leme da Rocha T (1970) Phases and states of sleep in the rat. Physiol Behav 5:1057-1062.

Tobler I (1995) Is sleep fundamentally different between mammalian species? Behav Brain Res 69(1-2):35-41.

Torii S (1961) Two types of pattern of hippocampal electrical activity induced by stimulation of hypothalamus and surrounding parts of rabbit's brain. Jap J Physiol 11:147-157.

Treves A, Rolls ET (1991) What determines the capacity of autoassociative memories in the brain? Network 2(4):371-397.

Trulson ME, Jacobs BL (1979) Raphe unit activity in freely moving cats: correlation with level of behavioral arousal. Brain Res 163:135-150.

Tsodyks MV, Skaggs WE, Sejnowski TJ, McNaughton BL (1996) Population dynamics and theta rhythm phase precession of hippocampal place cell firing: A spiking neuron model. Hippocampus 6:271-280.

Van Twyver H, Garrett W (1972) Arousal threshold in the rat determined by "meaningful" stimuli. Behav Biol 7:205-215.

Vanderwolf CH (1967) Behavioral correlates of theta waves. Proc Canad Fed Biol Soc 10:41-42.

Vanderwolf CH (1969) Hippocampal electrical activity and voluntary movement in the rat. Electroenceph Clin Neurophysiol 26:407-418.

Vanderwolf CH (1971) Limbic-diencephalic mechanisms of voluntary movement. Psychol Rev 78(2):83-113.

Vanderwolf CH (1983) The role of the cerebral cortex and the ascending activating systems in the control of behavior. In: Handbook of behavioral neurobiology: Motivation (Satinoff E, Teitelbaum P, eds), 6:67-104. New York: Plenum.

Vanderwolf CH (1988) Cerebral activity and behavior: control by central cholinergic and serotonergic systems. Int Rev Neurobiol 30:225-340.

Vanderwolf CH, Kramis R, Gillespie LA, Bland BH (1975) Hippocampal rhythmic slow activity and neocortical low-voltage fast activity: Relations to behavior. In: The hippocampus: Neurophysiology and behavior (Isaacson RL, Pribram KH, eds), 2:101-128. New York: Plenum.

Vanderwolf CH, Leung LS (1983) Hippocampal rhythmical slow activity: A brief history and effects of entorhinal lesions and phencycidine. In: The neurobiology of the hippocampus (Seifert W, ed), 275-302. London: Academic.

Vertes RP (1980) Brain stem activation of the hippocampus: a role for the magnocellular reticular formation and the MLF. Electroenceph Clin Neurophysiol 50:48-58.

Vertes RP (1981) An analysis of ascending brain stem systems involved in hippocampal synchronization and desynchronization. J Neurophysiol 46:1140-1159.

Vertes RP (1982) Brain stem generation of the hippocampal EEG. Prog Neurobiol 19:159-186.

Vertes RP (1984) A lectin horseradish peroxidase study of the origin of ascending fibers in the medial forebrain bundle of the rat: the upper brainstem. Neuroscience 11:669-690.

Vertes RP (1988) Brainstem afferents to the basal forebrain in the rat. Neuroscience 24:907-935.

Vertes RP (1992) PHA-L analysis of projections from the supramammillary nucleus in the rat. J Comp Neurol 326:595-622.

Vertes RP, Colom LV, Fortin WJ, Bland BH (1993) Brainstem sites for the carbachol elicitation of the hippocampal theta rhythm in the rat. Exp Brain Res 96:419-429.

Vertes RP, Crane AM, Colom LV, Bland BH (1995) Ascending projections of the posterior nucleus of the hypothalamus: PHA-L analysis in the rat. J Comp Neurol 359:90-116.

Vertes RP, Kocsis B (1997) Brainstem-diencephalo-septohippocampal systems controlling the theta rhythm of the hippocampus. Neurosci 81(4):893-926.

Vertes RP, Martin GF (1988) An autoradiographic analysis of ascending projections from the pontine and mesencephalic reticular formation and the median raphe nucleus in the rat. J Comp Neurol 275:511-541.

Vinogradova O (1970) Registration of information and the limbic system. In: Short term changes in neural activity and behaviour (Horn G, Hinde RA, eds), 95-140. Cambridge: Cambridge University Press.

Vinogradova O, Semyonova TP, Konovalov VP (1970) Trace phenomena in single neurons of hippocampus and mammillary bodies. In: Biology of memory (Pribram KH, Broadbent DE, eds), 191-222. New York: Academic.

Wallace DG, Gorny B, Whishaw IQ (2002) Rats can track odors, other rats, and themselves: implications for the study of spatial behavior. Behav Brain Res 131:185-192.

Wallenstein GV, Hasselmo ME (1997) GABAergic modulation of hippocampal population activity: Sequence learning, place field development, and the phase precession effect. J Neurophys 78(1):393-408.

Whishaw, IQ (1972) Hippocampal electroencephalographic activity in the Mongolian gerbil during natural behaviours and wheel running and in the rat during wheel running and conditioned immobility. Canad J Psychol./Rev Canad Psychol 26(3):219-239.

Whishaw IQ, Bland BH, Vanderwolf CH (1972) Hippocampal activity, behavior, self-stimulation and heart rate during electrical stimulation of the lateral hypothalamus. J Comp Physiol Psychol 79:115-127.

Whishaw IQ, Vanderwolf CH (1973) Hippocampal EEG and behavior: changes in amplitude and frequency of RSA (theta rhythm) associated with spontaneous and learned movement patterns in rats and cats. Behav Biol 8:461-484.

Wilson CL, Motter B, Lindsley DB (1976) Influences of hypothalamic stimulation upon septal and hippocampal electrical activity in the cat. Brain Res 107:55-68.

Wilson MA, McNaughton BL (1993) Dynamics of the hippocampal ensemble code for space. Science 261:1055-1058.

Wilson MA, McNaughton BL (1994) Reactivation of hippocampal ensemble memories during sleep. Science 265:676-679.

Winson J (1978) Loss of hippocampal theta rhythm results in spatial memory deficit in the rat. Science 201:160-163.

Wood ER, Dudchenko PA, Robitsek RJ, Eichenbaum H (2000) Hippocampal neurons encode information about different types of memory episodes occurring in the same location. Neuron 27:623-633.

Woodnorth M, Kyd RJ, Logan BJ, Long MA, McNaughton N (2003) Multiple hypothalamic sites control the frequency of hippocampal theta rhythm. Hippocampus 13:361-374.

Ylinen A, Bragin A, Nádasdy Z, Jandó G, Szabó I, Sik A, Buzsáki G (1995a) Sharp wave-associated high-frequency oscillation (200 Hz) in the intact hippocampus: network and intracellular mechanisms. J Neurosci 15:30-46.

Ylinen A, Soltész I, Bragin A, Penttonen M, Sik A, Buzsáki G (1995b) Intracellular correlates of hippocampal theta rhythm in identified pyramidal cells, granule cells, and basket cells. Hippocampus 5:78-90.

Yokota T, Fujimori B (1964) Effects of brain stem stimulation upon hippocampal electrical activity, somatomotor reflexes and autonomic functions. Electroenceph Clin Neurophysiol 16:375-382.

Zhang K, Ginzburg I, McNaughton BL, Sejnowski TJ (1998) Interpreting neuronal population activity by reconstruction: unified framework with application to hippocampal place cells. J Neurophysiol 79:1017-1044.